Author:
Boven, Ellen J P

Title:
Cerebro-cerebellar interactions for temporal information processing

Cerebro-cerebellar interactions for temporal information processing

Ellen Boven

A dissertation submitted to the University of Bristol in accordance with the requirements for award of the degree of Doctor of Philosophy in the Faculty of Life Sciences.

School of Physiology, Pharmacology and Neuroscience.

March 2022

Word count: 45062

Abstract

Brain networks support learning across the multiple time scales over which intelligent behaviour unfolds. One of the key challenges in learning adaptive behaviour is the problem of temporal credit assignment: the process of identifying which set of past actions and observations, and their underlying neural representations, lead to the behavioural outcome observed in the present. In this thesis, I explore how interactions between the cerebellum and the cerebral cortex contribute to temporal credit assignment. The thesis is divided into two parts: in the first part a computational model of cerebro-cerebellar interactions for temporal credit assignment is developed. In this model a cerebellar, feedforward, network communicates with a cerebral, recurrent, network for efficient temporal credit assignment. The cerebellar signal, which contains information about future feedback that the cerebral cortex receives, influences the cerebral network such that appropriate activity patterns can be acquired for precise behaviour. The cerebellum learns to predict this feedback based on the neural representation in the cerebral cortex, thereby decoupling learning in cerebral networks from future feedback. When trained in a simple sensorimotor task the model shows faster learning and reduced dysmetria-like behaviours, in line with normal cerebellar function. These results indicate that cerebellar feedback predictions enable the cerebral cortex to acquire adaptive representations effectively by increasing the amount of temporal information available to each cerebral network.

The cerebro-cerebellar model suggests that the cerebellum mediates behaviour by predicting feedback across a range of time scales. In the second part of the thesis I tested this hypothesis using an animal model. In particular I studied how the cerebellum contributes to interval timing, which is our ability to process temporal information in the seconds-to-minute range. The cerebellum is thought to be involved in the generation and updating of internal models for control of movements with sub-second timing. Here I hypothesise that the cerebellum may also be involved in learning an internal model of supra-second stimulus time intervals. In order to test the predictive function of the cerebellum in the supra-second range, I trained rats to associate a sound duration with reward delivery. The effects of chemogenetic inactivation of cerebellar output from the lateral nucleus was investigated in expert rats. Analysis indicates that when internal time estimation is required animals show premature temporal judgements when cerebellar outflow is disrupted. This suggests that the cerebellar contributions to time processing are not restricted to sub-second intervals, but also include longer time intervals associated with cognitive processes such as decision making. Overall, this work provides a better understanding of how cerebro-cerebellar interactions support efficient temporal information processing.

Dedication and Acknowledgements

I want to thank my supervisors Dr. Jasmine Pickford, Dr. Nadia Cerminara, Dr. Rui Ponte Costa and Prof. Richard Apps for their invaluable advice, fun discussions, crucial peptalks and continued support during these four years. I am very lucky to have been supported by such a diverse and complementary team of supervisors.

I would like to acknowledge the Wellcome Trust Neural Dynamics PhD program and the University of Bristol for the resources provided to complete this project. I also want to acknowledge the members of my progress panel, Conour Houghton and Paul Dodson.

I would like to thank Joseph Pemberton with whom I have worked closely on the computational modelling aspect of this PhD for all his help and support. I would also like to thank Rachel Bissett for her support during my PhD.

I would also like to thank all the members of the two labs I have been part of for the past four years: the Sensory Motor Systems Group and Neural and Machine learning group. It was great to share this experience with the fellow PhD students in the labs. I also want to thank Dr. Alex Swainson for sharing our interest in statistical analyses; Dr. Elena Paci, Dr. Haris Organtzidis for their friendship and Dr. Robert Drake for his advice.

Ultimately, I want to thank my parents and my sister for supporting me, believing in me and helping me out in so many ways. Also I want to thank my grandparents as they have always been very proud and supportive. As well thanks to my friends in England for supporting me and all the good times and to my friends in Belgium for maintaining the long-distance friendships, visiting England and supporting me.

Author's Declaration

I declare that the work in this dissertation was carried out in accordance with the requirements of the University's *Regulations and Code of Practice for Research Degree Programmes* and that it has not been submitted for any other academic award. Except where indicated by specific reference in the text, the work is the candidate's own work. Work done in collaboration with, or with the assistance of, others, is indicated as such. Any views expressed in the dissertation are those of the author.

Some of the content included in this thesis has been published as follows:

Boven, E., Pemberton, J., Chadderton, P., Apps, R., & Costa, R. P. (2022). Cerebro-cerebellar networks facilitate learning through feedback decoupling. bioRxiv. (accepted in Nature Communications)

Pemberton, J., Boven, E., Apps, R., & Costa, R. P. (2021). Cortico-cerebellar networks as decoupling neural interfaces. Advances in Neural Information Processing Systems, 34, 7745-7759.

Communications at conferences and invited talks:

Boven E., Pickford J., Costa P. R., Cerminara N., Apps R. (2022) Cerebellar contributions to interval timing. Poster S05-070 @ FENS (Paris)

Boven E. (2022) Cerebro-cerebellar circuits for temporal information processing. Invited talk @Erasmus MC Rotterdam, Cerebro-cerebellar Communication lab, Zenhuy Gao

Boven E. (2022) Cerebro-cerebellar circuits for temporal information processing. Invited online talk @NIH Washington D.C., Neocortex-Cerebellum Circuitry Unit, Mark J. Wagner

Boven, E., Pemberton, J., Chadderton, P., Apps, R., & Costa, R. P. (2022). Cerebro-cerebellar networks facilitate learning through feedback decoupling. Poster Cosyne

Boven, E., Pemberton, J., Chadderton, P., Apps, R., & Costa, R. P. (2021). Cerebro-cerebellar networks facilitate learning through feedback decoupling. Poster NeurIPS

Boven, E., Pemberton, J., Chadderton, P., Apps, R., & Costa, R. P. (2021). Cerebro-cerebellar networks facilitate learning through feedback decoupling. Poster Cosyne

The work presented in Chapter II was done in collaboration with my colleague Joseph Pemberton (JP), myself (EB) and my supervisor Rui Ponte Costa (RPC). JP and I have contributed equally to the conceptual developments of the cerebro-cerebellar model. Both have worked on the implementation of the model. Whereas JP has contributed significantly more to the development of the code itself, I have spent more time on the integration of the model results with the experimental literature. I performed the simulations presented in this work, however this would have not been possible without the support by JP. RPC has developed some of the schematics used in Chapter II. JP contributed to developing custom written python scripts to plot some of the data collected in Chapter II. Valentina Pauly and Callum Matthews contributed to processing histological tissue and subsequent analyses of the tissue using microscopy presented in Chapter III, this included, amongst others, determining expression level and cannula placement. Dr. Jasmine Pickford developed custom Matlab scripts used to analyse data collected in the open field behavioural test discussed in Chapter III. Dr. Alex Swainson has provided help with running the DeepLabCut models for analysing the open field.

SIGNED: ..... DATE:.....

Contents

List of Figures

List of Tables

List of abbreviations

ANOVA	Analysis of Variance
AP	Anteroposterior
BG	Basal Ganglia
CF	Climbing Fibres
CI	Confindence Interval
CNO	clozapine N-oxide
cRNN	Cerebral Recurrent Neural Network
ccRNN	Cerebro-cerebellar Recurrent Neural Network
dB	Decibel
DN	Dentate Nucleus
DV	Dorsoventral
DREADD	Designer Receptors Exclusively Activated by Designer Drugs
EGFP	Enhanced Green Fluorescent Protein
GC	Granule Cells
GLM	Generalised Linear Model
hM4Di	human M4 muscarinic (hM4) receptor DREADD subtype
IN	Interposed Nucleus
ITI	Inter-trial Interval
IR	Infrared
LCN	Lateral Cerebellar Nucleus
LMM	Linear Mixed-effects Model
LSTM	Long Short-Term memory
MF	Mossy Fibres
ML	Mediolateral
MN	Medial Nucleus
PC	Purkinje Cells
PCs	Principal Components
PCA	Principal Component Analysis
dPCA	demixed Principal Component Analysis
PFC	Prefrontal cortex
RL	Reinforcement Learning
RNN	Recurrent Neural Network
RPE	Reward Prediction Error
VL	Ventro-Lateral

Chapter 1

General introduction

1.1 Temporal information processing

The ability to encode temporal information across a wide range of time scales is essential for generating the adaptive behaviour that is key to our survival. Our capacity to behave adaptively results from our ability to learn by interacting with an environment in which states dynamically evolve across different timescales, ranging from slowly changing contextual states of the world to fast trajectories of bodily movement (Kiebel et al., 2008). For both a food-restricted rat anticipating the next reinforcement or a human commuting to work, accurately perceiving time is an important determinant of behaviour. In fact, it is known that neural circuits process temporal intervals during behaviour (Carr et al., 1993). For example, temporal information is encoded in single neurons that linearly change the firing rate with the duration between two events or in population activity that dynamically evolves over an action sequence. However, it is unclear how the brain integrates feedback from future events with internal representations of past experience in order to drive adaptive behaviour.

Our current understanding of the underlying neurobiological bases of temporal information processing is that, broadly speaking, it involves two main circuits (see Fig. 1.1, Buhusi et al., 2005). On the one hand it is thought that the cerebellum is important for tracking duration between events in the range of milliseconds. Indeed, the cerebellum is classically linked to a range of sensorimotor skills that require precise millisecond timing of the motor response (Garcia et al., 1998; Krupa et al., 1997; Mojtahedian et al., 2007). On the other hand, the basal ganglia and cerebral circuits, are thought to support interval timing: the perception of more slowly evolving events, at the scale of seconds to minutes which guides adaptive behaviours such as foraging and decision making. Neural substrates underlying interval timing include, amongst others, thalamo-cortical-striatal circuits, with cortical regions including the prefrontal cortex (PFC) and the posterior parietal cortex (PPC). Behavioural studies have shown involvement of the basal ganglia (BG), PFC and PPC in schizophrenia, a disease where interval timing is impaired. Also, interval timing depends on the ramping activity of medium spiny neurons (MSN) in the striatum

(Ponzi et al., 2022). Similarly, time intervals are represented by scaled ramping in the PFC (Xu et al., 2014).

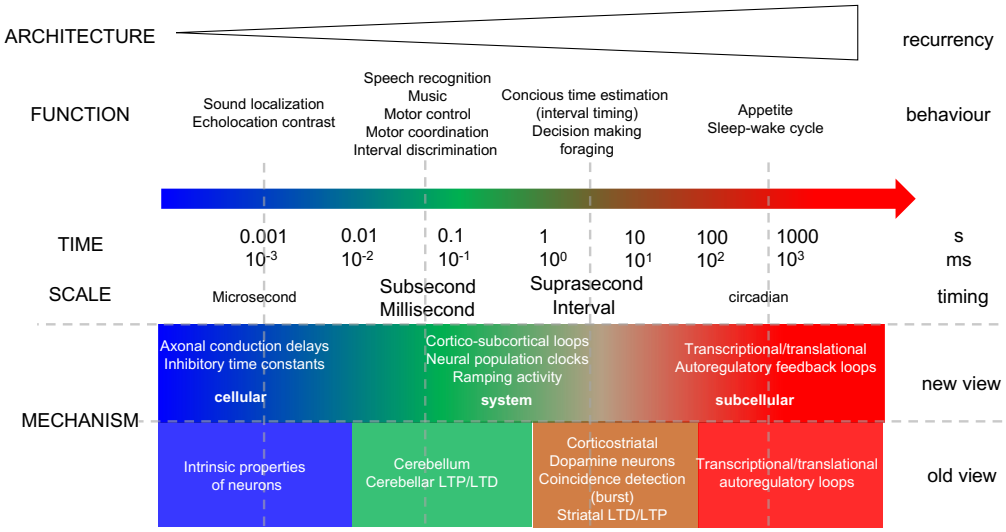

Figure 1.1: **Temporal information processing.** Schematic representing the complexity of behaviour, brain regions (old, Buhusi et al., 2005) and brain-wide feedback loops (new, Zhou et al., 2022) that underlie different scales of temporal information processing.

From a theoretical perspective the problem of learning what happens when, is known as the temporal credit assignment and is thought to be supported by a recurrent circuit architecture (Hardy et al., 2018). Characterised by reciprocal connections that provide inherent feedback loops of information, such networks are able to process time-dependent sequences. This is in stark contrast to a feedforward network, in which processing depends on current inputs without fluctuations of previous inputs propagating over time. Thanks to their ability of encoding temporally varying sequences, recurrent neural networks have been at the forefront as computational models for the neural basis of temporal information processing or timing. In fact, they are widely used in computational neuroscience to model behaviourally relevant sequences (Kaushik et al., 2023) and they also form the basis for freely available language processing tools such as Google translate (Murugan, 2018).

Together, neurobiological or theoretical tools, focussing on either a single brain region or a specific network architecture, have greatly contributed to our current understanding of temporal information processing. However, a striking feature of neural connectivity is nested feedback loops (see Fig. 1.1), that allows activity to propagate across areas, constantly exchanging signals, suggesting that multi-regional computations may underlie adaptive behaviour (Abbott et al., 2020; Cruz et al., 2022). One of the most prominent loops in the brain, that has expanded across evolution, is between the cerebrum and cerebellum (Sultan, 2002; Rilling et al., 1998). Despite the growing evidence that the cerebellum forms reciprocal functional and anatomical loops with sensory, motor, and associative cerebral areas (Gao et al., 2018; Li et al., 2020; Deverett et al., 2019; Pisano et al., 2021), the function of these biological feedback loops remains largely unknown.

The contribution of this thesis to understanding temporal information processing in

cerebro-cerebellar loops is two-fold. The first is to provide a theoretical account for cerebro-cerebellar interactions with a focus on how cerebellar output can modulate cerebral processing during learning of complex sequences. The second is to study the extent to which the cerebellum is necessary for temporal processing supported by the cerebral cortex when perceiving time intervals in the seconds to minutes range.

1.2 Cerebellum

1.2.1 Cerebellar architecture

The cerebellum is tightly interconnected with most other parts of the central nervous system, allowing it to integrate the multiplicity of signals that are processed during behaviour. Understanding its anatomical organisation is thus a prerequisite for studying how the cerebellum communicates with areas like the cerebrum. At the macroscopic level the cerebellum is divided into three compartments that are oriented in the rostro-caudal axis, with the vermis at the midline and paravermis and hemisphere further laterally on either side of the midline (Fig. 1.2a).

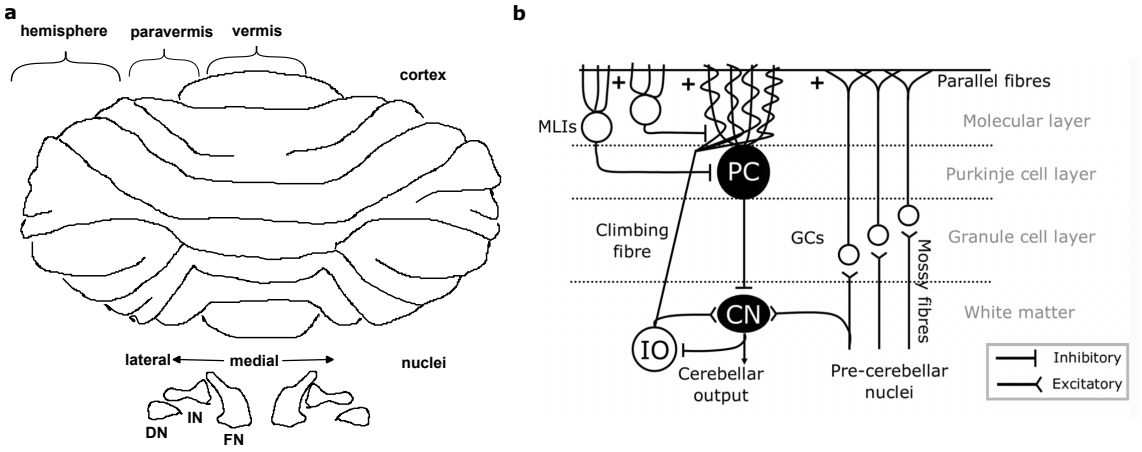

Figure 1.2: **Cerebellar architecture.** Schematic representation of cerebellar circuits. (**a**) On the top is a macroscopic view of the rat cerebellum with the vermis, paravermis and hemispheres. On the bottom is a schematic of the three cerebellar nuclei (CN) in a rat: dentate nucleus (DN), interpositus nucleus (IN) and fastigial nucleus (FN). (**b**) Schematic representation indicating the feedforward connectivity between the cerebellar cortex and the cerebellar nuclei: the main input output pathway of the cerebellum is feedforward: climbing fibers and mossy fibers enter via Purkinje and granule cells respectively and send collaterals to cerebellar nuclei. The latter mainly receive inhibitory input from the Purkinje cells and project to downstream target areas. Differences in cytoarchitecture as well as long distant projections together will eventually determine the functional processing of the cerebellar microcircuit. Image adapted from Gill et al., 2019 and Iosif et al., 2022.

The cerebellum consists of a mainly feedforward circuit architecture, existing of two components: the cerebellar cortex and the cerebellar nuclei (Fig. 1.2a, b). In brief, information enters the cerebellar cortex mainly via two excitatory pathways. On the

one hand the mossy fibres, originating principally in the pons, synapse on granule cells which in turn relay the information via parallel fibres to Purkinje Cells. On the other hand, there are the climbing fibres which arise exclusively from the inferior olive and synapse directly with Purkinje cells (Fig. 1.2c). Whilst the cerebellar cortex contains a variety of interneuronal cell types (not shown in Fig. 1.2, but for review see De Zeeuw et al., 2021), the Purkinje cells are the sole output, and form inhibitory synapses with neurons in the cerebellar nuclei.

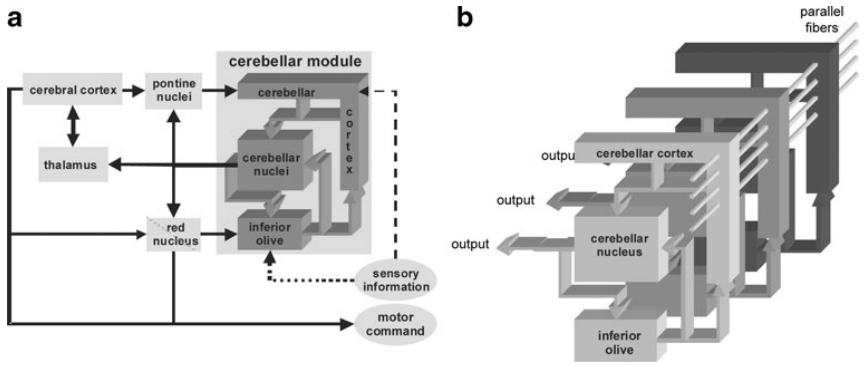

Figure 1.3: **Cerebellar module.** Schematic representation of a cerebellar module. (**a**) Functional specialization of each cerebellar module is determined by differences in global input and output connectivity with other regions in the central nervous system, ranging from sensory organs to higher-order associative areas in the cerebrum. (**b**) The boundaries of a cerebellar module are defined by where in the inferior olive the Purkinje cells receive climbing fibre input from and where in the cerebellar nuclei the Purkinje cells project to. Image by Ruigrok, 2011a.

The cerebellar cortex has a modular organization defined by climbing fibre input from the inferior olive, cellular properties of the Purkinje cells and their projection to specific downstream nuclei (Voogd et al., 1998). Within the cerebellum there exist three output nuclei, from medial to lateral on each side of the midline: the medial nucleus, the interposed nucleus and the lateral nucleus (Fig. 1.2a, bottom). Depending on whether Purkinje cells are located in the cerebellar cortical vermis, paravermis or hemisphere they provide a topographically organised cortico-nuclear projection to the medial, interposed and lateral nucleus respectively. The local input-output connectivity as well as certain molecular markers of the Purkinje cells have been used to identify anatomical units at the microscopic level: the cerebellar module (Fig. 1.3). On the one hand the boundaries of a cerebellar module are defined by where in the inferior olive the Purkinje cells receive climbing fibre input from and where in the cerebellar nuclei the Purkinje cells project to (Apps et al., 2005; Ruigrok, 2011a). It is thought the functional specialization of each cerebellar module is determined mainly by differences in global input and output connectivity with other regions in the central nervous system, ranging from sensory organs to higher-order associative areas in the cerebrum. On the other hand, experimental evidence points to localized diversity of molecular, cellular and physiological properties; for example regional differences in intrinsic properties in zebrin expression or the capacity to compensate for multiple delays in feedback about behavioural errors depending on local connectivity (Cerminara et al., 2015). This local circuit complexity provides a substrate for diverse processing mechanisms, thereby enhancing the computational capacity of cerebellar circuits. These modules are thus thought

to be non-uniform in their computational capacity. Together, this global and local diversity of the modular architecture enable the cerebellum to support a wide range of behaviourally relevant temporal contingencies.

1.2.2 Computational role of the cerebellum

Given that the cerebellar circuitry is relatively well-defined, the cerebellum has received long-standing interest from theoreticians to inspire computational modelling of how its structure can support functions such as motor control and sensorimotor learning (Kaiser et al., 2018). The original model is the Marr-Albus-Ito model, which postulated that two characteristics of the cerebellar circuit are central to the role of cerebellum in sensorimotor learning (for review see Yamazaki, 2021). These characteristics are the vast, but sparsely connected, mossy fibre expansion at the level of the granule cell and the modification of parallel fibre-to-Purkinje cell synapses guided by climbing fibre inputs. With the main feedforward connectivity at the centre point of this model, it shared a strong analogy with the perceptron (see Fig. 1.4, Rosenblatt, 1958), a basic supervised learning machine. Most theoretical studies of the cerebellum stem from this model, with a focus on local cerebellar circuit, particularly looking at the computations of input levels, i.e. granule cells, climbing fibres and Purkinje cells, of the cerebellar circuit (Jaeger, 2003; De Schutter et al., 1996; Dean et al., 2008).

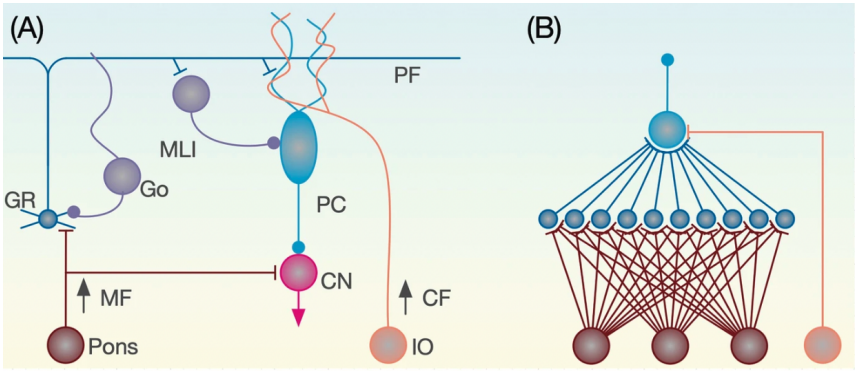

Figure 1.4: **Analogy between the cerebellar microcircuit and the perceptron.** Schematic illustrating the analogy between cerebellar microcircuit and the perceptron. (**a**) Cerebellar microcircuit with abbreviations MF mossy fibers, GR granule cells, Go Golgi cells, MLI molecular layer interneurons, PC Purkinje cells, PF parallel fibers, CN cerebellar nuclei, CF climbing fibers, IO inferior olive. (**b**) Representation of the Marr-Albus-Ito model as a perceptron. In this feedforward model two circuit characteristics are considered: the mossy fiber expansion onto granule cells and the inferior olive sending a learning signal via the climbing fibers. Brown indicates the MF input, orange relates to the CF input and blue indicate the PC. Image reproduced from Yamazaki, 2021.

However, as pointed out in section 1.1, the cerebellum does not operate in isolation. To date computational modelling of cerebellar interactions with other brain structures such as the cerebral cortex are based on the concept of internal models. This prevalent theory points towards the cerebellum as an "internal model" of the

nervous system (Wolpert et al., 1998), providing either efferent (inverse) or afferent (forward) predictions (Fig. 1.5a, b).

In the forward model of sensorimotor control, the cerebellum receives an efferent copy of the motor command from the motor cortex (Ito, 1970; Miall et al., 1993), and sensory feedback from movement (Fig. 1.5c). With these two inputs the forward model learns to predict the sensory consequences of motor commands, that in turn can be used as internal feedback to the cerebral cortex (Fig. 1.5c). The cerebellar internal feedback enables the cerebral cortex to perform accurate movements, as there is no need to wait for the actual sensory feedback generated by the movement. Since forward models are widely used in control theory, applications stemming from this field have been readily used to study the role of the cerebellum in motor control. The most famous example is the Kalman filter model (Paulin, 1989), in which an estimate of the current state results from the integration of a predicted state, which itself is derived from an internal model, and sensory afferents. It is thought that the cerebellum computes the Kalman gain, which calculates a weighted sum of these two components. By comparison, the inverse model of the cerebellum in motor control computes the predictions about the motor command given a target (or desired) motor response (Fig. 1.5d, Ito, 1970). Feedback errors are derived by comparing a motor command from the motor cortex with the predicted motor command in the cerebellum. Together, these models have enabled significant theoretical and experimental advances especially with respect to the understanding of motor control (Kawato et al., 2007).

It is thought that the cerebellar circuitry is well suited for the acquisition of such predictive models. The dimensionality expansion at the granule cell layer allows for input decorrelation and pattern recognition in Purkinje cells (Cayco-Gajic et al., 2019; Nguyen et al., 2022). In addition, these highly dimensional input patterns are thought to be reconfigured via modification of parallel-fibre synapses on Purkinje cells conditioned by climbing-fibre inputs (Grasselli et al., 2014). This comparison made at the Purkinje cell level relies on well-timed processing to avoid any mismatches between the two different inputs. These precisely timed signals enable the Purkinje cells to change their firing rate when unexpected signals are detected. This in turn will regulate activity in the cerebellar nuclei (Uusisaari et al., 2011), which then emits the appropriate efferent (inverse) or afferent (forward) signal to control behaviour. Together, these mechanisms are thought to establish learnt associations via reconfiguring incoming patterns via the mossy fibres following an instructive (salient) signal from the inferior olive. These mechamisms might in turn be shaped by local processes. Consistent with the non-uniform modular organization of the cerebellum (Apps et al., 2018; Cerminara et al., 2011; Ruigrok, 2011b), there likely exists a range of spatiotemporal predictions resulting from multiple internal models. It remains unknown exactly how these range of spatiotemporal predictions can be integrated into downstream circuits. Moreover, these models have so far only captured relatively simple sensorimotor control tasks.

While much experimental and computational research has focused on the role of the cerebellum in motor control, an increasing body of behavioural, anatomical and imaging studies points to a role of the cerebellum in cognition in humans and non-human primates (Ashida et al., 2019; Buckner, 2013; Diedrichsen et al., 2019).

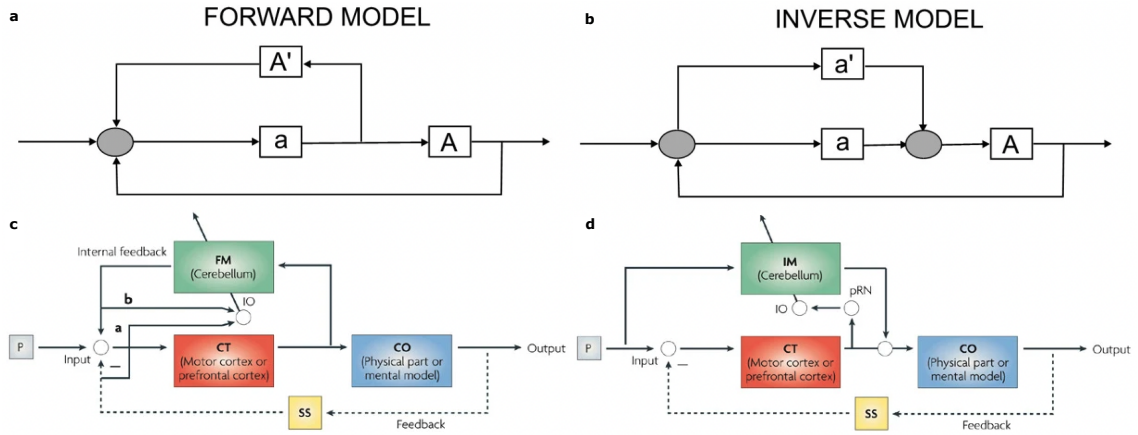

Figure 1.5: **Internal models.** (**a, b**) Simplified schematic illustrating the afferent and efferent flow in forward and inverse internal models respectively. (**c, d**) Detailed schematic of information flow in forward (FM) and inverse models (IM) respectively. An area (P) instructs a controller (CT), which could be the motor cortex or prefrontal cortex for example, to send out a command to the controlled object (CO), which could be a physical body part or a mental operation. This will elicit feedback from the sensory system (SS) that will be sent to the controller. Image adapted from Manto, 2009 and Ito, 2008.

Observed impairments of cerebellar patients range from tasks based on language (Deverett et al., 2019; Guell et al., 2015), planning (Baker et al., 1996), to emotional processing (Fiez et al., 1992); the enlarged size of the human dentate nucleus, a cerebellar output channel which projects to non-motor cerebral areas (Dum et al., 2003) provides evolutionary evidence for the proposed role of the cerebellum in higher order thinking (Leiner et al., 1993). Evidence in rodents also hints at a cerebellar role in some executive functions, for example the presence of a reinforcement error signal (Sendhilnathan et al., 2020) driven by reward-related signals during reward-based associative behavioural paradigms (Heffley et al., 2018; Kostadinov et al., 2019). However little research has directly measured cerebellar involvement in higher order behaviours. Similarly, it remains unclear how the theoretical accounts summarized above can be extended to learning and control of more complicated goal-directed behaviour (Cerminara et al., 2015; Diedrichsen et al., 2019).

1.3 Cerebral cortex

1.3.1 Architecture of cerebral cortex

The cerebral neocortex, or cerebral cortex, is made up of two hemispheres. The different cerebral areas in each hemisphere include layered cortical microcircuits which are characterized by recurrent connections (Douglas et al., 1998). There are the local recurrent connections which occur within and across layers and more global recurrent connections which arise from projections from other cerebral areas but also subcortical areas (Fig. 1.6) (Douglas et al., 1995; Berezovskii et al., 2011; Harris

et al., 2015). The inputs resulting from this dense reciprocity enter the cerebral cortex in such a way that distinct information streams terminate within distinct pathways. On the one hand there are feed-forward streams that are thought to carry information from sensory processing from lower layers to higher layers in the cerebral cortex (Fig. 1.6). On the other hand there is the feedback information streams that enter via outer layers and carry information between cerebral and subcortical areas (Fig. 1.6).

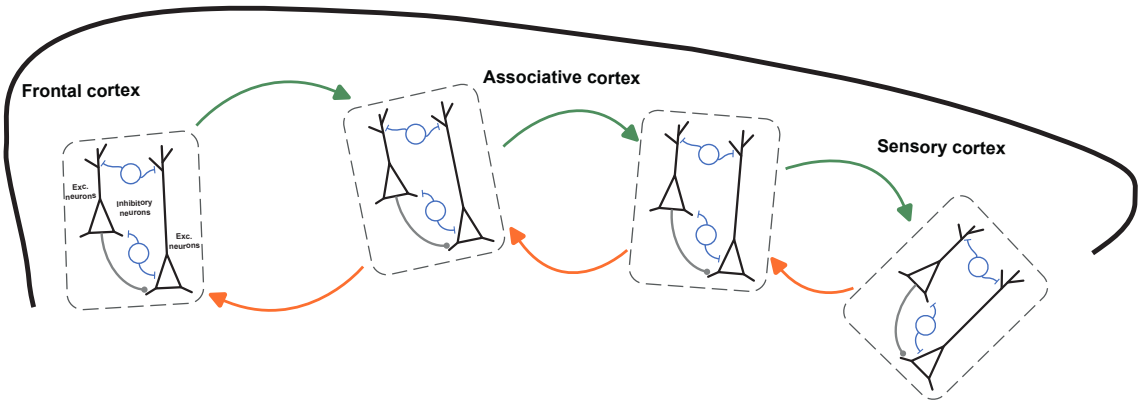

Figure 1.6: **Schematic of cerebral architecture.** Schematic illustrating the recurrent local microcircuit, formed between excitatory and inhibitory neurons, in each different cerebral areas and the global feedforward (orange) and feedback (green) inputs into the cerebral cortex.

1.3.2 Computational role of cerebral cortex

The ability to learn the temporal relations between fast sensorimotor signals and sparse, adaptive, behavioural outcomes is thought to be supported by the neocortex (Tanji et al., 2008; Chen et al., 2013; Ebbesen et al., 2017). Moreover, it is thought that the anatomy of the cerebral cortex captures the temporal hierarchy present in the dynamics of environmental states (Kiebel et al., 2008; Hasson et al., 2008; Chen et al., 2015). This reinstates the idea that each cerebral area integrates task-specific information related to a functionally distinct behavioural module: while the motor cortex enables the execution of precise goal-directed movements, the prefrontal cortex allows the formation of thoughts and actions guided by internal goals. Studies show that the population dynamics of different cerebral areas, measured as temporal correlations in ongoing activity, evolve over different timescales (Wolff et al., 2022). Whereas fast fluctuations in sensory areas enable the precise representation of rapidly changing sensory inputs, slower environmental dynamics are encoded in higher-order areas via temporally extended representations (Cavanagh et al., 2020; Raut et al., 2020). This has led to the idea that the temporal correlations, or intrinsic timescales, of each area contribute a temporal hierarchy of population dynamics across the neocortex (Murray et al., 2014).

The cerebral cortex involvement in integrating dynamics across different timescales is what enables humans and animals to anticipate future events (Raby et al., 2007)

and to implement intelligent behaviour (Gallistel, 1990). However, it is unclear how the cerebral cortex learns to associate events across a wide range of timescales. This is known as the temporal credit assignment problem (tCA, Sutton, 1984): the difficulty of understanding which past events, and the underlying neural representations, have lead to a favourable behavioural outcome. A framework that allows to study how hierarchical representations are formed to represent the complex temporal correlations of events is that of the recurrent neural network (RNN) (Lillicrap et al., 2019). RNNs are brain-inspired artificial architectures that have the capability of performing tasks that are considered to require intelligent behaviour. This has led to the idea that there is some equivalence between these cerebral circuits and these networks (for review see Richards et al., 2019b). RNNs are able to perform difficult tasks as a result of the efficient credit assignment algorithms they employ. More specifically, given their capability to represent information over time through reciprocal connections between neurons, the problem of tCA can be formalized using RNNs (see Fig. 1.7a, Lillicrap et al., 2019). When considering a sequence of network representations h, the RNN state at each timestep will be a function f of the input at that timestep and the RNN state at the previous timestep applied on the network connections θ:

$$h_t = f(x_t, h_{t-1}; \theta) \tag{1.1}$$

In order to relate the temporal network representations of an input sequence to a desired output behaviour, RNNs are presented with a learning goal (or objective function, Richards et al., 2019b). The problem of temporal credit assignment can then be formalized as the problem of changing the RNN connections such that the behavioural learning goal is achieved. The canonical algorithm for performing temporal credit assignment in an RNN is the back-propagation through time algorithm (BPTT; see Fig. 1.7b; for detailed discussion see Lillicrap et al., 2019). In brief, BPTT recursively calculates the required change in network connections with respect to the learning goal, $\frac{dL}{d\theta}$. The required change is signalled via an error which results from comparing the final network state h_T to the desired output. In order to mathematically calculate the change required for the time-dependent network connections to achieve an improved representation of the input-ouput relationship, the error for each time step can only be derived once the input sequence is fully processed. This means that the network must be capable of storing the full history of network activations in order to calculate the subsequent error signals. Thus, when using BPTT, error is assigned backward in time, from more recent to earlier states.

Although these mathematical learning rules suffer from such biological implausibilities (see Lillicrap et al., 2020 for review), the theoretical framework of (temporal) credit assignment has been readily applied to understanding learning in the brain (Richards et al., 2019b), as studying learning in *in vivo* biological, recurrent, networks is a practically hard endeavour (Maass et al., 2002; Eyono et al., 2022). With an attempt to reduce the gap between the mathematics of BPTT and biology recent studies indicate that learning in cerebral network can approximate the back-propagation algorithm (Whittington et al., 2019), with a focus on understanding the mechanisms of local synaptic plasticity for temporal credit assignment. However, how interactions between different brain areas can support efficient temporal credit assignment remains currently unexplored (Eyono et al., 2022).

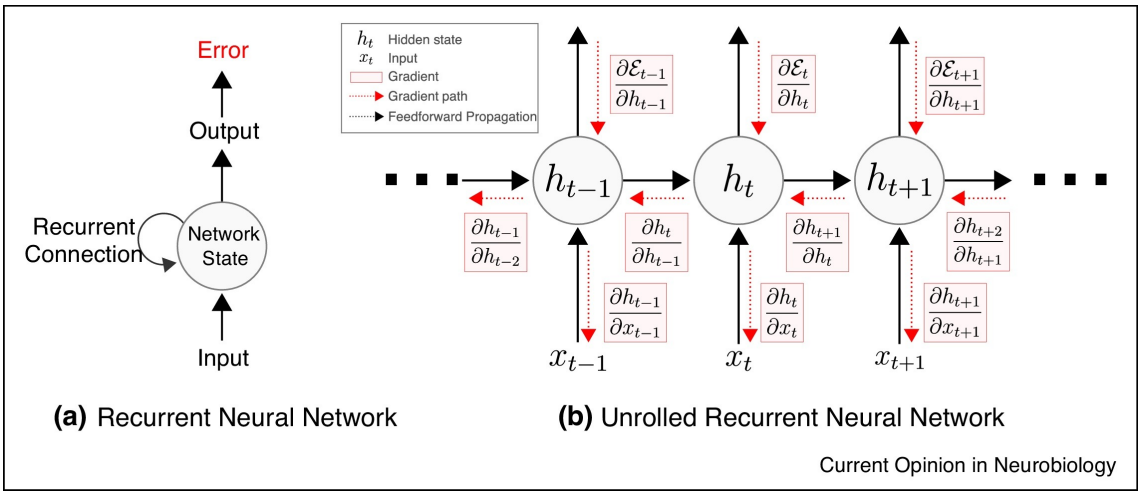

Figure 1.7: **Temporal credit assignment in recurrent neural networks.** (**a**) Schematic illustrating a simple RNN, in which reciprocal connections enable network representations to evolve over time. (**b**) Schematic illustrating the information flow and temporal credit assignment in RNN. Black arrows indicate the forward propagation of input and network representations over time. Red arrows indicate the backward propagation of error that signals behavioural adjustments derived from the learning goal back to the network. Image reproduced from Lillicrap et al., 2019.

1.4 Cerebro-cerebellar circuits

Evidence showing that sensory areas (Buetfering et al., 2022) and subcortical structures such as the cerebellum (see section 1.2.2), contain signals related to motor planning, choice and working memory questions the idea of strict functional separation in the brain. Altogether this suggests that functional specializations of behaviour emerge from distributed networks across the brain. It is possible that regions might differ in the way they process and integrate information: whereas the cerebellar processes information feedforwardly, the cerebral cortex integrates signals via recurrent connections. However, in order to fuly appreciate the contributions of these circuits to behaviour, it is important to look at their interactions.

1.4.1 Anatomy of cerebro-cerebellar circuits

The cerebellum is bidirectionally connected to the cerebrum via cerebro-cerebellar circuits (Fig. 1.8, Apps et al., 2013). In one direction, information descends from different parts of the cerebral cortex towards the cerebellum, via several structures in the brainstem. Several studies highlight the impact of a range of cerebral areas (sensory, motor and association areas) onto the cerebellum via the mossy fibres coming from the pons (Odeh et al., 2005; Legg et al., 1989). This is called the cerebro-ponto-cerebellar projection, which forms one of the most dense fibres tracts in the mammalian brain (Armstrong, 2022). Besides the pontine mossy fiber system, cerebro-cerebellar communication is also mediated by the climbing fiber system,

called the cerebro-olivo-cerebellar pathway, via projections through the mesodiencephalic junction (MDJ). For example, one study using trans-neuronal tracing has revealed that connections from the cerebral cortical areas onto different olivary subnuclei are topographically organized (Wang et al., 2022).

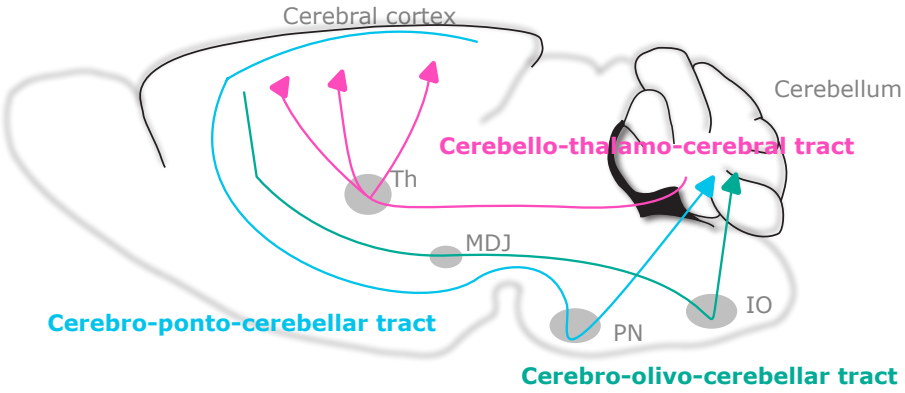

Figure 1.8: **Cerebro-cerebellar circuits.** Schematic of rodent brain summarizing the key features of cerebro-cerebellar reciprocal connectivity. Different areas of the cerebral cortex project to the cerebellum via cerebro-ponto-cerebellar pathway (blue) and cerebro-olivo-cerebellar pathway (green). The cerebellum provides feedback connections to different cerebral areas via the cerebello-thalamo-cerebral tract (pink). Abbreviations are Th, thalamus; MDJ, mesodiencephalic junction; PN, pontine nuclei or pons; IO, inferior olive.

In the other direction, the ascending, feedback, pathway originates in the cerebellar output nuclei and projects, via the thalamus, to the cerebrum (Fig. 1.8). The traditional view is that the cerebello-thalamic projections arising from the three output nuclei project primarily project to the motor cortex. However accumulating evidence shows that the cerebellar paths to the cerebral cortex are more distributed, including a wide range of areas. For example, the enlarged size of the human dentate nucleus, a cerebellar output channel which projects to non-motor cerebral areas (Dum et al., 2003), provides evolutionary evidence for the proposed role of the cerebellum in higher order thinking (Leiner et al., 1993). The cerebellar ascending pathways to frontal areas of the cerebral cortex have now as well been identified in rodent models (Pisano et al., 2021). The principal route of cerebellar feedback projections to the cerebrum occurs via the ventral thalamic nuclei, including the ventral medial (VM), ventral anterior (VA), ventral lateral (VL), ventral posteriomedial (VPM), and ventral posteriolateral (VPL) nuclei. However, distinct thalamic routes have been identified, such via the reticular thalamic nucleus which is thought to provide a substantial modulatory cerebello-cerebral pathway (Pisano et al., 2021). Although other, indirect, routes via subcortical and brainstem structures such as basal ganglia and tegmental areas are possible, the cerebello-thalamic projections are rapidly conducting, thus providing a substrate for reciprocal communication between cerebellum and the cerebral cortex (Watson et al., 2009; Watson et al., 2014).

1.4.2 Computational role of cerebro-cerebellar circuits

One line of evidence that has raised important questions regarding cerebellar interactions with the cerebral cortex comes from observing reward related signals at the level of cerebellar input (Heffley et al., 2018; Kostadinov et al., 2019). Several studies in animals have shown that both the climbing fiber as well as mossy fiber pathways can carry reward signals into the cerebellum (Kostadinov et al., 2022). In addition, several human studies have observed a functional parcellation of task-related activity in the cerebellum ranging from sensorimotor to higher-order signalling (King et al., 2019; Popa et al., 2019). This suggests that the cerebellar input not only carries reward related information but also other types of higher order signals. Depending on how this information is processed by local cerebellar circuits and downstream brain circuits, the cerebellum seems able to generate a variety of predictive computations (see section 1.2.2).

Several studies on how the neural dynamics of cerebral cortex and cerebellum depend on each other have supported the notion that the cerebellum contributes to higher order processing via cerebro-cerebellar interactions. Evidence from *in vivo* recordings and theoretical studies have indicated that diverse neural representations can be faithfully transmitted between the cerebral cortex and cerebellum via the intermediate structures (Wagner et al., 2019), which are thought to enable optimal transformation of the representations (Muscinelli et al., 2022). Moreover, studies focused on how the cerebellar output influences cerebral representations, implicate the cerebellum as a driver of cerebral representations. More specifically, using optogenetics combined with *in vivo* electrophysiology Gao et al., 2018 have found that the cerebellum is required to sustain the preparatory motor activity, that is necessary for task execution, in the premotor cortex. Another study contributed to this idea by showing that the cerebellum learns to predict the timing of upcoming rewards in order to sculpt the preparatory representations in the cerebral cortex (Chabrol et al., 2019).

From a theoretical perspective the idea of the cerebellum as a driver of cerebral dynamics seems plausible given the characteristic computational features that arise from the contrasting circuit architectures. Artificial recurrent neural network models have been successful at approximating the cerebrum as a dynamical system (Mante et al., 2013; Song et al., 2016; Rajan et al., 2016; Laje et al., 2013). The recurrent connections allow for input information to be sustained and propagated over time, whereas processing in a feedforward network only depends on current inputs, so the encoded information depends less on information carried over from previous events. A recurrent neural network is also known to be difficult to train and control because it may exhibit chaotic behaviour (Sompolinsky et al., 1988; Sussillo et al., 2009; Laje et al., 2013). A feedforward neural network, on the other hand, is stable because its output depends not on previous inputs but only current inputs and a fluctuation at one point of time does not propagate over time. Previous theoretical studies have shown that stable activity patterns in recurrent neural network can be generated by adding a non-recurrent feedback connection from the output to the recurrent units (Sussillo et al., 2009; Ben-Shushan et al., 2017). Taken together, experimental and theoretical evidence supports the idea that the cerebellum drives cerebral dynamics

by predicting the next state based on the copy of cerebral dynamics it receives. Based on this Tanaka et al., 2020 propose that the computational role of the cerebellar descending pathway is to stabilizes recurrent cerebral dynamics by predicting the expected activity of the cerebral cortex (Fig. 1.9).

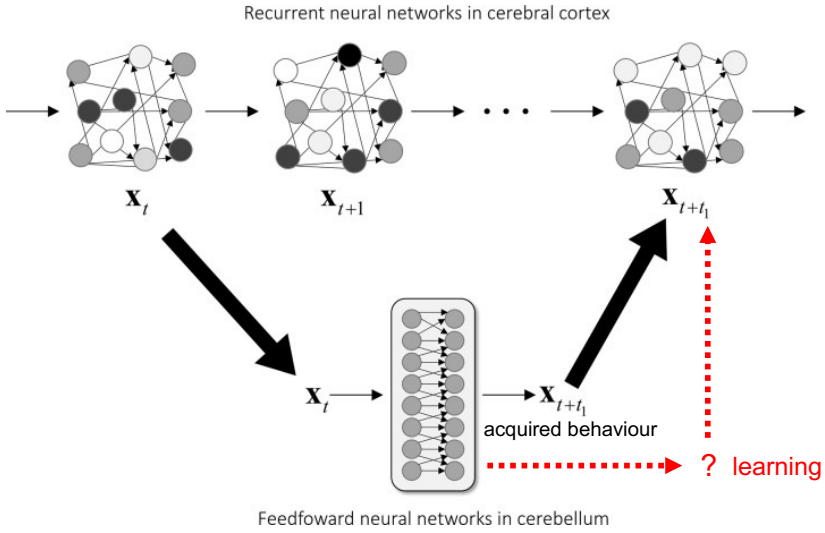

Figure 1.9: **Cerebro-cerebellar loop as artificial neural networks.** Schematic representation of the cerebro-cerebellar loop using artificial neural networks. While the cerebrum is characterized by a, mainly, recurrent local connectivity, the cerebellum can be approximated by a feedforward neural network. During skilled behaviour, the cerebellum uses the current cerebral state to predict the next. On the contrary, based on current information, there is no computational account of how the cerebellum interacts with the cerebral cortex during learning. Image adapted from Tanaka et al., 2020.

The work and ideas summarized above are based on experiments performed in a setting where skilled behaviour has already been acquired. For most complex behaviours, however, skill acquisition occurs through modification and organization of neural representation such that the relevant stimulus features and action sequences are appropriately associated through learning and memory processes. Work on how the cerebellum could control plastic changes in the cerebral cortex stem mostly from human studies. One study suggests that the cerebellum modulates excitability in the cerebral cortex in such a way that induces coupling between the relevant input signals and behavioural outputs (Molinari et al., 2002). In addition, studies suggest that defective cerebellar processing leads to abnormal plasticity in motor areas preventing the acquisition of precise motor programs (Kishore et al., 2014). Another study implicates the cerebellum in shaping motor commands in the motor cortex by conditioning cerebral plasticity using predictions of sensory feedback (Popa et al., 2013). The idea that the cerebellum learns internal models of sensory feedback together with its modular organization support this idea (see section 1.2.2). Moreover, the existence of non-uniform cerebellar modules, composed of topographic-specific global connections and local diversity in cerebellar circuitry, suggest that the cerebellum can facilitate tuning of task-specific representations by simulating feedback across a range of modalities, including physical and internal states. To date, there is little to no theoretical work that postulate constraints on how the cerebellum interacts with the cerebral cortex during acquisition of skilled behaviour. One attractive

framework comes from the idea that associative learning in cortical networks can approximate the back-propagation algorithm (Whittington et al., 2019, see section 1.3.2).

Together, two gaps in the understanding of cerebro-cerebellar networks can be identified. On the one hand most studies looking at cerebro-cerebellar have focussed on tasks that engage cerebellar interactions with motor and premotor cerebral areas, while studying the role of the cerebellum in tasks that engage different cerebral areas remain unexplored (Fig. 1.9). On the other hand there is the idea that the cerebellum exerts a, potentially complementary (Sohn et al., 2021), modulatory role on cerebral areas during learning, an interaction which is currently unaccounted for in computational models of these circuits.

1.5 Outline of this thesis

At the start of this general introduction I argued that in order to understand how humans and animals achieve complicated sequences of adaptive behaviour it is important to move beyond our understanding of single-region contributions to behaviour. I present the case that cerebro-cerebellar connectivity is an important component of a distributed, brain wide network that underpins adaptive behaviour. I have layed out the main characteristics of the homogenous cerebellar circuit organisation to form predictive models to enable successful task performance.

In this thesis I consider two main research questions. The first question will identify a computational role of cerebro-cerebellar interactions during learning across task domains. As evidenced above, most of our current understanding of how the cerebellum can drive cerebral dynamics comes from studying well trained subjects. However, extrapolating from the role of cerebellum in motor learning and research from human studies in associative learning indicates that there is a critical window during learning in which the cerebellum might be important for controlling and adjusting cerebral dynamics. This will be the focus of the first chapter and will be done via computational modelling using deep learning models. The power of using these types of models is that they can be easily trained on a range of complex tasks and therefore the computation executed by the model can be tested in a range of different settings. In order to understand cerebro-cerebellar circuits this seems key as most models of the cerebellum consider a single purely sensorimotor behaviour. Through a series of simulations I explore different task conditions where the advantages of having a simulated cerebellar module become integrated with cerebral cortical operation.

The second question centres around the role of the cerebellar output nuclei in well-defined cognitive behaviours. The feedforward architecture of the cerebellum seems well suited for information processing at the millisecond timescale, however it remains unclear if the cerebellum has useful contributions to longer time scales that are relevant for goal-directed and higher order behaviours. Therefore in the second results chapter the behavioural contribution of the cerebellar output nuclei and cerebello-thalamo cerebral pathway during interval timing is explored. In order to probe the role of the cerebellum during this cognitive-demanding task I will use chemogenetic techniques to reversibly manipulate cerebellar output in animals that have been trained to estimate the duration of a supra-second interval.

Chapter 2

Cerebro-cerebellar networks facilitate learning through feedback coupling

2.1 Introduction

Learning is key to adaptive intelligent behaviour as it allows the individual to adjust to a changing environment (Lee, 2020). According to this view the brain adapts, over time, to the environment by acquiring an improved model of the world via changes in neuronal substrates (Dussutour, 2021). Neuronal substrates should thus learn to capture the causal dynamics and structure in the environment (i.e. external feedback) that will ultimately result in the desired output behaviour (Adams, 1968). However, external feedback from the environment is inherently delayed and incomplete, thereby reducing the effectiveness by which the brain can extract information to build meaningful representations. This has implications for the rate and extent of learning in the neuronal circuits that underlie adaptive behaviour (Herzog et al., 1997). Together, these observations suggest that the brain may implement a general mechanism to facilitate learning when external feedback is not readily available.

The cerebellum interacts with the cerebral cortex while an animal learns to adapt to its environment. The cerebellum is specialised in building internal models that predicts the sensory consequences of actions (Wolpert et al., 1998; Wolpert et al., 2000, section 1.2.2). The output of such internal models enable cerebral areas such as the motor cortex to implement motor commands accurately using internal feedback instead of relying on feedback from the real object (Manto, 2009). In line with this proposal are a wide range of experimental observations in primates and rodents for which cerebellar dysfunction is known to lead to deficiencies in motor learning (Sanes et al., 1990; Gerlai et al., 1996; Dash et al., 2014; Criscimagna-Hemminger et al., 2010). The functional contribution of the cerebellum during learning is not restricted to the sensorimotor domain as cerebellar dysfunction has also been associated with impaired language processing, cognitive associative learning and working memory (Fiez et al., 1992; Rahmati et al., 2014; Guell et al., 2015; Locke et al., 2018). Similarly, it is thought that dysmetria, one of the cardinal symptoms of cerebellar deficit, is caused by an impairment in the ability to form such internal predictive models. In the classical motor domain dysmetria is defined as the lack of coordination and fine control during voluntary movements due to cerebellar damage and is observed in patients are unable to perform accurate motor movement. (Sanes et al., 1990; Hore et al., 1991). In one clinical test for motor dysmetria, subjects are asked to point from their nose to a target in a straight line. Cerebellar patients however fail to perform this goal-directed behaviour in a smooth manner and exhibit undershooting and overshooting of the target trajectory. Recently, dysmetria has been extended to cognitive behaviours, in which cerebellar patients are thought to exhibit inappropriate responses in the non-motor domain. One of the experiments that has provided evidence for this "dysmetria of thought" proposal studied deficits in language processing in cerebellar patients and controls (Guell et al., 2015). However, despite growing experimental evidence that the cerebellum is important for both motor and non-motor learning, little computational work has postulated constraints on how the cerebral cortex uses information from this key subcortical structure during learning of adaptive behaviour.

Like humans, machine learning (ML) models make mistakes during learning and need a feedback loop to confirm or invalidate their decisions. Feedback loops allow

ML models to know what they did right or wrong, giving them data that enables them to adjust their parameters to perform better in the future. One field of ML that has excelled at modelling learning is that of deep learning. In deep learning intelligent models are built from a learning algorithm implementing feedback loops that enable feature extraction. The most efficient learning algorithm in deep learning is backpropagation. The backpropagation algorithm consists of feedback loops, where input data is used to learn by changing connection weights through error feedback from comparing the model output with the desired target behaviour. Classically, backpropagation recursively calculates the required change in the network connections with respect to a predefined learning goal (see section 1.3.2 for BPTT, the temporal variant of backpropagation). However there exist new models in deep learning that do not rely on precise derivation of learning signals via backpropagation, but that use a combination of backpropagated feedback signals and internally generated learning signals (Werfel et al., 2003; Jaderberg et al., 2017; Czarnecki et al., 2017). These internally generated feedback signals are generated by one network and are used to adjust another neural network.

In general, artificial neural network models can be analyzed and experimentally manipulated analogous to studies of brain function using interventionist approaches. Moreover, the model provides the ability to run tests across many different conditions, which is not possible in experimental neuroscience. One way is to perform synthetic or *in silico* neurophysiology and use standard analysis tools for neural dynamics such as Principal Component Analysis (PCA) (Mante et al., 2013; Goudar et al., 2018), or study model behaviour while certain parts of the network model are made dysfunctional. In addition, using ANNs to understand brain function and study brain circuits can be highly valuable as they have the potential to reduce animal usage (Lewis, 2019). Though animals models are invaluable and necessary, computational models provide ideal substrates for initial hypothesis testing which can aid to disambiguate between different possibilities regarding behaviour and neural dynamics (Sejnowski et al., 1988).

In this chapter I build on recent advancements in deep learning and use model validation techniques to introduce a computational model of cerebro-cerebellar networks. More specifically, given the capacity of the cerebellum to build internal models (see section 1.2.2), in this study the cerebellum is hypothesized to predict future cerebral feedback signals given current cerebral activity. This feedback predicted by the cerebellum is then sent back to the cerebral network to drive learning. A given cerebral area is modelled as a recurrent neural network (Mante et al., 2013; Song et al., 2016; Rajan et al., 2016; Laje et al., 2013, see section 1.3.2) which receives feedback predictions from a feedforward, cerebellar, network. As a first step towards model validation, the model is tested on a simple sensorimotor task inspired by drawing and reaching tasks often used to study cerebellar function in animals and humans. The role of the cerebellar predictions is studied by probing learning and behaviour of the model with and without the cerebellar component. Additionally, by recording the cerebro-cerebellar activity during learning and examining the contributions of cerebellar output and the inferior olive, predictions for future experiments are proposed. Together, this work postulates constraints on how the cerebellum communicates with the cerebral cortex during learning.

2.2 Material and Methods

2.2.1 Model architecture

Cerebro-cerebellar circuits were modelled using artificial neural networks. The artificial neural network model used in this study was characterized by a network architecture that deviates from the following standard implementation. In standard deep learning models (Fig. 2.1a), the input x, or feedforward information, is propagated through the different processing stages of the network. These processing stages, h, could be different network layers, in the case of a feedforward network, or processing of different time steps in a sequence when considering a recurrent neural network. Once this forward sweep of the inputs has been completed, the network's predictions are compared to a target y to achieve the following learning goal L. This in turn generates error signals, or feedback signals, that are backpropagated through the network. In this classical scheme of information flow in neural networks, which is viewed as the cerebral centric scheme (see section 2.2.1.1 for details), the different stages of processing are dependent on each other: feedforward information needs to be propagated through the whole network before error feedback can be used to update the connectivity weights and guide learning.

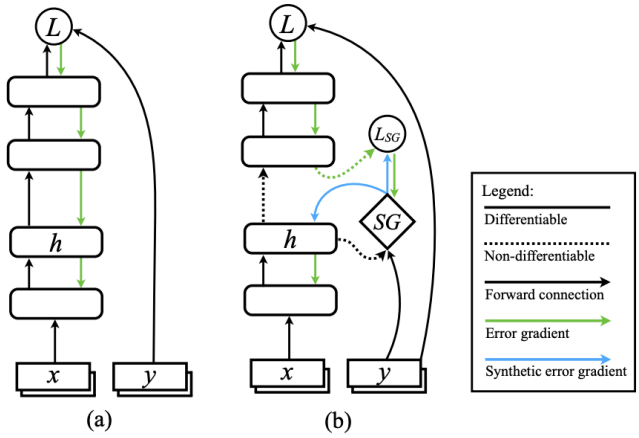

Figure 2.1: **Feedback decoupling as a solution to the complete feedback dependency in artificial, feedforward, neural networks.** (a) Visualisation of a regular deep learning architecture, which is locked both in the feedforward (black arrows) and feedback phase (green arrows). (b) Solution to the locking problem based on predicted gradients. Adapted from Czarnecki et al., 2017. L = Loss or difference between actual output and predicted output from the network. LSG = difference between predicted feedback and true feedback; x = input; y = correct output label given x. Image reproduced from Jaderberg et al., 2017.

More specifically, the model implementation used in this study was based on decoupled neural interfaces (DNIs), a neural network in which the feedforward and feedback information flow is decoupled (Fig. 2.1b, Jaderberg et al., 2017). In DNI this dependency was broken by introducing a loop between two separate networks,

where one network SG (synthetic gradient, see section 2.2.2 for further detail) effectively learns, via a separate learning goal L_{SG}, a model of the different processing stages of the main network. The main network then integrates these internal feedback signals. Here, such a two-learner system was mapped on cerebro-cerebellar networks, a closed loop system existing of two distinct functional and anatomical brain regions: a cerebral network and a cerebellar network. The model of cerebro-cerebellar interactions comprised of two network modules, each characterized by a distinct architecture, a recurrent network as the main network and a feedforward network as the SG network.

2.2.1.1 Cerebral network

The main network was considered to be the cerebral network which existed of a cerebral area A modelled as a recurrent neural network (RNN) in which all units N were recurrently connected via parameters θ (Fig. 2.2). The RNN units were modeled as long short-term memory units (LSTM units; Hochreiter et al., 1997), a type of units that contain internal mechanisms, called gates, which regulate the amount of information that can be stored in the network. LSTMs have been mapped onto the cerebral microcircuitry, with the function of the gates being mapped onto inhibitory neurons (Costa et al., 2017). For computational efficiency, the activity states of these LSTM units, a_t, were encoded in a time-discrete manner (Song et al., 2016). However, approximate timescales of the RNN were derived using the approach by Song et al., 2017. In brief, each timestep in the time-discrete model was considered to be 100 ms in continuous-time dynamics, derived from previous studies (Song et al., 2017; Yang et al., 2019 and see Boven et al., 2022 for more details).

The cerebral RNN (cRNN) was trained to perform experimenter-designed tasks (Fig. 2.2). Each task existed of two temporally varying sequences of length T: a sensory input sequence, x_T, and a target output sequence, o_T. The model was trained to generate o_T by sequentially processing input at every timestep, x_t. In order to train the cRNN, the LSTM activities, a_t, were sent through a linear readout generating the model output, $\hat{o}_t$, that is compared to the target output to generate external feedback. In order to model a more realistic setting of task feedback, a temporally sparse external feedback sequence was derived from the target sequence. This means that the generated model output was only corrected when external feedback was available. Unless stated otherwise, external feedback was available at every other timestep. The interval between available feedback is referred to as the *external feedback interval*. A supervised error module E^{task}, which is the same as L in Fig. 2.1, was then used to calculate the mismatch between the model output and the desired output to generate true sensory feedback. This also known as the prediction error $E^{task} = \mathcal{E}(o_t, \hat{o}_t)$, where $\mathcal{E}$ is the learning goal or objective function. The error with respect to the sparse external feedback was reported as *error*. This error was in turn integrated back in the cRNN via error-derived feedback signals fb_t, here referred to as *cerebral feedback*. These were modelled as error gradients $\text{fb}_t = \dfrac{\mathrm{d}E}{\mathrm{d}a_t}$, for each timestep t, using standard gradient descent methods with backpropagation

through time (BPTT; see section 2.2.2, Werbos, 1990). In addition, a *dysmetria score* was derived by considering the total error with the output at every timestep at the end of training, whether available during training or not. This quantifies the "smoothness" of the model output, quantified as the straightness of the line between two available targets.

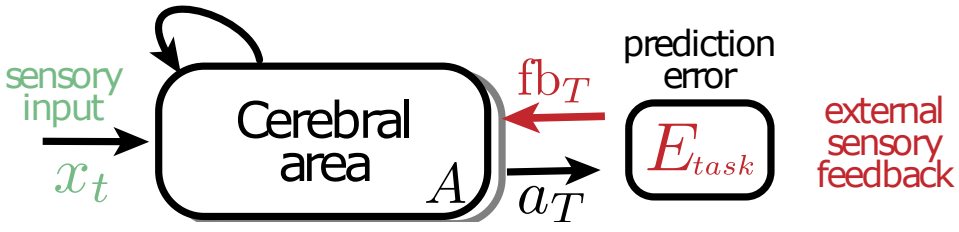

Figure 2.2: **Cerebral RNN.** Schematic representation of the cerebral module. A cerebral area modelled as RNN (cRNN) learns input dependent, x_t, activity representations a_T from external sensory feedback using a supervised prediction error module E^{task} to generate feedback signals fb_T. The black and red arrows represent the forward and feedback pathway respectively. Image adapted from (Boven et al., 2022).

2.2.1.2 Cerebellar network

The cerebellar module C, which is the SG network in Fig. 2.1, was modelled as a feedforward network with independent parameters Ψ. The cerebellar module was bidirectionally connected to the cerebral module in order to form the cerebro-cerebellar RNN model (ccRNN; Fig. 2.3 and Fig. 2.4). The ccRNN thus consisted of a cerebral network with N number of cerebral neurons and M number of cerebellar units. The ratio of cerebral to cerebellar units was $\frac{M}{N} \sim 4$. At every timestep, the cerebellar module received a copy of the cerebral units activity a_t and sent back a prediction of the future cerebral feedback with respect to that activity, $C(a_t) \approx fb_t$. The functionality of the predicted cerebral feedback, or *cerebellar feedback*, could be understood when considering the learning algorithm of the cerebral network.

2.2.2 Cerebral learning using backpropagation through time

The parameters θ of the cerebral network were learnt using feedback signals, classically refferred to as gradients, generated by backpropagation through time (BPTT, see section 1.3.2) in order to minimize the prediction error which is generated when task feedback is available, E^{task}. In brief, BPTT computes the temporal feedback error signal as the change in prediction error, E^{task}, with respect to the parameters, θ, via the sequence of model activities, a_T (see eq. 2.1). In order to update the network parameters across the whole sequence, feedback from the prediction error with respect to the cerebral activity at each point in time a_t is generated backward in time and is referred to as cerebral feedback fb_t.

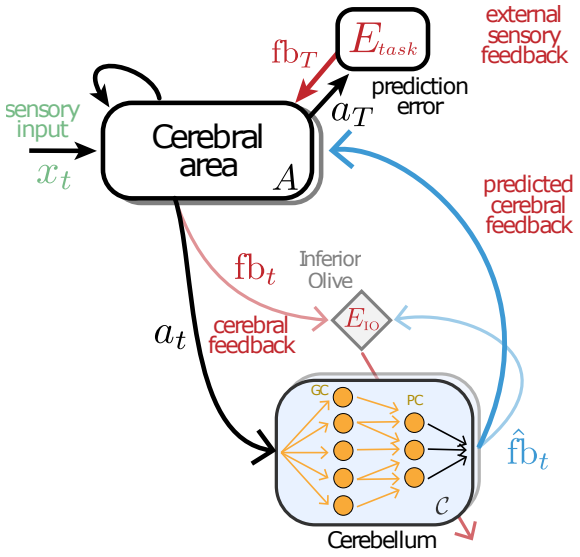

Figure 2.3: **Schematic representation of the cerebro-cerebellar model.** A cerebellar feedforward network is connected to the cerebral module presented in Fig. 2.2. The cerebellum continuously predicts the feedback expected by the cerebral network $\hat{fb}_t$ (blue) given current cerebral activity a_t (black). The cerebellar network, consisting of granule cells (GC) and Purkinje cells (PC) (see section 2.4.1 for interpretation), learns through prediction errors (bottom red arrow) computed at the inferior olive (diamond) by comparing predicted cerebral feedback $\hat{fb}_t$ with actual cerebral feedback fb_t (light blue). Image adapted from (Boven et al., 2022).

$$\sum_{t'=t}^{T} \frac{\partial E_{t'}}{\partial \theta} = \left(\sum_{t'=t}^{T} \frac{\partial E_{t'}}{\partial \mathbf{a}_t} \right) \frac{\partial \mathbf{a}_t}{\partial \theta} = \mathbf{fb}_{t'} \frac{\partial \mathbf{a}_t}{\partial \theta} \tag{2.1}$$

Here a more realistic setting was implemented such that temporal information can only be integrated over a limited horizon K, which is known as truncated backpropagation through time (tBPTT). This constraint reduced the temporal dependency that can be learned. Here, this limited horizon K was referred to as the *cerebral feedback horizon* and was postulated to be analogous to the idea that intrinsic timescales of cerebral areas restrict the time horizon across which task-relevant signals, such as feedback errors, can be integrated (see section 1.3.2; Spitmaan et al., 2020).

However, from a behavioural perspective, to allow smooth state transitions for example, it seemed reasonable that the feedback error signals beyond the K horizon were available to the cerebral network. In this work it was postulated that the cerebellar module provides predictions of future feedback errors. In particular, in ccRNN, the cerebellum is tasked with predicting future feedback giving the current state of the cerebral RNN (Eq. 2.2.2, Fig. 2.4), thereby providing feedback estimates to the RNN that go beyond the K-horizon. This effectively increased the amount of task-specific information available to the cerebral RNN. The final feedback error used by the RNN then forms a combination of cerebral (red) and cerebellar feedback (blue) as shown in eq. 2.2.

$$
\begin{aligned}
\sum_{t'=t}^{T} \frac{\partial E_{t'}}{\partial \theta} &= \left(\sum_{t'=t}^{K} \frac{\partial E_{t'}}{\partial \mathbf{a}_t} \right) \frac{\partial \mathbf{a}_t}{\partial \theta} + \left(\sum_{t'=K+1}^{T} \frac{\partial E_{t'}}{\partial \mathbf{a}_K} \right) \frac{\partial \mathbf{a}_K}{\partial \theta} \\
\sum_{t'=t}^{T} \frac{\partial E_{t'}}{\partial \theta} &\approx \left(\mathbf{fb}_{t'} + \hat{\mathbf{fb}}_{t'>K} \frac{\partial \mathbf{a}_K}{\partial \mathbf{a}_t} \right) \frac{\partial \mathbf{a}_t}{\partial \theta} \\
\Delta\theta &\approx \left(\underbrace{\mathbf{fb}_t}_{\text{cerebral feedback}} + \underbrace{C(\mathbf{a}_K)}_{\text{cerebellar feedback}} \frac{\partial \mathbf{a}_K}{\partial \mathbf{a}_t} \right) \frac{\partial \mathbf{a}_t}{\partial \theta}
\end{aligned}
\tag{2.2}
$$

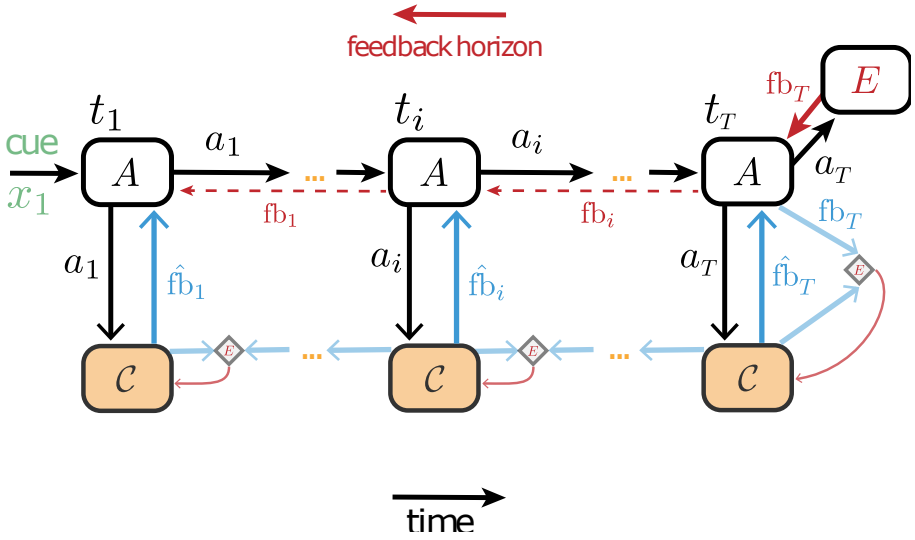

Figure 2.4: **ccRNN unfolded in time.** Example of cerebro-cerebellar model unfolded in time in which the cerebral network learns to associate a cue given at t_1 (x_1, green) with feedback received at the end of the task, t_T (for example see Fig. 2.6). At the end of the task the cerebral network A receives external sensory feedback fb_T (red), which is transmitted to the cerebellar network as cerebral feedback fb_T (light blue). Here the case of cerebral feedback horizon stopping at the end of the task T is highlighted, but feedback may also be available earlier in the task (dashed red arrows). The cerebellum generates cerebral feedback predictions $\hat{fb}_T$ (blue) given cerebral activity a_T (black), and learns using inferior olive (diamond) error signals (red arrow). Before t_T cerebral feedback may not be readily available, thus the cerebellum learns through self-predictions. In this case the inferior olive (diamond) compares old cerebellar predictions (e.g. $\hat{fb}_i$) with the new one (e.g. $\hat{fb}_T$) to generate cerebellar learning signals (red arrow; see main text for details). Image and legend reproduced from (Boven et al., 2022).

2.2.3 Cerebellar learning

The cerebellar network learned, by updating its parameters ψ, to provide effective predictions of cerebral feedback by comparing its predictions to the target cerebral

feedback signals, which is analogous to the function of the inferior olive: $E_t^{\text{IO}} = ||C(a_t) - \frac{\bar{\partial E}}{\partial a_t}||$.

Since the true cerebral feedback signals were only provided within the cerebral feedback horizon, the time window across which the cerebellar module can learn to predict feedback will be limited as well. In order to effectively extend the temporal horizon of predicted cerebral feedback beyond the cerebral feedback horizon, the true feedback signals within the imposed truncation were combined with bootstrapped future cerebellar predictions (see red arrow in Fig. 2.4). This was originally proposed by (Jaderberg et al., 2017). Formally, using the same notation as equation 2.2, the trained target for $C(a_T)$ then becomes:

$$\frac{\bar{\partial E}}{\partial a_T} = \frac{\partial E_{\leq 2T}}{\partial a_T} + C(a_{2T})\frac{\partial a_{2T}}{\partial a_T} \tag{2.3}$$

2.3 Experimental details

In general, hyperparameters such as learning rate and batch size were decided by the experimenter by doing test runs and all neural network models were implemented using the PyTorch library (Stevens et al., 2020). In particular, the DNI implementation is based on code available at `https://github.com/koz4k/dni-pytorch`. The code used for the experiments is available at `https://github.com/neuralml/ccDNI`.

Before training, the network model was initialized using random initialization. Specifically, for the cerebral network the parameters θ were drawn from a uniform distribution defined by the number of units in the cerebral network: $\mathcal{U}(\frac{1}{\sqrt{N}}, \frac{1}{\sqrt{N}})$. The weights of the readout network and the feedforward weights of the cerebellar network (other than the final layer) were initialised according to $\mathcal{U}(-b_k, b_k)$ where b_k denotes the "kaiming bound" as computed in He et al., 2015 (slope $a = \sqrt{5}$), and the biases are draw from $\mathcal{U}(\frac{1}{\sqrt{n_{\text{inp}}}}, \frac{1}{\sqrt{n_{\text{inp}}}})$, where n_{inp} denotes the input size of the layer. During training the cerebellar predicted gradient was scaled (eq. 2.2) by 0.1 (Jaderberg et al., 2017), to avoid instability. Both cerebral and cerebellar parameters were optimised using ADAM (Kingma et al., 2014).

Training the model involved iterating many times (training sessions/epochs) over a given dataset, split into batches. In theory when using tBPTT, the model parameters could be updated at each truncation. However, since training involved temporally sparse task feedback, some truncations rely solely on cerebellar predictions, optimising each truncation would lead to more weight updates and faster ADAM optimisation. In order to compare a model with, ccRNN, and without, cRNN, cerebellar component directly, updates from the feedback signals were accumuulated and applied at the end of each batch.

Unless stated otherwise, during learning, tBPTT was implemented by dividing a given input sequence of T timesteps $x_1, x_2, \ldots, x_T$ into 10 truncations of size 1.

2.3.1 Varying cerebral feedback horizon

The effect of the interaction between predicted cerebellar feedback and the cerebral feedback horizon was studied by varying K. Depending on the length of the sequence, T, and the value of K, the sequence was divided following $T = mT + r$ for positive integers m, r with $0 \leq r < K$, with any remainder going to the last truncation. In other words, the sequence is now made up truncations of $(x_1, \ldots, x_K)$, $\ldots, (x_{(m-1)K+1}, \ldots, x_{mK})$, $(x_{T-r}, \ldots, x_N)$.

2.3.2 Varying external feedback

The effect of the interaction between predicted cerebellar feedback and availability of temporally sparse external feedback was studied by varying the task feedback interval. Thus given an external feedback interval n, the target was only available every n timesteps.

2.3.3 Cerebellar output and cerebellar learning ablation

Ablation studies were performed by removing the output of the cerebellar module or the learning signals used by the cerebellum from the model graph.

2.3.4 Delta/normalised error

The delta/normalised error with respect to a given model was calculated by the difference/ratio of total errors during learning (all epochs). For example, the normalised error of ccRNN with respect to cRNN was $\frac{\text{error(ccRNN)}}{\text{error(cRNN)}}$. In the case of ablation experiments, the comparison is made against an unaffected ccRNN and only consider the respective errors post-ablation. e.g. the normalised error for a model with cerebellar ablation at epoch 50 is $\frac{\text{error(ablated)}_{>50}}{\text{error(ccRNN)}_{>50}}$.

2.3.5 Computing details

All experiments were conducted on the BluePebble super computer at the university of Bristol; on CPUs (Intel(R) Xeon(R) Silver 4112 CPU @ 2.60GHz).

2.3.6 Line drawing task

The line drawing task was simulated in 10 timesteps with seven distinct discrete sensory inputs and seven position-dependent targets expressed as 2D coordinates. More specifcally, the sensory input was designed as a vector of length 10, where

the discrete cue occurred at the first time step. The input at the first timestep thus corresponded with $\in \{\pm 1, \pm 2, \pm 3\}$ activity level setting and the input at the remaining nine time steps was zero. The position-dependent outputs were defined as six lines specified by an x and y coordinate. These coordinates were generated as a linearly spaced vector of length 10 using a circle with radius 10 where the end point of the six lines lie equidistantly from each other. The x and y coordinates of the 7th target were vectors of 0. The latter considered the case in which the network had to remain quite, equivalent to a monkey remaining at the centre of a drawing screen (Fig. 2.6). These position-dependent output vectors were used to generate the external sensory feedback vector based on sparsity. The model is trained to minimise the mean squared error (MSE) between its output and the cue-based external feedback.

The cerebral network consisted of one layer of 50 LSTM units and the cerebellar network contained one hidden layer of 400 neurons. The initial learning rate was set to 0.001. Each training session contained 20 batches of 50 randomised examples. Unless stated otherwise, a truncation size of $T = 1$ which covers 10% of the total task duration. Model results were obtained for 10 random seeds where each seed determines the initial weights of the network.

2.3.7 Line drawing task with a simple actuator

The line drawing task was also modelled using a simplified model of an actuator that is responsible for the motion of drawing. The line drawing task was simulated as before with 10 timesteps, discrete inputs and seven position-dependent targets. The simplified actuator was implemented as a point-mass with inertia $m = 0.1$ kg that obeys the laws of motion. In this setting, the network generated a muscle-like output with an x- and y- actuator modelled as a pair of orthogonal forces (F^x, F^y). From there the position-dependent information in terms of x and y coordinates was derived using Newton's second law of motion (acceleration=force/mass) to calculate the task error at timestep t is $E = ||(x_t, y_t) - (\hat{x}_t, \hat{y}_t)||_2$ where $(\hat{x}_t, \hat{y}_t)$ is the position-dependent target. Thus, the network was trained to translate the discrete external input to an associated temporal trajectory of the point mass object. To predict the forces (F_t^x, F_t^y) the RNN also received as input the prior coordinates (x_{t-1}, y_{t-1}) and speed (v_{t-1}^x, v_{t-1}^y) of the object. The initial coordinate x_0 and velocity v_0^x are both set to zero. The motion dynamics was discretised into time windows of length $\Delta t = 0.1s$. To obtain the cerebral feedback signal of the task error with respect to the model-applied force, i.e. $\frac{\partial E_t}{\partial F_t^x}$, backpropagation occurred through the motion dynamics above but was limited to the current timestep.

The cerebral network consisted of one layer 50 LSTM units and the cerebellar network contained one layer of 400 neurons. The initial learning rate ws set to 0.0003. Each epoch contained 20 batches of 50 randomised examples. Unless stated otherwise, a truncation size of $T = 1$ which covers 10% of the total task duration. Model results were obtained for 10 random seeds where each seed determines the initial weights of the network.

2.3.8 Cosine similariry

The performance of the cerebellar module in predicting useful feedback was quantified as the cosine similarity - "cossimilarity" - between the predicted feedback and the true, fully backpropogated gradients, where for two arbitrary vectors $\mathbf{x}$ and $\mathbf{y}$

$$\text{cossimilarity}(\mathbf{x}, \mathbf{y}) = \frac{\mathbf{x} \cdot \mathbf{y}}{||\mathbf{x}||_2 ||\mathbf{y}||_2} \tag{2.4}$$

Where $\cdot$ denotes the dot product and $||||_2$ the Euclidean norm.

2.3.9 Quantification of cerebro-cerebellar model representations over learning

2.3.9.1 Cortico-cerebellar coupling

To analyse how the coupling between the network representations in the two model components changed over learning (inspired by Wagner et al., 2019), the Pearson correlation between a given LSTM unit (both cell and output states) and a given unit in the cerebellar hidden (granular) layer over different bins during training was calculated. Values presented in the results were the average over all RNN/cerebellar hidden unit pairs. Subsequent PCA analysis was performed on the matrix containing changes in cerebro-cerebellar pairwise correlation coefficient of 600 active pairs over time.

2.3.9.2 Demixed Principal component Analysis

To study the response dynamics specific to task variables demixed principal component analysis (dPCA) was performed (Kobak et al., 2016). Demixed PCA extracts low-dimensional components that explain maximum population variance constrained by task-specific variables, such as the input stimulus. As a result, principal components that are specific to task variables were obtained. The simulated neural data provided as input to dPCA was a three-dimensional array (n, s, t) with neuronal activity (concatenated across seeds), stimulus identity and time, respectively. In order to compare the cue-specific variance explained for each principal component across models it was normalised against the variance explained for each principal component. In order to quantify how well the cue-specific variance was separated the Euclidean distance between the seven cues of the RNN dynamics corresponding to the two leading dPCA components was computed.

2.3.10 Data Processing

Most analyses of the models were done using custom-written scripts Python (version 3.9), the dPCA analysis was performed in Matlab (2021a) using scripts available at `https://github.com/machenslab/dPCA`.

2.4 Results

2.4.1 A systems-level computational model of cerebro-cerebellar interactions

The proposed systems-level model of cerebro-cerebellar interactions in which the cerebellum learns to adjust the cerebral cortex was based on a recent deep learning algorithm (Jaderberg et al., 2017). The individual network structures followed the dominant anatomical features of each brain region (Fig. 2.3a). A cerebral area A was characterized by recurrent connections and was modelled as a recurrent neural network (RNN) (Mante et al., 2013; Song et al., 2016; Rajan et al., 2016; Laje et al., 2013). The cerebellum consistted of a dominant feedforward connectivity and was thus modeled as a simple feedforward network, with the input and output layer mirroring the Granule Cell (GC) and Purkinje cell (PC) layers respectively (Marr, 1969; Albus, 1973; Raymond et al., 2018). To capture the dimensionality expansion observed between cerebral and cerebellar networks the model was constraint with $M \gg N$, where M corresponds to the number of GCs, N the number of cerebral neurons and use the same ratio found experimentally $\frac{M}{N} \sim 4$ (Herculano-Houzel, 2009; Diedrichsen et al., 2019).

The behavioural tasks used to train the model were inspired by behavioural tasks found in humans and animals that learn to associate an input with a desired goal behaviour. In order to acquire task specific representation that underlie good task performance, the cerebral RNN relied on external sensory feedback (red top right arrow in Fig. 2.3) to generate its own feedback error signals, here called cerebral feedback (see section 2.2.1.1). In line with experimental evidence indicating that only limited amount of information can be stored in the population code of cerebral areas (Spitmaan et al., 2020), the timescale over which the model can learn input-output dependencies was limited. This is referred to as the cerebral feedback horizon with length T. Thus, given a sequential sensory input, x_{t-T} the RNN will generate an output, a_T, that is compared to task-specific external feedback fb_T. This task-specific external feedback could in theory also be interpreted as sensory input and is therefore referred to as sensory feedback. The difference between the output predicted by the RNN and the external feedback was calculated via a prediction error module E^{task}, this in turn leads to feedback error signals (or prediction error signals) of length T that were used by the cerebral area for learning.

In contrast to the RNN that learned with a temporal dependency of length T, the cerebellar module C continuously learned to predict cerebral feedback fb_t given cerebral activity a_t (Fig. 2.3). The cerebellar network itself learned through error signals computed by comparing the actual cerebral feedback fb_t at time t with the cerebellar predicted cerebral feedback $\hat{\text{fb}}_t$. This comparison was performed separately via a separate comparator, thought to be present in the inferior olive, $E_t^{\mathcal{IO}} = (\text{fb}_t - \hat{\text{fb}}_t)^2$, that generates error signals which were used to optimise the cerebellar network (see section 2.2.3). However, since the cerebral feedback is limited by cerebral feedback horizon, the cerebellum learned using its own feedback predictions when cerebral feedback is not available (Fig. 2.4) (Jaderberg et al., 2017). This leads to the fol-

lowing target feedback $\bar{\text{fb}}_t \sim \text{fb}_t + C(a_{t+1})$ where fb_t is the true cerebral feedback and $C(a_{t+1}) = \hat{\text{fb}}_{t+1}$ is a self-prediction term which enabled the cerebellum to learn online (see section 2.2.3). The use of self-predictions, also known as bootstrapping, is generally used in reinforcement learning and in is essential for ccRNN as is enables the cerebellar module to learn to provide effective, future, cerebral feedback predictions.

Together this model of cerebro-cerebellar interactions act as feedback prediction machines, in which continuous prediction about future feedback from cerebellum enable the cerebral network to learn temporal task efficiently by effectively increasing the amount of feedback information available to the RNN. Such functional feedback modules can be applied accros multiple cereberal areas and cerebellar areas (represented as the shaded boxed in Fig. 2.3).

2.4.2 Cerebro-cerebellar model mapped onto internal models

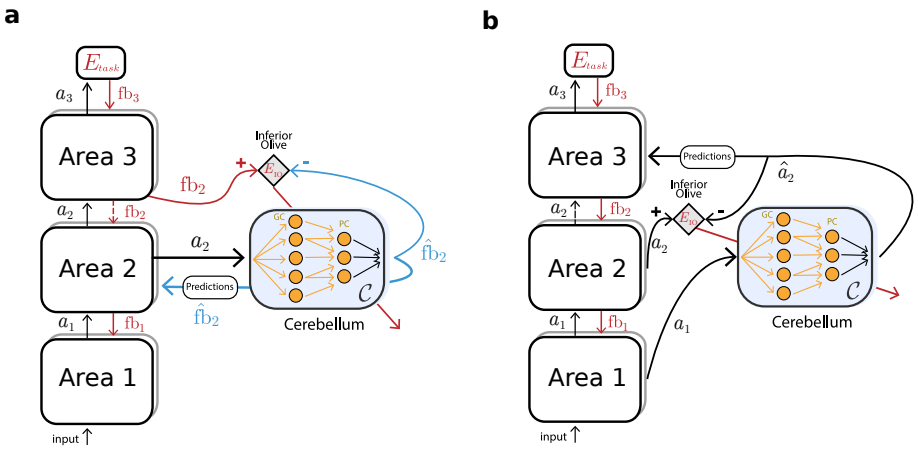

Figure 2.5: **Cerebellum as decoupling machine in feedforward multi-area networks.** (**a**) Illustration of decoupling feedback processing. The cerebellum makes predictions of the feedback expected by brain area 2, decoupling the main network from downstream brain areas (dashed red arrow). (**b**) Case of decoupling feedforward processing. The cerebellum predicts the forward activity expected by brain area 3, thereby approximating (and decoupling) the forward computations between brain area 1 and 3 (dashed black arrow). Note that the cerebellum could, in principle, approximate feedback and feedforward processing across many more brain areas, for example brain area 2 could be expanded in multiple brain areas). Image and legend reproduced from Boven et al., 2022.

The ccRNN shared common features with classical internal models of the cerebellum (Fig. 2.5; see section 1.2.2 and Fig. 1.5 for description of internal models). In order to simplify the comparison with internal models, the cerebro-cerebellar interactions were presented in the feedforward case considering information flow between brain areas (see Fig. 2.1 and section 2.2.1). The cerebro-cerebellar module was compared using the main components of internal models: the controller, which generates the commands, input and output of the internal model (see Table 2.1). In the forward

model case, the controller represents a cerebral area which in the decoupling framework is approximated by an artificial neural network (RNN in the temporal case or feedforward neural network in the spatial case). The input to the cerebellar module was an efference copy of motor command or cerebral activity. The output was the future state, modelled as future feedback in the recurrent case or downstream feedback in the spatial case. This output was directed to the controller. Thus in the forward model case, the cerebellar module learned to predict feedback predictions coming from a distant brain area (area 3), thereby decoupling information flow across brain directed areas. The cerebellar module learned accurate feedback predictions by receiving input from the distinct brain area. This is analogous to the forward internal model in which the cerebellar receives a motor command from the motor cortex (area 2 in Fig. 2.5a) that is sent to lower motor centres (area 3 in Fig. 2.5a). Additionally, it receives sensory feedback from the lower sensorimotor centres that inform the cerebellum on the current state. With these two inputs the forward model in the cerebellum can learn to predict the next state which in turn provides internal feedback to update cerebral activity in the motor cortex.

In theory, the cerebro-cerebellar model presented here could also be used as an inverse model. Again the controller is a certain cerebral area of which the cerebellum learns to approximate the command based on an instructive command regarding the desired directory (from area 1 in Fig. 2.5b) and the actual command (from area 2 in Fig. 2.5b) . The output of the cerebellum is the feedforward command implementing the instruction that gets send downstream to what could be another cerebral area or a controlled object.

In conclusion, comparison of the information flow in feedforward multi-area networks interacting with a cerebellar module to the information flow in internal models indicates that there exist a analogous relationship between internal models and DNIs (Fig. 2.1; Jaderberg et al., 2017). In the rest of the chapter the forward model case, or feedback decoupling, will be studied using recurrent neural networks.

Table 2.1: **Relationship between the internal models of the cerebellum with decoupling machines** (Jaderberg et al., 2017). The properties of the forward model of the cerebellum can be set against those of feedback decoupling (blue); similarly, the properties of the inverse model of the cerebellum can be set against those of forward decoupling (red). The internal models here focus on the classical motor control setting but can be extended to cognition, where for example a "mental model" replaces the "controlled object" (Ito, 2008). Abbreviations: MM, main model; temp., temporal; spat. spatial. Table and legend reproduced from Boven et al., 2022.

	Forward Model	Feedback Decoupling	Inverse Model	Forward Decoupling
controller	cerebral (motor) cortex	main model (MM)	(motor) cortex	main model
input	motor state/command	neural network state	sensory/desired state	(temp.) area state* (spat.) upstream state*
output prediction	future state	(temp.) future gradient (spat.) downstream gradient	motor command	(temp.) future state (spat.) downstream state
output destination	controller	MM: same area	controlled object	(temp.) MM: same area (spat.) MM: downstream area

2.4.3 Cerebro-cerebellar model trained on a line drawing task

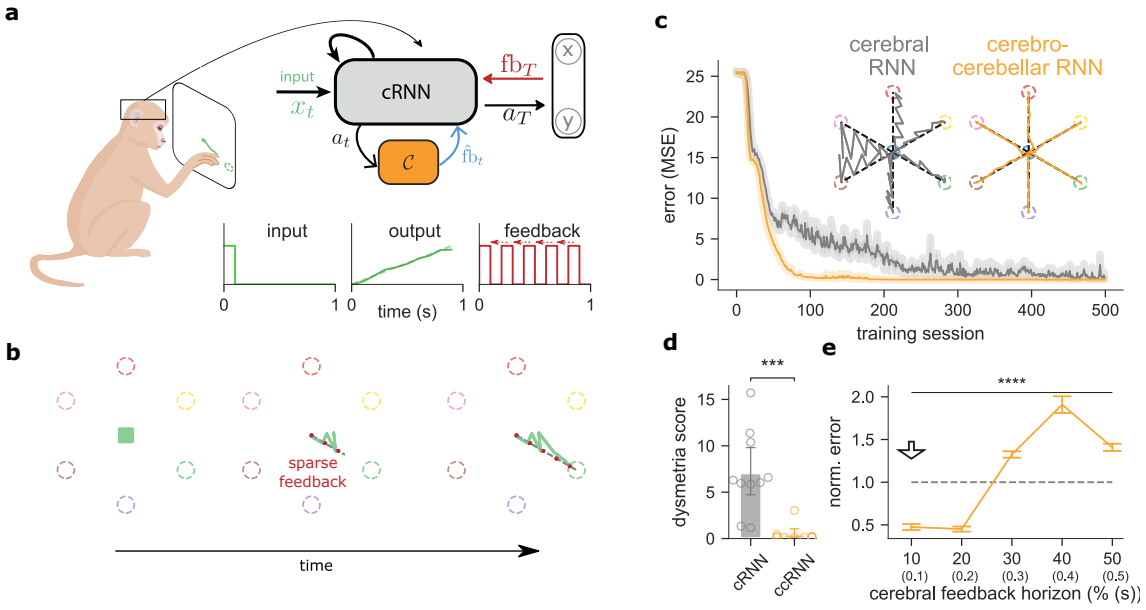

Figure 2.6: **Cerebro-cerebellar model improves learning in a simple line drawing sensorimotor task.** (**a**) Schematic of a macaque monkey performing a simple line drawing task (top left). A cerebro-cerebellar RNN (ccRNN) in the macaques brain receives cue-specific input and learns to produce the desired trajectory (top right). The temporal profile of input, output (dashed gray line represents the target trajectory) and feedback are also shown (bottom right). (**b**) There are 6 possible targets (coloured dashed circles) and feedback (dashed black line) is provided at a regular interval (bottom; see section 2.3.6 for details). In the example shown the model must draw a straight line towards the green target. (**c**) Error between model output and desired target trajectories for cerebellar RNN (gray, cRNN) and cerebro-cerebellar RNN (orange, ccRNN). Insets: Model trajectory produced for all cues after learning. (**d**) Dysmetria score for cRNN and ccRNN. The dysmetria score quantifies how smooth the movement is after learning (see section 2.2.1.1). (**e**) Normalized model mean squared error (MSE) after learning for different cerebral feedback horizons. Feedback horizon is denoted as percentage of the total task sequence. Arrow indicates feedback horizon used by the cerebral network in the other panels. ***: $p < 0.001$, ****: $p < 0.0001$. Error bars represent mean ± SEM across 10 different initial conditions of the model. Figure and legend adapted from Boven et al., 2022.

In order to validate ccRNN as a systems-level computational model of cerebro-cerebellar architecture the model was tested on a task based on classical sensorimotor control and compared to a cRNN model. A line drawing task (Fig. 2.6a, b) was designed inspired by classical sensorimotor studies in the cerebellum, which include line drawing and target reaching tasks (Butcher et al., 2017; Nashef et al., 2019; Sanes et al., 1990; Streng et al., 2018; Tseng et al., 2007). A cerebro-cerebellar RNN (ccRNN) and a cerebral RNN (cRNN) were trained to perform this task. In this task each model was trained to draw a straight line in a two-dimensional space towards one of seven target locations given a target-specific cue provided only at

the start of the task (Fig. 2.6a, b). The models learned to associate 6 input cues with their respective target locations or to remain silent when there was no input cue. During learning the output generated by the cerebral network was compared to external feedback based on the optimal trajectory (Fig. 2.6a). When this feedback is available at time t the global prediction error as $E = (y_t - \hat{y}_t)^2$ was calculated, where y_t and $\hat{y}_t$ denote the desired and current model output. In particular, this external feedback was available at every other time step, which models a more realistic setting in which sensory feedback, such as visual information, is not always readily available. Temporal cerebral feedback signals were derived from this external feedback with a feedback horizon (see section 2.2.2) of 10% of the total duration for this task. This relatively short temporal dependency models biologically relevant conditions due to the short timescales cerebral RNN dynamics involved in these tasks (Spitmaan et al., 2020).

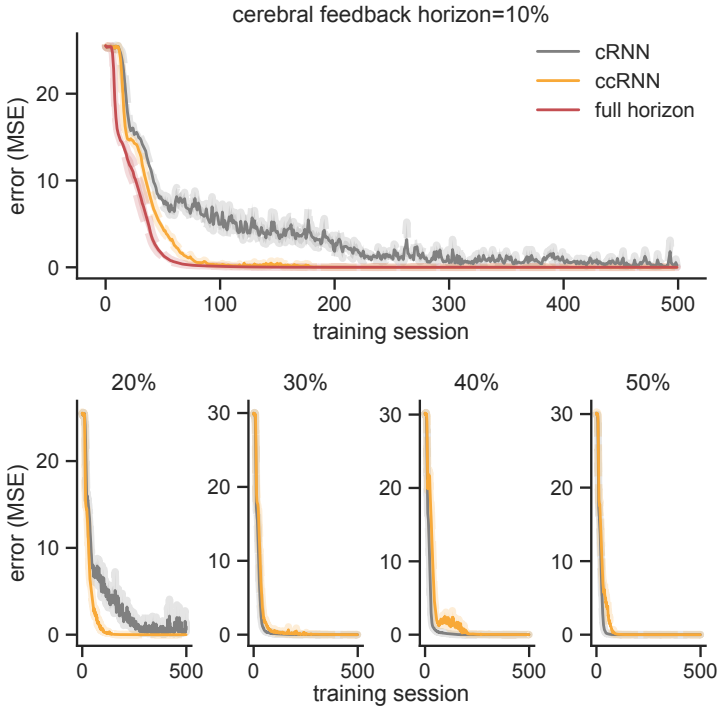

Figure 2.7: **Learning for different cerebral feedback horizons for the line drawing task.** (see Fig. 2.6d for comparison). Feedback horizon is given as percentage of task duration (10 time steps). Results presented in main text (Fig. 2.6b) shown on top row along with RNN trained with full horizon, which is the cerebral feedback horizon = 100%). Figure and legend adapted from Boven et al., 2022.

The ccRNN achieved near-zero error in less training sessions than the cRNN, which learned much more slowly and with higher variability (Fig. 2.6c). In addition, there were differences at the level of model output trajectories. While the ccRNN produced smooth and straight trajectories, the cRNN, which lacks the cerebellar component, generated a more variable trajectory towards all targets (Fig. 2.6c). This suggests that the ccRNN model might also capture one of the defining features of cerebellar deficits, dysmetria (see section 2.1). The degree of dysmetria-like output in both models was measured as the error between the model output and the optimal trajectory, which is a straight line in this case (see section 2.3.6). When

applying this measure, the ccRNN showed a reduced dysmetria-like behaviour than cRNN (Fig. 2.6d). In addition the cRNN model generated trajectories that under and overshoot the target, which is another key observation in cerebellar malfunction (Hore et al., 1991).

Moreover, to study under which conditions the cerebellum may facilitate learning in cerebral networks, different conditions of cerebral feedback horizon were tested. The results showed that the ccRNN model only facilitates learning when the temporal dependencies that the RNN can learn were relatively short ($< 30\%$; Fig. 2.6e and Fig. 2.7). When comparing the ccRNN and cRNN with feedback horizon of 10% to an RNN that was able to learn temporal dependencies across the whole sequence, the ccRNN closely approximated the cRNN with full feedback horizon. This indicates that the cerebellar module of the ccRNN is able to learn truthful estimates of the feedback that is required for the RNN to learn the task (Fig. 2.7).

2.4.4 Comparison with classical cerebellar and cerebral models

In order to demonstrate the benefits of ccRNN for modelling sequential behaviour a comparison to a classical cerebellar and cerebral model was made (Fig. 2.8). For the first a classical Albus-Marr type of model was implemented. This model consisted solely of a feedforward cerebellar network and completely failed to learn the line drawing task (purple line in Fig. 2.8). For the latter, a model in which the cerebrum (RNN) does not change its connectivity pattern was considered, which is equivalent to a reservoir RNN (Tanaka et al., 2019). This model as well performed substantially worse than ccRNN (green line in Fig. 2.8). Since neither of these control models were capable of learning input-output temporal dependencies, the models failed in exhibiting the same learning properties as the ccRNN.

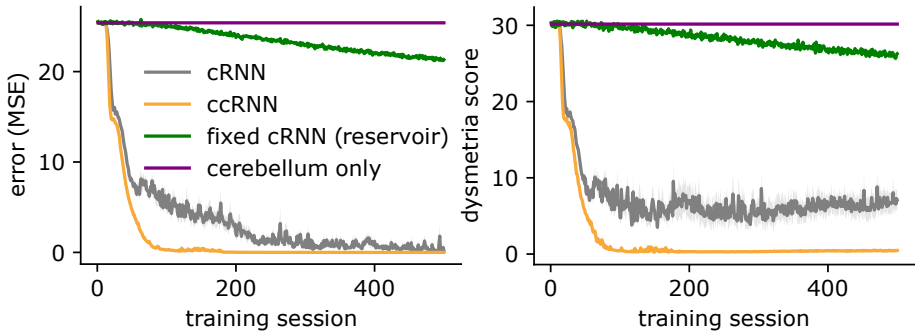

Figure 2.8: **cRNN and ccRNN models compared to a fixed RNN with fixed weights (reservoir RNN) and a model with only the feedforward cerebellar network.** For the lone cerebellar network there is no recurrency in the network at all and must directly translate the current external input to desired output; for the simple line drawing task which requires memory of the initial cue this removes the possibility of any learning at all (optimal case shown). Error bars represent mean ± SEM across 10 different initial conditions. Figure and legend adapted from Boven et al., 2022.

2.4.5 Cerebellar-mediated learning facilitation depends on task feedback interval

Next, a systematic study of the main variables of interest, which are the time points of feedback, and the cerebral feedback horizon was performed. More specifically, the assumptions were that the temporal dependencies that a cerebral area can learn are limited and that sparse feedback is an inherent property of virtually any task. In Fig. 2.6e it was shown that the cerebellar predictions were valuable when the cerebral area can learn relatively short temporal dependencies. Next, it was tested how effective cerebellar prediction depends on the timing external feedback. Therefore both the cRNN and ccRNN models were trained on the line drawing task across a range of external feedback interval (Fig. 2.9a). When external feedback was given at every time time step (Fig. 2.9a-c, short or 10% case), there was little benefit of the cerebellar feedback predictions on the dysmetria score (Fig. 2.9a, b, short or 10% case) and the training error (Fig. 2.9c).

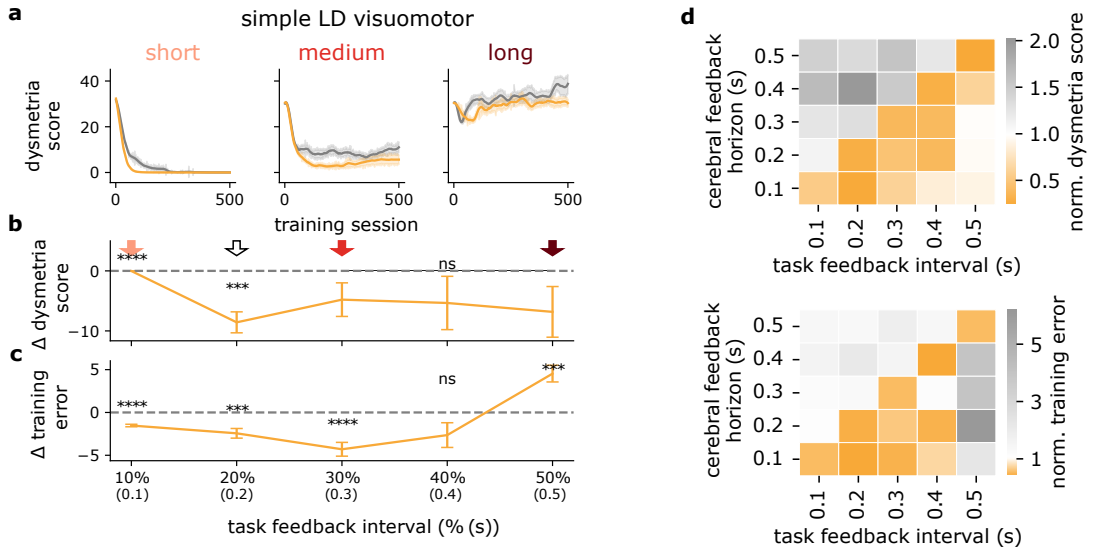

Figure 2.9: **Cerebellar-mediated facilitation of learning depends on task feedback interval.** (**a**) Dysmetria score during learning for short (light red), medium (red) and long (dark red) levels of feedback interval in both models cRNN (gray) and ccRNN (orange).(**b**) Difference in dysmetria score between ccRNN and cRNN for varying degrees of task feedback intervals (not significant, p=0.3176 for simple LD). Degrees of red in arrows indicate the respective interval in (**a**) while the white arrow indicates the feedback interval used in Fig. 2.6. Task feedback interval given as a percentage of the total task time. (**c**) Difference in training error between cRNN and ccRNN for varying degrees of task feedback interval. (**d**) Normalised dysmetria score integrated over learning (top) and training score at end of learning (bottom) of ccRNN with respect to cRNN for varying degrees of cerebral feedback horizons and task feedback intervals for simple LD. **: $p < 0.01$, ***: $p < 0.001$, ****: $p < 0.0001$. Error bars represent mean ± SEM across 10 different initial conditions. Figure and legend adapted from Boven et al., 2022.

In contrast, increasing the interval between the timepoints at which external sensory feedback was delivered resulted in improved dysmetria and training scores for the ccRNN model compared to the cRNN model. However, when the external feedback interval was too long, neither cRNN nor ccRNN were able to learn the task as the external feedback was too sparse. In addition, when considering the interaction between feedback interval and horizon, the ccRNN model particularly improved learning and dysmetria-like outputs for medium-to-hard regimes of feedback interval, provided that the cerebral feedback horizon is not longer than the feedback interval (Fig. 2.9d). Together, these results indicate that cerebro-cerebellar facilitation of learning shown above depends on the ability of the cerebellum to provide the cerebral network with effective feedback predictions and that cerebellar feedback is mostly beneficial points in time in which there is no feedback readily available.

2.4.6 Cerebro-cerebellar feedback alignment

Since the effect of cerebellar feedback predictions on learning depends on how well these align with the optimal task feedback, the cosine similarity between the cerebellar predictions and the optimal cerebral feedback was calculated (see section 2.3.8). First, in order to allow for a more straightforward interpretation of the similarity between the optimal cerebral feedback and cerebellar feedback, the cosine similarity was calculated in a setting of the line drawing task where external sensory feedback was only provided at the end of the sequence. In this end-only feedback case the cosine similarity should decay gradually from the end to beginning. The results indicated that the cerebellar-cerebral feedback similarity is high closer to the point in which external sensory feedback is available, in this case at end of the task (Fig. 2.10a and Fig. 2.6 for comparison), and remains high over learning in particular for later points in the task (Fig. 2.10b).

When calculating the cosine similarity for conditions in which external feedback is available throughout the task the patterns become more complex. In the line drawing task the predictions made during earlier points in the task were more similar than those at later points throughout learning (Fig. 2.10c, d). These results suggest that for tasks with feedback only at the end cerebro-cerebellar feedback alignment should decay rapidly, and for tasks with regular external feedback it predicts that cerebro-cerebellar feedback alignment should be stronger when more external feedback is provided. Overall, these comparisons of similarity between cerebellar predicted feedback and optimal cerebral feedback indicate that the cerebellar module effectively learns a mapping between the cerebral activity and predicted cerebral feedback. This has implications for how the coupling between the cerebellar and cerebral unit representations change throughout learning, which was explored next.

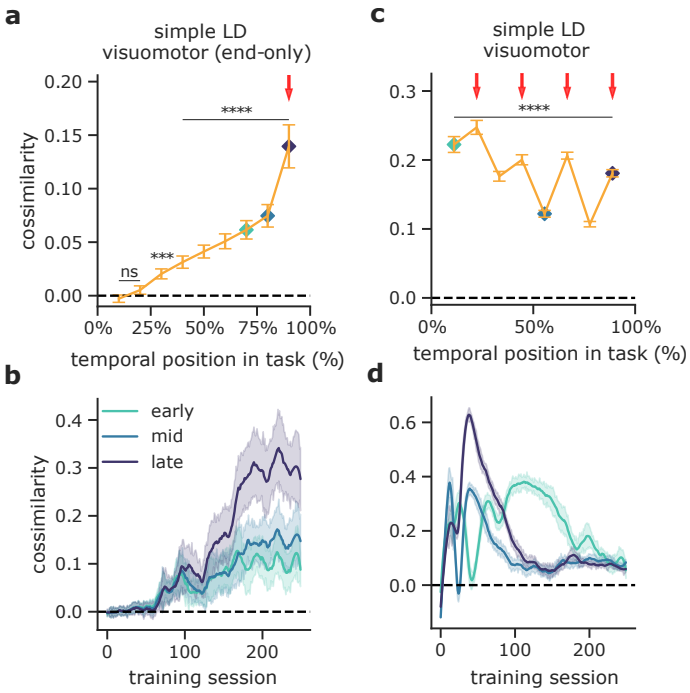

Figure 2.10: **Similarity between cerebellar and cerebral feedback is task and learning dependent.** (**a**) Cerebro-cerebellar cosine similarity throughout tasks sequences which do not require intermediate external feedback: simple line drawing with feedback only at the end of the task (LD end-only) and online visual discrimination (n.s. p=0.212 (0%), p=0.520 (25%)). Here and in subsequent panels red arrows indicate points in which external feedback is available. Cosine similarity throughout the tasks is calculated across all training sessions (see section 2.3.8 for details). (**b**) Cerebro-cerebellar cosine similarity over learning for three time points in the task: early (turquoise), mid (blue) and late (purple) in the task (see (a) for comparison). (**c**) Cerebro-cerebellar cosine similarity throughout the sequence for tasks with intermediate external feedback. (**d**) Cerebro-cerebellar cosine similarity over learning for three different time points in the task (early, mid and late as in (b)). Dashed black line represents zero similarity. **: $p < 0.01$, ***: $p < 0.001$, ****: $p < 0.0001$. Error bars represent mean ± SEM across 10 different initial conditions. Figure and legend adapted from Boven et al., 2022.

2.4.7 Cerebro-cerebellar model representations during learning of line drawing task

To understand how the activities of the cerebro-cerebellar network change over learning, the pairwise correlation between cerebral and cerebellar representations was calculated. A small increase in correlation was observed early in learning, followed by a consistent decrease in correlation (Fig. 2.11a). Next, standard principal component analysis was applied on the correlation matrix to understand more subtle changes in the correlation structure (Fig. 2.11b). The first principal component reflected the changes in the average cerebro-cerebellar coupling (Fig. 2.11b). The second principal component showed a delayed increase with respect to the first, followed by a sustained decrease in the cerebro-cerebellar coupling (see Fig. 2.12 for remaining components). These results were consistent with the idea that early in

learning model performance is more reliant on effective feedback predictions from the cerebellar module than late in learning. These results were confirmed when considering the changes in correlations of cerebro-cerebellar pairs during early, mid and late learning respectively (Figs. 2.11c). Early in learning, there was a higher number of pairs that show an increase in correlations, whereas late in learning only a small number of pairs show increase in correlation. Together these results suggest that early in learning cerebro-cerebellar coupling is highest and the need for the cerebellar module to provide effecitve feedback predictions is the highest.

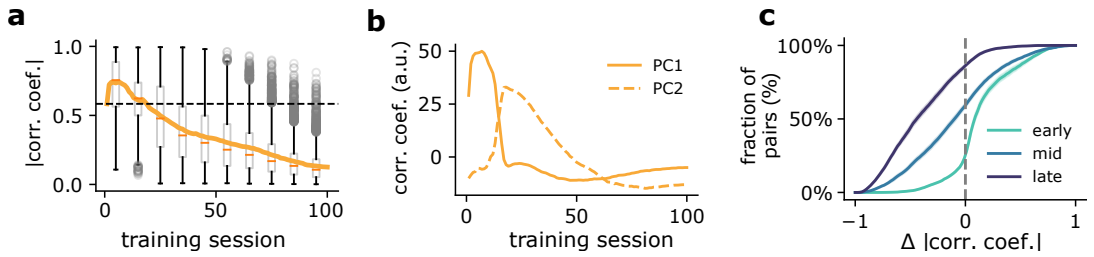

Figure 2.11: **Cerebro-cerebellar neuronal activity coupling over learning.** (**a**) Box plot showing the mean and distribution of pairwise cerebro-cerebellar absolute correlation coefficients over learning. Fully fixed ccRNN, which means without any form of plasticity, is given for reference (dashed line). (**b**) Change in first two principal components of cerebro-cerebellar pairwise correlation coefficients over learning (all components available in Fig. 2.12). (**c**) Cumulative plot of cerebro-cerebellar pairs with positive and negative changes in absolute correlation coefficients in early (session 1), mid (session 25) and late (session 80) learning. Error bars represent mean ± SEM across 10 different initial conditions. Figure and legend adapted from Boven et al., 2022.

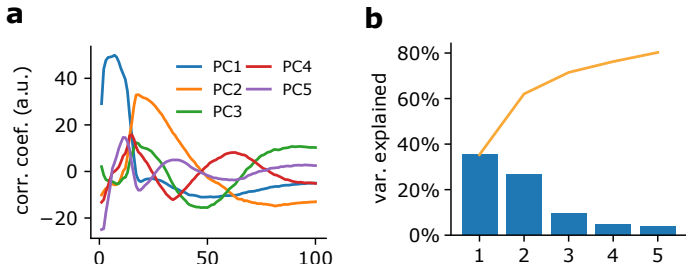

Figure 2.12: **Pairwise correlations over learning.** (**a**) extension of Fig.2.11 for top 5 principal components. (**b**) Variance explained by each component (accumulation in orange). Figure and legend adapted from Boven et al., 2022.

Next, the change in task-specific cerebral and cerebellar representations was quantified in order to gain a deeper understanding on how the cerebellar predictions shapes cerebral processing. This was done using using a dimensionality reduction method (demixed PCA; see section 2.3.9.2) that enables to extract task-related low-dimensional representations from the network activities. In the case of the line drawing task the task-related variables are: cue (or stimulus), time and the interaction between cue and time. Here the cue-specific principal components (PCs) were considered as encoding cue information, which was critical for the line drawing task. First, cue-specific representations in the recurrent neural network activities

were compared between cRNN and ccRNN. This was done by calculating the two-dimensional Euclidean distance across the 7 different possible cues at each timestep which resulted in a measure of how separate the cue-related representations in each model were (see section 2.3.9.2). The ccRNN cerebral network acquired a higher separation of stimulus components over learning than the cRNN (Fig. 2.13a and b).

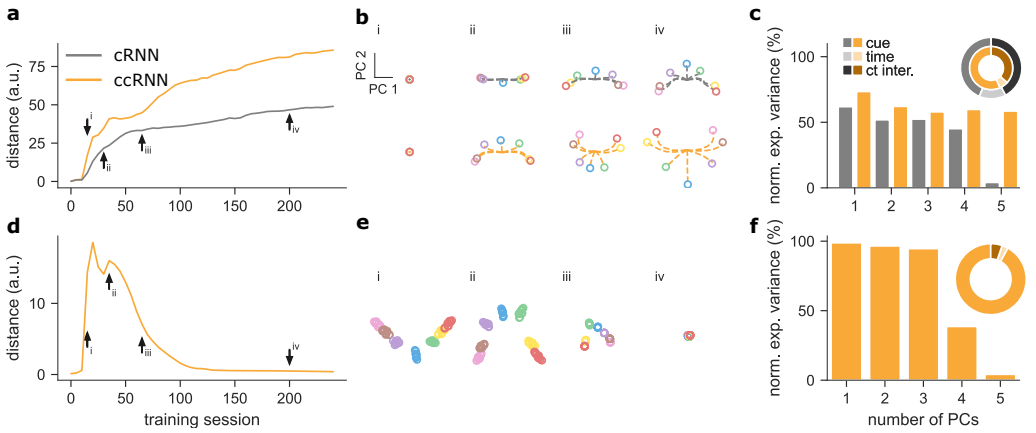

Figure 2.13: **Cerebro-cerebellar model improves learning and task output in a simple line drawing sensorimotor task.** (**a**) Euclidean distance between the cue-specific cerebral RNN dynamics corresponding to the two leading cue-specific principal components. Results are given for both the cRNN (grey) and ccRNN (orange) models. Arrows highlight training sessions of cue-specific demixed principal components (dPCs) plotted in (**b**) for early (i), early-mid (ii), mid (iii) and late (iv) learning, for both cRNN (top) and ccRNN (bottom). Dashed lines represent the trajectory of the 2D neural dynamics throughout the task (circle represents last timestep). (**c**) Normalised cue-specific explained variance of the RNN for both models cRNN (gray) and ccRNN (orange). Circular plot shows the total explained for cue (medium-dark colours), time (light colours) and cue-time interaction (dark colours) task variables. (**d**) Euclidean distance of the cue-specific two-dimensional neural activity for the cerebellar network (orange, ccRNN model). Arrows indicate training sessions highlighted in (**e**) as in (b). In contrast to the cerebral network here there is no task trajectory encoded – multiple circles represent the temporal points during the task. (**f**) Normalised explained variance for cue-specific dPCs of the cerebellar network. Figure and legend adapted from Boven et al., 2022.

To contrast task-specific components with general temporal information, the level of cue-specific and time-specific explained variance, normalized by the total variance for each model were compared across both models. Overall, ccRNN captured more cue-specific explained variance when compared with cRNN (Fig. 2.13c). This was also the case when performing dPCA at the beginning and at the end of learning (Fig. 2.14 for cRNN and Fig. 2.15). At the beginning of learning the overall variance explained by dPCA was the same as for regular PCA (Fig. 2.14a and Fig. 2.15a) and was largely explained by the first PC which was time-specific (Fig. 2.14b, c and Fig. 2.15b, c). At the end of learning, cue-related variance was higher in the ccRNN and the separability between cue-related activity was achieved much earlier in the sequence compared to cRNN (Fig. 2.14g, f and Fig. 2.15g, f). Overall, pairwise correlations between components are all close to zero and most pairs are orthogonal to each other (Fig. 2.14h and Fig. 2.15h)

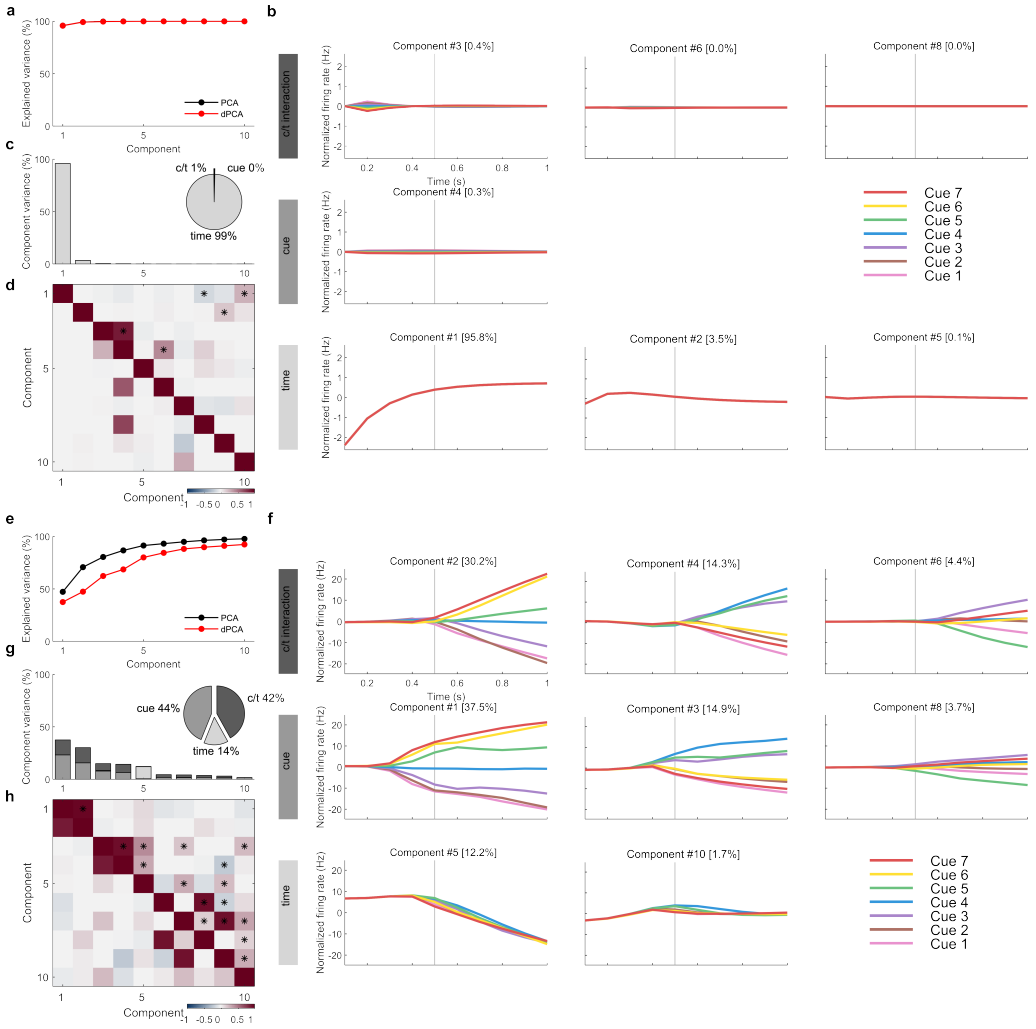

Figure 2.14: **Demixed PCA of cRNN network at the beginning and end of learning.** (see Fig. 2.13a, c). Early and late learning corresponds to training session 1 (top a-d) and 200 (bottom e-h), respectively. (**a, e**) Cumulative variance explained by PCA (black) and dPCA (red) components. (**b, f**) Demixed principal components for cue, time and cue/time interaction task variables. In each subplot there are 7 lines corresponding to the 7 cues (see Fig. 2.6a). (**c, g**) Explained variance for individual demixed principal components. Pie chart shows how the total variance is split between different task variables. (**d, h**) Dot product between all pairs of the first 15 demixed principal components (upper-right triangle) and correlations between all pairs of the first 10 demixed principal components (bottom-left triangle). Stars denote statistical significance ($p < 0.05$). Figure and legend adapted from Boven et al., 2022.

When applying dPCA to the activity of the cerebellar module, the distance between cue-related activity changed over learning with an increase in distance early in learning followed by a decrease (Fig. 2.13d, e). Representations in the cerebellar feedforward network were dominated by task-specific information (Fig. 2.13f). Similarly to the cerebral network, when considering all components for all task variables, the overall variance explained by dPCA was close to normal PCA at the beginning and end of learning (Fig. 2.16a, e) and was explained by the first two PCs which, at the beginning of learning, depend on time but become cue-dependent at the end

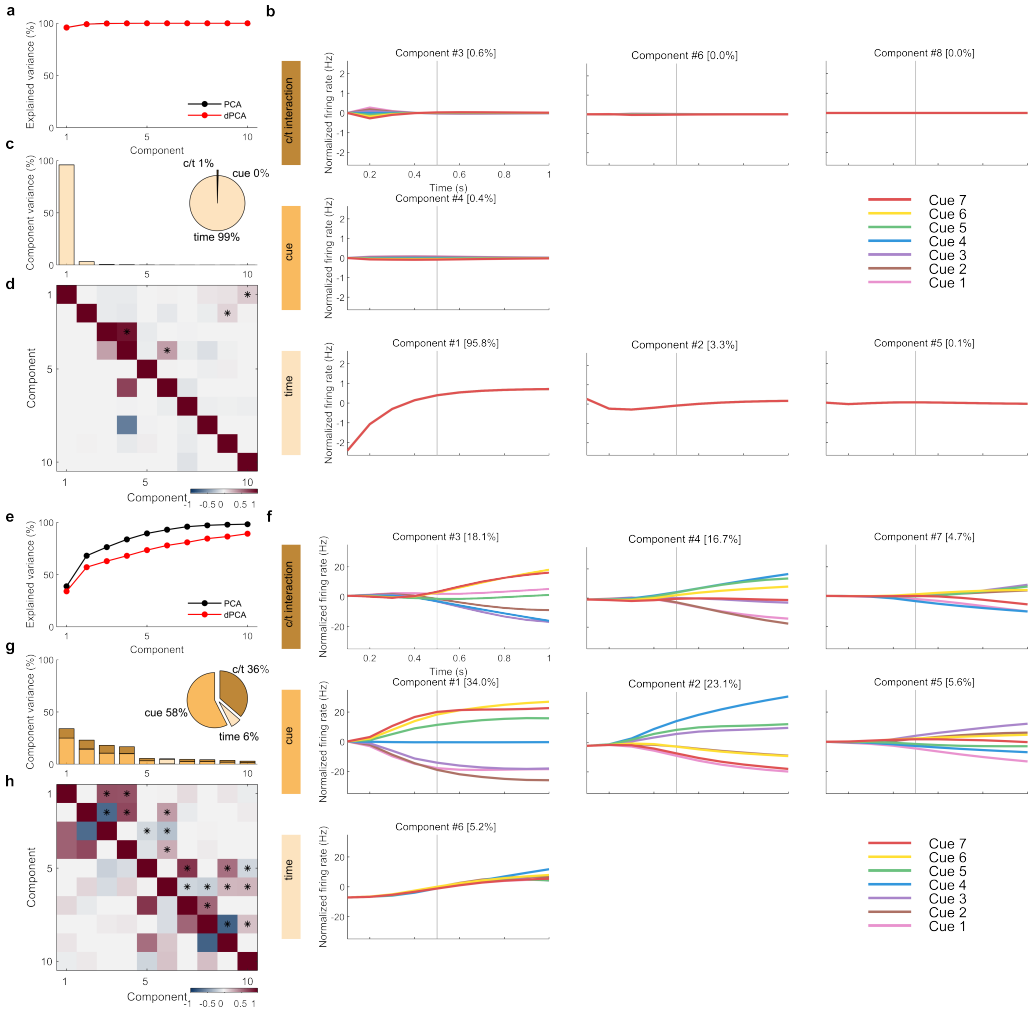

Figure 2.15: **Demixed PCA of ccRNN cerebral network at the beginning and end of learning.** (see Fig. 2.13a, c). Early and late learning corresponds to training session 1 (top a-d) and 200 (bottom e-h), respectively. (**a, e**) Cumulative variance explained by PCA (black) and dPCA (red) components. (**b, f**) Demixed principal components for cue, time and cue/time interaction task variables. In each subplot there are 7 lines corresponding to the 7 cues (see Fig. 2.6a). (**c, g**) Explained variance for individual demixed principal components. Pie chart shows how the total variance is split between different task variables. (**d, h**) Dot product between all pairs of the first 15 demixed principal components (upper-right triangle) and correlations between all pairs of the first 10 demixed principal components (bottom-left triangle). Stars denote statistical significance ($p < 0.05$). Figure and legend adapted from Boven et al., 2022.

of learning (Fig. 2.14b, c). Although there was some separability in the first cue PC there was almost no separability in the second cue PC, which was consistent with the decreased, but non-zero, distance observed in Fig. 2.13d. When performing dPCA it is important to consider pairwise correlations as well as orthogonality between the different components in order to verify if components represent independent signals corresponding to different task parameters (time, cue and cue-time interaction). Overall, pairwise correlations between components are all close to zero and most pairs are orthogonal to each other (Fig. 2.16h).

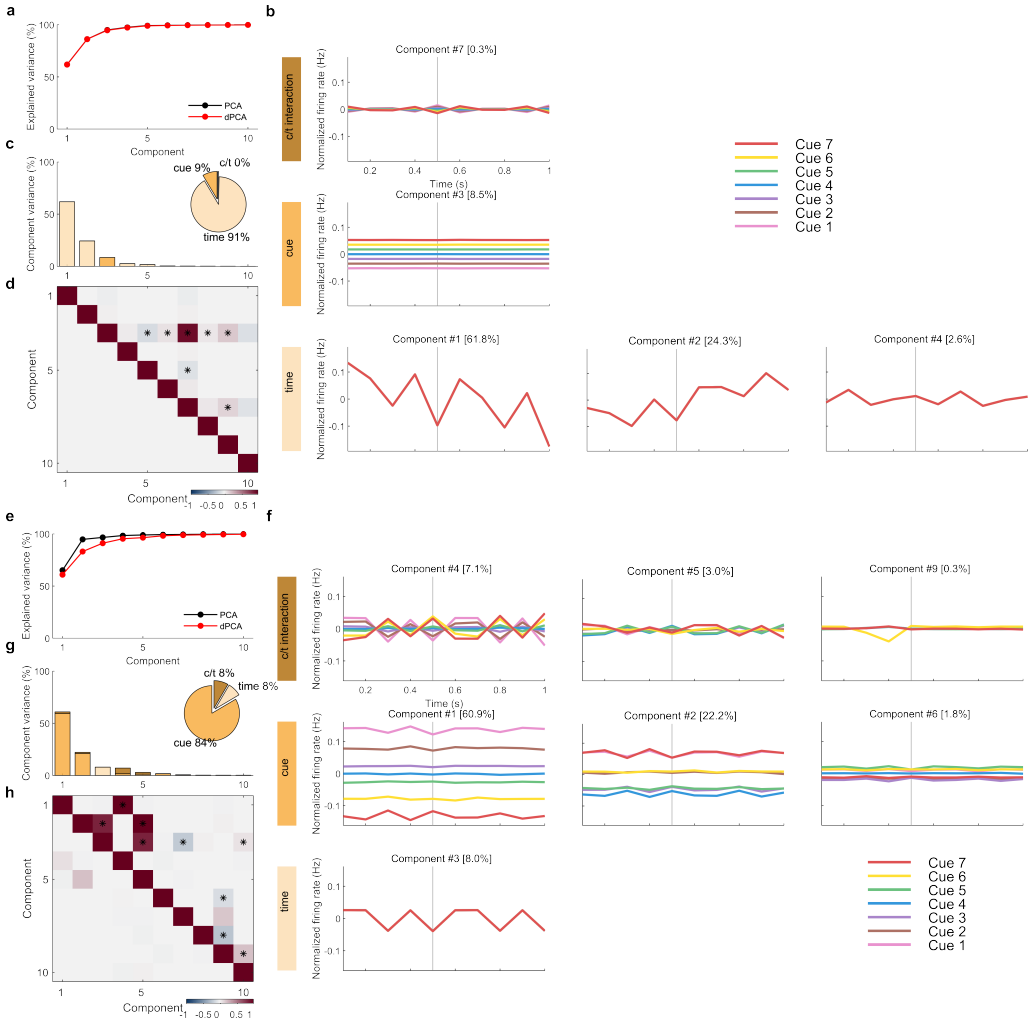

Figure 2.16: **Demixed PCA of ccRNN cerebellar network at the beginning and end of learning** (see Fig. 2.13d, f for comparison). Early and late learning corresponds to training session 1 (top a-d) and 200 (bottom e-h), respectively. (**a, e**) Cumulative variance explained by PCA (black) and dPCA (red) components. (**b, f**) Demixed principal components for cue, time and cue/time interaction task variables. In each subplot there are 7 lines corresponding to the 7 cues (see Fig. 2.6a for comparison). (**c, g**) Explained variance for individual demixed principal components. Pie chart shows how the total variance is split between different task variables. (**d, h**) Dot product between all pairs of the first 15 demixed principal components (upper-right triangle) and correlations between all pairs of the first 10 demixed principal components (bottom-left triangle). Stars denote statistical significance ($p < 0.05$). Figure and legend adapted from Boven et al., 2022.

Together, these results indicate that the cerebral network in ccRNN encoded more task-relevant information compared to cRNN and that the cerebellar network facilitates cue-to-target learning during the phase of learning where the presence of cerebellar predictions was most critical. Overall, these results suggest that when using a simple sensorimotor task cerebellar-mediated decoupling of cerebral feedback enables faster learning and smoother behavioural output. In addition, it makes a number of experimentally testable predictions in terms of the joint evolution of task-specific cerebro-cerebellar representations throughout learning.

2.4.8 Differential impact of cerebellar output and inferior olive on learning

Analogous to perturbation studies commonly used in experimental paradigms, *in silico* lesion experiments were performed to probe the impact of the cerebellar predictions during learning (see section 2.3.3). Cerebellar output was ablated early, mid and late in learning. Overall, inactivating cerebellar output impaired subsequent learning and final model performance (Fig. 2.17a, b). This was in line with the general idea that cerebellar predictions enable smooth learning. Interestingly, when the cerebellar output was removed early in learning, the subsequent learning trajectory was worse than the baseline model, presumably because the initial cerebellar predictions have modified the learning trajectory of the model. In comparison, when the cerebellar output was removed late in learning there was less impact, as the cerebral module has already achieved good performance and was less reliant on the cerebellar predictions. Similarly, when cerebellar learning was impaired (see section 2.2.3), learning was reversed as now the cerebellar network predictions are perturbed. Inactivating cerebellar learning had the same impact at any stage in learning, making the model return to naive performance (Fig. 2.17c, d). This was due to the cerebellum driving learning in the cerebrum with noisy estimates, thus corrupting the true cerebral feedback with noise.

2.4.9 Cerebro-cerebellar model trained on a line drawing task with simple actuator

In order to demonstrate the capacity of ccRNN in a more realistic motor output setting, the models were trained to perform the line drawing task with a simple actuator (see section 2.3.7). Whereas before the model directly predicts 2D coordinates, in this setting the output of the cerebral network was a muscle-like with an x- and y- actuator, expressed as a pair of orthogonal forces (F^x, F^y) to move a point mass m with inertia. As expected this new model made learning more challenging, but the relative comparison between cerebellar and non-cerebellar models remained the same in terms of (i) faster learning (Fig. 2.18a), (ii) reduced ataxia (Fig. 2.18a, b), (iii) dependency on feedback horizon (Fig. 2.18c) and (iv) dependency on task feedback sparsity (Fig. Fig. 2.18d, e). Together, these results demonstrate that the key results of ccRNN also extend to a more realistic motor model.

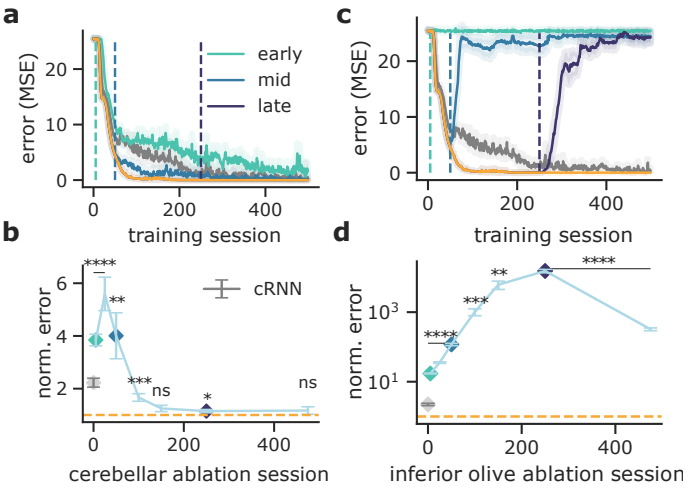

Figure 2.17: **Inactivating cerebellar output and inferior olive have a differential impact on learning.** (**a**) Complete cerebellar lesion at different points during learning. Vertical lines represent at which point during training the cerebellar was inactivated in the ccRNN model. In gray and orange show the baseline performances of the cerebral RNN and ccRNN, respectively. (**b**) Normalised error after cerebellar lesion throughout learning with respect to ccRNN (n.s. p=0.062 (session 150), p=0.162 (session 475)). Gray denotes normalised error for cRNN. (**c**) Complete inferior-olive lesion at different points during learning. Vertical lines represent point of lesion of the ccRNN model. In gray and orange are shown the baseline performances of the cerebral RNN and ccRNN, respectively. (**d**) Normalised error after inferior-olive lesion throughout learning with respect to ccRNN. Gray denotes normalised error for cRNN. *: $p < 0.05$, **: $p < 0.01$, ***: $p < 0.001$, ****: $p < 0.0001$. Error bars represent mean ± SEM across 10 different initial conditions. Figure and legend adapted from Boven et al., 2022.

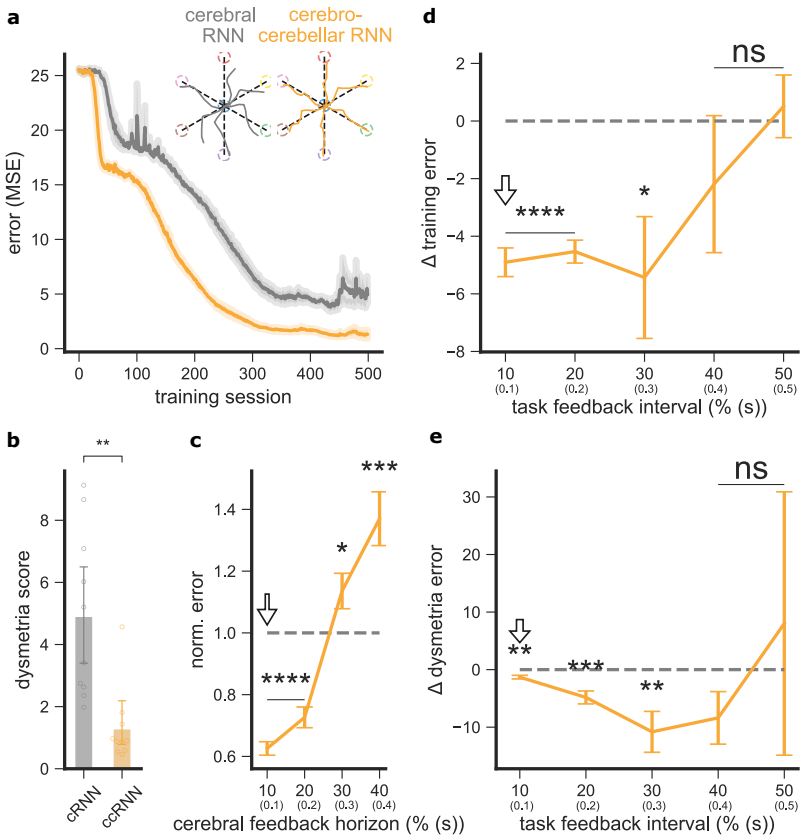

Figure 2.18: **Cerebro-cerebellar model improves learning and output behaviour when using a point-mass model in the line drawing sensorimotor task.**(**a**) Error between model output and desired target trajectories for cerebellar RNN (gray, cRNN) and cerebro-cerebellar RNN (orange, ccRNN) over learning. Insets: Model trajectory produced for all cues after learning. (**b**) Dysmetria score for cRNN and ccRNN. The dysmetria score quantifies how smooth the movement is after learning (Methods). (**c**) Normalized model mean squared error (MSE) after learning for different cerebral feedback horizons. Feedback horizon is denoted as percentage of the total task sequence. Arrow indicates feedback horizon used by the cerebral network in the other panels. (**d**) Difference in training error between for varying degrees of task feedback interval. (**e**) Difference in dysmetria score between ccRNN and cRNN for varying degrees of task feedback intervals. Task feedback interval given as a percentage of the total task time. **: $p < 0.01$, ***: $p < 0.001$, ****: $p < 0.0001$. Error bars represent mean ± SEM across 10 different initial conditions. Figure and legend adapted from Boven et al., 2022.

2.5 Discussion

In this chapter I have introduced a systems-level computational model of the largest circuit in the brain, cerebro-cerebellar circuitry. Modelling the cerebrum and cerebellum following their dominant anatomical structure it was proposed that a computational role of the cerebellum is to estimate feedback signals that are broadcasted to the neocortex to drive learning. The proposed model is novel in two ways: (i) it explicitly considers the cerebro-cerebellar structure and (ii) it deals with temporal problems, which are at the heart of naturalistic behaviour. The results from this study are largely consistent with observed empirical consequences of cerebellar damage, with cerebellar patients often suffering poorer performance in motor-related tasks; the occurrence of dysmetria, as well as a general reduced ability to learn motor tasks (Holmes, 1917; Sanes et al., 1990; Deuschl et al., 1996; Butcher et al., 2017; Nashef et al., 2019).

While in this chapter the model of cerebro-cerebellar interactions was tested using a relatively simple implementation of a sensorimotor task, testing the model on the sensorimotor task with simple actuator provides evidence that the key model predictions also apply to a more realistic motor model. Moreover, in the resulting publications of this work the model was tested on more challenging tasks that simulate more naturalistic conditions by using nonlinear input-output mappings (Pemberton et al., 2021; Boven et al., 2022). Overall the key results and predictions of the model remain the same. Although these more challenging/realistic tasks also make the important point that when the model converges to a non-zero error solution the cerebellum is still important after learning, which is not the case in the simpler line drawing task.

2.5.0.1 Cerebro-cerebellar networks for efficient temporal credit assignment

The model predicts that the cerebellum is particularly important for temporally challenging tasks, offering a potential explanation for recent experimental observations (Locke et al., 2018). This is due to the fact that the cerebro-cerebellar model enables efficient temporal credit assignment (see section 1.3.2). Therefore this work suggests that the cerebellum reduces the need for strong temporal credit assignment in the brain. This predicts that when the cerebellum is perturbed the cerebrum must encode and learn with richer temporal signals to achieve a similar performance when compared with healthy controls. Moreover, the cerebellum has long been known to be involved in timing prediction (Ivry et al., 2002; O'Reilly et al., 2008). The model is related to these observations in that the cerebellar module learns to predict cerebral feedback at specific points in time. Although in the model these predictions are used directly for learning, it is possible that these temporal predictions have a broader impact on network dynamics and information processing in the brain (Pemberton et al., 2022). In addition, the model makes the prediction that the benefits provided by cerebellar networks are not uniform throughout learning. More specifically, the model predicts that cerebro-cerebellar networks facilitate learning

early on, but after this first phase of learning the model suggests that cerebellar predictions may indeed impair learning. This suggests the need to gate cerebellar predictions throughout learning, a process that might involve the thalamus which mediates cerebellar-cerebral communication (Chabrol et al., 2019). Moreover, this is line with the idea that the cerebral cortex retains what the cerebellum learns (Galea et al., 2011)

This study constrained the model using biologically realistic assumptions regarding how much information can be stored in the cerebral cortex, or cerebral horizon, and the availability of external sensory feedback. Additionally, in sensorimotor tasks there are inherent physiological constraints which impose limits on the rate of sensory feedback (Kitazawa et al., 1995; Ikegami et al., 2012; Levy et al., 2010. This delay is important for how cerebellar predictions are learned, as ultimately the cerebellar predictions must be compared to sensory feedback (Sanes et al., 1990; Synofzik et al., 2008). Given these constraints, the behaviour observed in a cerebral model without cerebellar module is akin to learning and behavioural performance deficits of cerebellar patients. Systematically studying the effect of these constraints on network behaviour with and without a cerebellar component shed light under which conditions the cerebellum may play an important role. First I show that the cerebellum is of particular importance when a cerebral area is limited in the temporal dependencies it can process. This makes the prediction that the cerebellum is particularly important for cerebral learning in conditions in which cortical networks fail to learn on their own (Fig. 2.6d), consistent with experimental observations showing that the cerebellum is more detrimental when in the presence of large than small task-specific errors (Criscimagna-Hemminger et al., 2010).

The systematic analysis of varying cerebral feedback horizon and feedback interval indicates that the cerebellum plays a role particularly in the case where the cerebral feedback horizon is no longer than the feedback interval. This is to be expected, as cerebellar feedback in the model would be mostly beneficial for points in time in which there is no feedback readily available. Although different studies have considered the influence of external feedback on learning (Foulkes et al., 2000; Honda et al., 2012) and it is known that cerebellar function relies on the precise timing of feedback (Beppu et al., 1984; Cerminara et al., 2009), the optimal properties of task feedback for learning remain to be explored. Taken together, the results presented in this study suggest that cerebellar circuit facilitates cerebral learning if external feedback is sparse. Moreover, the cosine similarity results indicate that the alignment between cerebellar feedback predictions and actual cerebral feedback depends on the properties of the external sensory feedback. In particular, the model predicts that for tasks with feedback only at the end of the task there is a gradual decay of the cerebellar alignment with cortical feedback for earlier points in the task, whereas for tasks with intermediate feedback this relationship becomes non-trivial. Experimentally such alignment might be possible to measure by comparing cerebellar output with spiking burst rates, which is believed to underlie credit assignment in neocortical networks (Payeur et al., 2021).

2.5.0.2 Cerebellar bootstrapping

In addition, the cerebellar error function used in the model is proposed to be computed by the *inferior olive*, which is known to mediate learning in the cerebellum via the climbing fibres, also in line with classical internal cerebellar models (Marr, 1969; Raymond et al., 2018). The model requires the cerebellum to be trained with feedback from the cerebral cortex, but also with its own self-predictions (also known as bootstrapping). The combination of true feedback and self-predicted feedback is important for the cerebellar module to learn to predict effective cerebral feedback. Feedback from the cerebral cortex can be directed via the cerebro-olivo-cerebellar pathway via the mesodiencephalic junction (Wang et al., 2022). The latter, that is the idea of self-predictions, is highlighted in Fig. 2.4 and is analogous to the reinforcement learning literature, where the value function in temporal difference learning is also reliant on bootstrapping and allows to account for future rewards (Sutton et al., 2018). Similar signals have been previously observed to be present in climbing fibers (Ohmae et al., 2015). This echoes existing evidence that cerebellar circuits can condition on their own outputs, and hence learn to execute specific sequences of effects based on triggering context signals (Ohmae, 2022; Wang et al., 2020). Moreover, this reinforces the idea that the cerebellum must learn fast in order to provide effective feedback to the rest of the brain (Shadmehr et al., 2010). Together, this raises the prediction that the inferior olive processes cerebellar predictions which may originate from different, perhaps functionally distinct, cerebellar modules that generate cerebellar learning signals when more direct teaching signals (as provided by the cerebral cortex in ccRNN) are not available. This could be implemented via having multiple predictive forward models working in hierarchical fashion. This idea has been proposed previously (Haruno et al., 2003), however in this study it is predicted that multiple forward models cooperate by predicting cerebral feedback for different points in time. The prediction of the model emphasizes the importance of divergent and convergent connections between cerebellar modules in implementing such role. More specifically in which the predicted feedback of one module is used to instruct learning of another module. This prediction of the model implies that there exist nucleo-olivary projections that carry output signals from one module that target a climbing fiber population of another module. This is consistent with the connectivity from cerebellar output to the inferior olive observed experimentally (Wang et al., 2020).

2.5.0.3 Cerebro-cerebellar representations

The results from the representational analysis presented in this study suggests that the cerebellum develops task-specific representations. Recent functional MRI studies have observed that different regions of the cerebellum encode task domain-specific representations (King et al., 2019; Ashida et al., 2019). The model predicts the need for different cerebellar regions to cooperate with the cerebral cortex across different task domains. In addition, results about the coupling between cerebellar and cerebral neural activity demonstrate a general decay in the coupling over learning. However, this study observed increases in coupling for sub-populations at particular points in the learning process. In particular sub-populations with high initial corre-

lations tend to decrease over learning, whereas those with initially low correlations tend to increase, consistent with recent experimental observations (Wagner et al., 2019).

2.5.0.4 Differential role of the cerebellum and the inferior olive throughout learning

The cerebellar ablation results echo the existing literature in that though shared cerebro-cerebellar dynamics might emerge during the acquisition of a novel motor sequence, these dynamics can become less interdependent once knowledge becomes consolidated (Doyon et al., 2003; Galliano et al., 2013). However, the nonlinear ablation results predicted by the model have not been explored experimentally. Moreover, the inferior olive ablations predict a detrimental role of the inferior olive in enabling cerebellar-mediated learning, such that without it task performance is likely to be severally impaired, which is consistent with experimental results that observed disrupted inferior olive activity during learning together with deficits in behavioural performance (Llinás et al., 1975; Silva et al., 2022).

2.5.0.5 Cerebro-cerebellar interactions via thalamus

Different lines of evidence suggest that the cerebellum can influence cerebral learning processes via its projections to the thalamus (Hua et al., 1997; Penhune et al., 2005; Kishore et al., 2014; Tanaka et al., 2018). For example, the cerebellum plays an important role in scaling plasticity by controlling the afferent inflow into the cerebral cortex through thalamus (Popa et al., 2013). One of the limitation of the proposed framework is that the model does no consider the long-range projections via the thalamus and pons that mediate cerebro-cerebellar interactions. This is in line with previous research which proposes that intermediate structures like the pons provide bottlenecks that filter out non-relevant information in order to enable optimal routing (Muscinelli et al., 2022) and in the case of cerebello-thalamo-cerebral connections would allow the cerebellum to provide more efficient feedback signals. This is an interesting line of future research.

2.5.0.6 Learning with prediction errors

The work presented in this chapter is based on the assumption that cerebral prediction error modules, which compare the output of a given cerebral area with a teaching signal, exist in the brain. The classical example in the brain of such prediction errors are those computed by the VTA, which are also known as reward-prediction errors (Schultz et al., 1997; Keiflin et al., 2015) and other studies have provided evidence for the existence of prediction errors across different brain areas, for example sensorimotor prediction errors in the neocortex (Attinger et al., 2017; Jordan et al., 2020) or the prediction error signals from the locus coereleus facilitate plasticity in the sensorimotor cortex (Jordan et al., 2022). For simplicity this study

considered supervised prediction errors, but this can in principle be extended to unsupervised or reward-based prediction errors (Schultz et al., 1997; Mnih et al., 2015). In future work it would be of interest to explore how this shapes learning and neuronal dynamics across cerebral and cerebellar networks (Carta et al., 2019; Sendhilnathan et al., 2020). Indeed the model is of particular relevance to reinforcement learning due to prevalence of sparse and delayed rewards (see Fig. 2.9). Resulting from the assumption of supervised cerebral prediction error, the model predicts the need for feedback signals in the form of gradients to (i) be calculated in the cerebral cortex and (ii) propagated across cerebral and cerebellar networks. Recent developments have introduced biologically plausible solutions to how the brain encodes gradients (Lillicrap et al., 2019; Guerguiev et al., 2017; Sacramento et al., 2018; Richards et al., 2019a; Payeur et al., 2021; Ahmad et al., 2020). Regarding spatial backpropagation of gradients (for example from the prediction error module to the recurrent cerebral network), Sacramento et al., 2018 demonstrated that biological networks do not need to explicitly send gradient information, but rather that this can be reconstructed locally in dendritic cerebral microcircuits. Indeed, at the single-neuron level, credit signals are thought to drive dendritic non-linearities that produce unique spiking patterns (Richards et al., 2019a). One prediction of the model is that if the cerebellum sends a credit signal, this means that cerebellar activation should have the ability to produce such distinct activity patterns that can be distinguished from ongoing processing. This is a prediction that could theoretically be tested by experiments given the advancements in viral tracing and perturbation tools (Nectow et al., 2020; Prestori et al., 2020). On the other hand Bellec et al., 2019 showed that temporal gradients can be approximated by eligibility traces that transmit information forward in time. In addition, Payeur et al., 2021 demonstrated that short-term synaptic plasticity can be used to decode deep learning gradients. In light of the work presented here this suggests a potential mechanism by which the cerebral cortex and the cerebellum could exchange feedback signals encoding gradient information. It is in principle possible to integrate these elements in the systems-level model, but this remains to be explored. In addition, the interplay between the two types of feedback may have a very powerful organizing effect on the generation of ordered, biologically meaningful activities (Schöll et al., 2009).

2.5.0.7 Summary of predictions from the model

1. The cerebellum is particularly important for temporally challenging tasks. This predicts that when the cerebellum is perturbed the cerebrum must encode and learn with richer temporal signals to achieve a similar performance when compared with healthy controls.

2. Cerebellar facilitation of cerebral processing is not uniform throughout learning, but is more prominent early in learning.

3. Cerebellar-mediated feedback predictions are particularly important for temporally challenging tasks with sparse feedback.

4. For tasks with feedback only at the end of the task the alignment of cerebellar predictions with cerebral feedback will gradually decay. This could be experi-

mentally tested using spike burst as the learning/feedback signal in neocortical networks (Greedy et al., 2022).

5. It proposes that in order for the cerebellum to learn rapidly it uses learns via its own predictions, a concept known as bootstrapping in the machine learning literature.

6. Cerebro-cerebellar coupling decays over learning

7. Cerebellar activation should have the ability to produce learning/feedback specific signals that are distinct from other activity patterns resulting from ongoing processing in pyramidal cells in the cerebral cortex.

Chapter 3

Role of the cerebellum in interval timing

3.1 Introduction

The mechanisms of temporal credit assignment seem to be strongly linked to the ability of biological networks to process temporal information (Medina et al., 2000; Lim et al., 2020). At the moment our understanding of the biological networks underlying different scales of temporal information processing is changing (Fig. 1.1), with evidence such as the cerebellum being involved in higher cognitive behaviours (see Section 1.2.2). This suggests that the cerebellum should be involved in encoding supra-second time intervals.

In fact several studies, including human lesion cases and functional brain imaging, support a role for the lateral cerebellum in the supra-second timing range (Gooch et al., 2010; Mangels et al., 1998; Nichelli et al., 1996; Tracy et al., 2000). For example, Gooch et al., 2010 observed overestimation as well as underestimation of supra-second time intervals in cerebellar patients with damage to the lateral parts of the cerebellum. In addition, a study observed co-activation of the cerebellum with prefrontal cortex during supra-second timing tasks (Parker, 2016). Another study in zebrafish observed how Purkinje cells use prediction errors to acquire an internal model of supra-second stimulus timing (Narayanan et al., 2021). Together, these reports question the dogma that the cerebellum exclusively influences sub-second timing performance (Ohmae et al., 2017), indicating that the apparent division between sub- and supra-second timing systems might not be as clear cut as previously thought (see Fig. 1.1).

A first step in understanding the temporal range of the cerebellum's involvement in timing, is to consider the regions with which the cerebellum interacts. Most studies pointing to a subsecond timing role of the cerebellum rely on behaviours that mainly involve premotor and motor cortices. Indeed, most animal studies focusing on probing the behaviourally relevant interactions between cerebellum and cerebral cortex look at behaviours that involve the motor cortex (Gao et al., 2018; Wagner et al., 2019). Thus the role of the cerebellum in behaviours that involve cerebral areas like the PFC remains elusive. Although, recent animal studies have observed co-activation of the cerebellum with prefrontal cortex during supra-second timing tasks (Parker, 2016), its behavioural contributions to supra-second timing remain relatively unexplored.

Supra-second timing behaviours are mostly studied using behavioural paradigms of interval timing: tasks that involve monitoring time in the seconds-to-minute range to drive goal-directed behaviours and decision making (Oprisan et al., 2014). However, it is known that behavioural readouts of timing in animals involve the development of stereotyped movement sequences or motor strategies (Aronov et al., 2011; Gouvêa et al., 2014; Kawai et al., 2015; Monteiro et al., 2020). Together with the central role of the cerebellum in state-dependent control such as motor control and coordination, it is often hard to dissociate its contributions to time-dependent control (Diedrichsen et al., 2007).

In order to explore cerebellar contributions to supra-second time processing, the results presented in this chapter involved rats performing an interval timing task that

controlled for motor strategies used in rats. The behavioural task requires the rat to estimate time instructed by a sound duration, by terminating a nose poke hold at the right time, followed by poking into a different port to receive reward (Fig. 3.10). Moreover, this interval timing task is known to recruit the prefrontal cortex but not the adjacent motor cortices. More specifically, Xu et al., 2014 have previously shown that cooling of medial PFC, but not motor cortex, slows the ability of rats to estimate time. Therefore, the present study sought to replicate the behavioural paradigm to investigate the role of the cerebellum in this task.

The area of the cerebellum in rodents that is likely to relay information to other supra-second timing regions like the striatum and the PFC is the lateral cerebellar nucleus (LCN), also known as the dentate nucleus (DN) (Shipman et al., 2020). Considering the dentate nucleus, the motor loop is defined by the dorsal dentate nucleus and lobules I-VI of the cerebellum and primary motor and premotor cortex of the neocortex. The cognitive loop on the other hand is defined by ventral dentate nucleus and lobule VI, Crus II, lobule VIIb and vermal VIIIb of cerebellar cortex and the anterior cingulate cortex, caudate nucleus and the thalamus projecting to various regions of the cortex (Shipman et al., 2020). The thalamus also transmits signals from other structures such as the BG to the cerebral cortex. It is therefore a strong candidate for the transmission and integration of information from key nodes in the supra-second network to the cerebral cortex where the final behavioural response is assumed to be generated.

In this thesis chapter I used experimental approaches in rats to evaluate the role of the LCN in interval timing. Given that the connections between cerebellum and prefrontal cortex are mainly via the lateral cerebellum, the present experiments employed a chemogenetic approach (Zhu et al., 2014; Sternson et al., 2014; Roth, 2016; Campbell et al., 2018) to evaluate the role of the DN in interval timing. This allowed to probe the functional contributions of lateral cerebellar output to interval timing behaviour. In this case DREADD virus was targeted to the DN and following transfection, the projections of these transfected neurons were manipulated in two ways. The first invovled reversibly manipulating all the cerebellar output projections by systemic injection of a selective ligand (clozapine N-oxide, CNO). Systemic injection of the ligand allows manipulation of the output of the cerebellar nucleus as a whole during behaviour. In addition, the terminals of DREADD expressing cerebellar neurones projecting to the ventrolateral (VL) thalamus were also targeted. When the ligand (CNO) is administered by intracranial infusion directly targeted to the VL thalamus the ligand acts on virally transfected terminals modifying neurotransmission from the cerebellar output projection. The manipulation was applied at the stage where the animals had acquired the behaviour and were regarded as expert subjects.

Together, the combination of an interval timing paradigm and experimental manipulation technique that allows targeted circuit manipulation allows me to test the hypothesis that cerebellar output projections, potentially via cerebello-thalamic projections, are recruited during a behaviour that involves supra-second time processing.

3.2 Material and methods

3.2.1 Experimental animals

All animal procedures were performed in accordance with the UK Animals (Scientific Procedures) Act of 1986, they were approved by the University of Bristol Animal Welfare and Ethical Review Body and carried out under the authority of a UK Home Office Project licence (PPL number PA26B438F). Experiments were conducted on 20 male Lister Hooded rats (HsdOla:LH, 330-480g at time of surgery, Envigo). Animals were housed in pairs under a 12:12 hour reverse light–dark cycle (light phase 20:15-08:15, target conditions: 20°C and 45–65% humidity). Experiments were therefore performed during the dark phase when they are naturally most active. Food and water were available *ad libitum* prior to and during recovery from surgical procedures. Water was available *ad libitum* throughout the experiment. After recovery from surgical procedures (see section 3.2.3) animals were fed approximately 16 g of standard laboratory chow per day, in addition to food rewards obtained during behavioural tasks. For tasks involving food reward, 45 mg grain-based sweetened reward pellets (TestDiet LabTab AIN-76, 5TUL, catalogue number 1811155) were used. Weights of the animals were monitored 5 days a week to ensure they did not drop below 90% of the normal growth curve. Animals were habituated to the experimenter and experimental room for five consecutive days. Handling occurred daily one-week prior to surgery and during the recovery phase. During the experiment animals were handled every weekday. The experiment occurred over two batches, one batch (n=8) was run between March - September 2021 and a second batch (n=12) between November 2021 – May 2022.

3.2.2 Viral vectors

In order to study the role of cerebellar projections during interval timing chemogenetics were used. To modulate the output activity from the cerebellar nuclei, a red fluorescent inhibitory Designer Receptor Exclusively activated by a Designer Drug (DREADD), hM4Di, was injected bilaterally into the LCN in 10 animals (AAV5-hSyn-hM4D(Gi)-mCherry, Addgene, USA; titre $8.6 \times 10^{12} \frac{GC}{ml}$). In order to control for nonspecific Clozapine N-Oxide (CNO) effects a control group of animals (n=10) received bilateral injection into LCN of a green fluorescent tagged virus (AAV5-hSyn-EGFP, Addgene, USA; ; titre $1.2 \times 10^{12} \frac{GC}{ml}$).

3.2.3 Surgical procedure

All surgical procedures were performed under aseptic conditions. General anaesthesia was induced by initially administering gaseous isoflurane, followed by an intraperitoneal injection with ketamine/medetomidine (initial dose $\frac{50}{0.3}$ $\frac{mg}{kg}$, Vetalar/Domitor). Depth of anaesthesia was regularly monitored throughout surgery by

testing the hindpaw withdrawal reflex and additional doses of ketamine/medetomidine were given as necessary to maintain surgical anaesthesia. Each animal was mounted in a stereotaxic frame with atraumatic ear bars. During anesthesia, a rectal thermometer was inserted to provide feedback to the heated blanket on which the animal was placed. Body temperature of the animal was maintained at approximately 37°C. Eye ointment (LacriLube) was placed on the eyes to to prevent corneal injury due to drying. The incision site was treated ahead with local anaesthetic cream. A midline scalp incision was made to access the skull. The skull was scraped to allow for good dental acrylic attachment and cleaned using hydrogen peroxide (3%). Bregma and lambda were measured to ensure the skull was level in the dorsoventral plane. Coordinates relative to bregma were measured to allow precise positioning of burr holes for viral injections, cannula and skull screw placement. For viral injections the dentate nucleus of the cerebellum was targeted (AP -11.2mm, ML +/- 3.4mm and DV -4mm relative to surface). For cannula placement the thalamus was targeted (AP -2.76mm, ML +/- 1.5mm and DV -5.2mm). Bilateral AAV-virus injections targeting the cerebellum were delivered using a pulled glass micropipette connected to a 25 µl syringe (Hamilton, Bonaduz, Switzerland) via tubing filled with mineral oil, and was then backfilled with 1 µL of the viral vector using a syringe driver (AL-1000, World Precision Instruments). A volume of 0.5 nl was injected at 200 $\frac{nl}{min}$ and the pipette was then left in place for approximately 10 min after injection, in order to minimise leakage of the tracer back up the pipette track. Stainless steel bilateral guide cannula (26 gauge, 3mm apart, Plastics One, Bilaney, UK) were placed in the thalamus such that the tips of the internal cannula (33-gauge with 1 mm projection) targeted the thalamus dorsally. Dummy cannula (26 gauge, Plastics One, Bilaney, UK) secured with dust caps kept the cannula patent between infusions. Dental acrylic was used to close up burr holes and secure the bilateral cannula to the skull via 4 screws, 2 on either side of the frontal skull bone and 2 on either side of the interpariatel skull bone. At the end of each surgery, rats were given the medetomidine antidote atipamezole (Antisedan, 0.1 mg intraperitoneally), analgesic (Metacam, 1 $\frac{mg}{kg}$ subcutaneously) and saline (10 $\frac{ml}{kg}$ subcutaneously). Rats were singly housed for 7 days following surgery and then returned to their original pairings. A minimum period of 6 weeks was allowed for stable expression of the viral vector before any experimental manipulations. Infusions were performed no sooner than 8 weeks following surgery. During this period animals underwent behavioural training on the interval timing task.

3.2.4 Behavioural testing

3.2.4.1 Single-Interval timing task

3.2.4.1.1 Hardware

The interval timing task was performed in a standard rat operant chamber (Fig. 3.1; dimensions 30.5 x 24.1 x 21.0 cm; Med Associates, OpCoBe Ltd., UK), placed in a light-resistant and sound attenuating cubicle. The operant chamber contained a stainless steel grid floor, two identical ports (Fig. 3.1A; trough type with 6.0"

opening, Med Associates), a pellet dispenser (Fig. 3.1E) and a speaker (Fig. 3.1F).

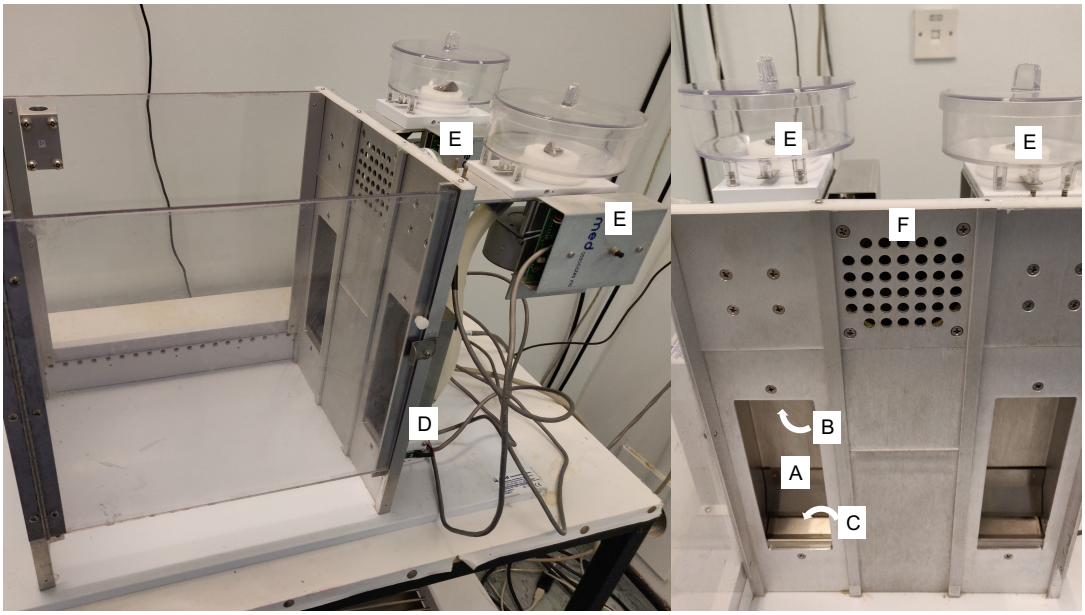

Figure 3.1: **Annotated photograph of rat operant chamber.** A side view (left) and front view (right) photograph of a representative operant chamber where rats performed the interval timing task, with operant chamber ports (A) equipped with stimulus light (B) and receptacle (C) with IR head entry detector (D). The left port is the "hold port" in which rats have to sustain nose poke fixation during a sound emitted through the speaker (F). The right port is connected to a pellet dispenser (E) and is thus used as the "reward port".

Each port included a stimulus light (Fig. 3.1B; 1" White Lens, light source of 28 V) at the top and a nose poke receptacle with infrared (IR) photobeam (Fig. 3.1C, D) at the bottom. The stimulus light was used as a reinforcer during the behavioural paradigm. The photobeam served as a head entry detector for nose pokes in each port (Fig. 3.1D) and was created by a single infrared (IR) light source and receiver. When the beam was uninterrupted, the IR receiver maintained a high output signal, when the rat's head entered the port the IR beam would be broken, and the receiver would set the output signal to low. One of the ports served as the "hold port" in which the rats maintained head fixation, while the other port served as the "reward port" for reward collection. Relative positions of the hold and reward port were fixed across the whole experiment, with the right port the reward port (Fig. 3.1). A rubber tube connected the pellet receptacle of the reward port to the pellet dispenser (Fig. 3.1E). An audio generator (ANL-926, Med Associates, OpCoBe Ltd., UK) produced tones that were delivered to each chamber via a speaker placed at the top of the chamber, in between the two ports (Fig. 3.1F). The signals coming from the different components in the operant chamber were recorded through connection panels that feed the signals into input/ouput cards. In the interface cabinet (MED-SYST-8-USB, MedAssociates), the input/output cards were connected to a decode card that interfaced with a computer.

3.2.4.1.2 Software

The K-Limbic software (Conclusive Solutions Ltd., UK) operated as an interface between the operant chamber hardware and a computer. Custom-written programs in K-Limbic were used to control the parameter conditions for each of the behavioural training stages (see below). It managed all input parameters to the chamber, such as duration of sound emission, dispensing pellets and switching lights on and off. The software further controlled the audio generator used for sound emission. It received chamber output through registering changes in IR photobeam state, sound emission, light onset, which it turned into a Microsoft Excel file (.xlsx format) after the end of each session.

3.2.4.1.3 Training stages

In the single-interval time estimation task, food restricted rats learnt to estimate a 2.5 s sound duration through positive reinforcement. Rats indicated the estimated time by exiting from the hold port; if this action was around the target duration of 2.5 s, rats could nose poke into the reward port which would trigger delivery of a food pellet. The behavioural protocol used for this experiment is based on the interval timing task described by Xu et al., 2014. Rats were habituated to the operant chambers in two successive sessions of 20 minutes per session. During habituation, food pellets were pulverized in the bottom of the ports to encourage exploration.

Behavioural training occurred through reinforcement of four successive approximations of the target behaviour (Skinner, 1971), called training stages. The different training stages with the respective number of sessions needed to achieve criterion for moving to the next stage are presented in order in Table 3.1. Training sessions took place 5 days per week, Monday to Friday.

Table 3.1: **Training stage criteria for single-interval time estimation task.** Training stages are shown along with the number of sessions it took for the both batches to graduate each stage and the corresponding graduation criteria. Cerebellar manipulation experiments were performed at stable performance on both the single-interval timing with predictable and unpredictable time cue.

Training stage	Duration (sessions)	Criterion
Instrumental conditioning	2	100 trials in 30 mins
Action suppression	10	$> 50\%$ accuracy on required duration
Single-interval timing with predictable time cue	10	$> 50\%$ accuracy on two consecutive sessions $< 30\%$ too early responses
Single-interval timing with unpredictable time cue	10	$> 50\%$ accuracy on two consecutive sessions $< 30\%$ too early responses

3.2.4.1.4 Instrumental conditioning stage

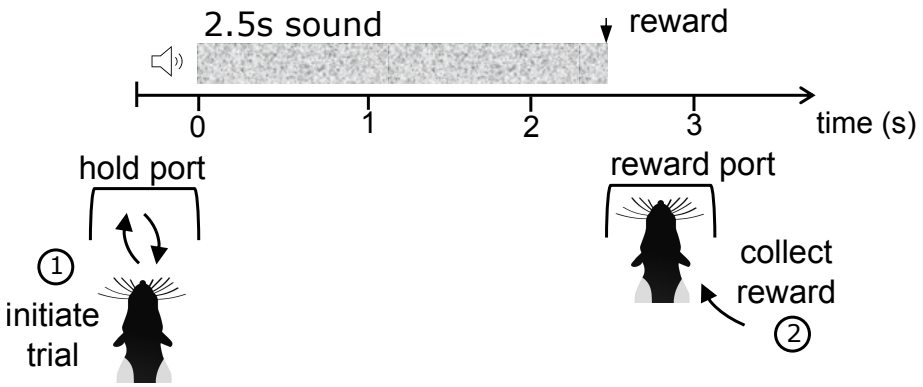

Figure 3.2: **Graphical representation of trial sequence in the instrumental conditioning phase.** The timeline gives the sequence of stimulus events in the operant chamber and the numbers indicate the action sequence of the rat. A rat initiates a trial by poking into the hold port (1), triggering a 2.5 s long auditory stimulus after which an automatically dispensed reward can be collected from the reward port (2).

The instrumental conditioning stage consisted of a self-initiated action-cue-reward learning procedure to link the nose poke into the hold port to the auditory stimulus. After repeated trials food-restricted rats learned that a nose poke into the hold port resulted in automatic food delivery in the reward port on termination of a 2.5 s auditory cue (white noise, 75 dB) (Fig. 3.2). The sound onset was contingent on the first head entry into the hold port or automatically triggered every 2 min (Fig. 3.3). During periods in which the sound was off, the stimulus light in the hold port was illuminated in order to encourage exploration of the operant chamber ports. The criterion for determining successful task performance was 100 rewarded trials in 30 min on two consecutive days.

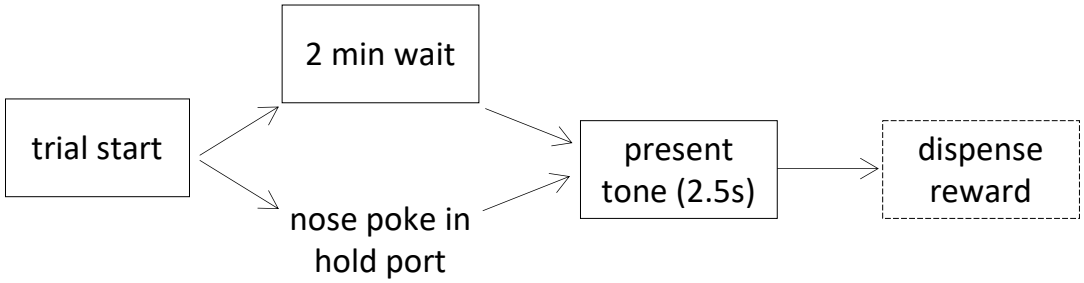

Figure 3.3: **Trial structure in the instrumental conditioning phase.** Boxes represent states during a trial, unboxed text indicate action required from the rat, arrows indicate transitions between states. Dashed box indicates final trial state before returning to the start and initiating a new trial. Trials can be self-initiated by poking into the hold port which triggers the onset of a sound with 2.5 s duration. A reward is dispensed at tone offset. If a trial has not been initiated for 2 minutes a tone onset will be automatically triggered after which a reward will be dispensed.

3.2.4.1.5 Action suppression phase

After rats could reliably dispense a food pellet in the reward port by poking into the hold port, they were moved on to the action suppression phase in which rats were trained to actively hold a nose poke for 2.5 s (Fig. 3.4 and Fig. 3.5). Rats could self-initiate a trial by poking into the hold port which would lead to the immediate onset of the auditory stimulus. This was followed by a hold period in which rats had to sustain their nose poke in the hold port during sound emission. The duration of sound emission was gradually increased by the experimenter from 0.5 s to the target duration of 2.5 s according to individual rat's performance. Fig. 3.4a depicts the trial sequence at the start of action suppression training and Fig. 3.4b depicts the trial sequence at the end of action suppression training when rats are considered expert. The criterion was to sustain the nosepoke for the required duration at least 50% of the trials across 2 sessions. If the rat successfully held the nose poke during the hold period, a pellet would be dispensed and available for collection in the reward port (1.5 s). This response was recorded as a correct trial. Failing to sustain the nose poke in the hold port for the required hold period lead to a time-out period that served as a negative reinforcer. During the time-out the stimulus lights in both the hold and reward port were illuminated for 16 sec. These type of responses were recorded as incorrect trials. Training to sustain a nosepoke for 2.5 s occurred over several sessions, with each session consisting of a minimum of 100 trials. All rats learned to hold for 2.5 s in 10 sessions.

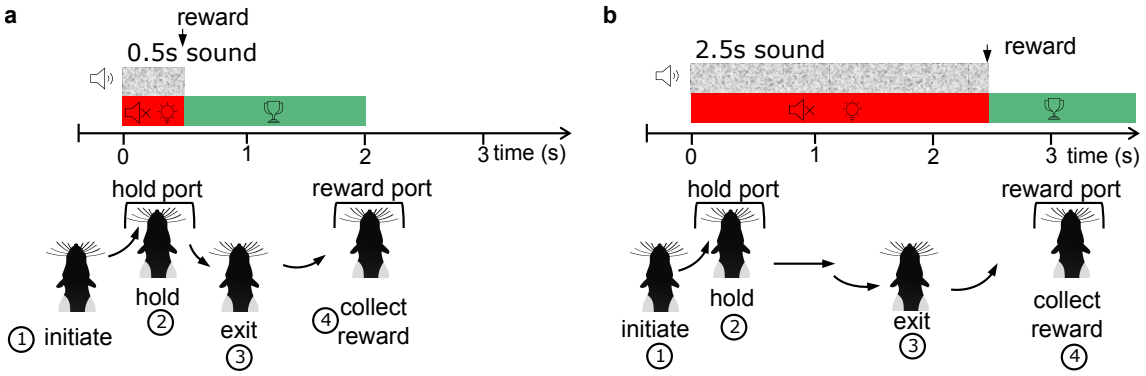

Figure 3.4: **Trial sequence in the action suppression phase.** The timeline gives the sequence of stimulus events in the operant chamber and the numbers indicate the action sequence of the rat. **(a)** Trial sequence at the start of action suppression training. A rat initiates a trial by poking into the hold port (1), triggering an auditory stimulus of 0.5 s during which the rat has to fixate its nose in the hold port (2). The trial outcome depends on when the rat exits the hold port indicated by the red in the case of incorrect trials and green in the case of correct trials. If the rat exits (3) after the tone offset, a reward was available for collection (4). This trial outcome is indicated in green. If the rat exits before the tone offset this will lead to an incorrect trial in which the sound is turned off and the stimulus lights turned on. **(b)** Same as in (a) but for a trial at the end of action suppression training when the rat is considered expert. Now a nosepoke will trigger an auditory stimulus of 2.5 s during which the rat has to sustain the nosepoke into the hold port.

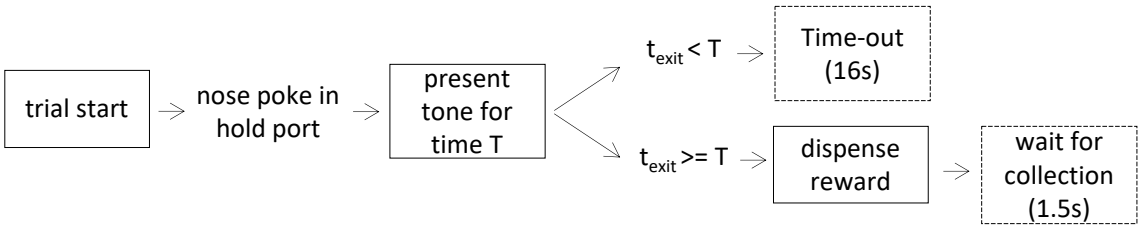

Figure 3.5: **Trial structure of the action suppression stage.** Boxes represent states during a trial, unboxed text indicate action required from the rat, arrows indicate transitions between states. Dashed boxes indicates states that go back to the start and initiate a new trial. Trials are self-initiated by poking into the hold port which triggers the onset of a sound of length T that varies between 0.5 s and 2.5 s during training. If the time at which the rat exits from the hold port is below T, this will lead to time-out. If the rat is able to sustain the nose poke for the minimum required period of T a reward will become available for collection.

3.2.4.1.6 Single-interval timing task with predictable time cue

After the rats had learnt to reliably maintain their nose poke in the hold port during emission of the sound, the rats were exposed to the single-interval timing task with predictable time cue (Fig. 3.6 and Fig. 3.7). At each trial the duration of the sound was fixed to 2.5 s and served as a cue for the rat to exit from the hold port at sound offset. As the sound offset conveys predictive information for reward availability this is referred to as a time cue (Freestone et al., 2013). To ensure final shaping of the behaviour, a random delay, reward window and intertrial interval (ITI) were introduced in addition to time-out period instituted in the action suppression phase.

First, a random delay (drawn from a uniform distribution within 0.5–1.5 s) between the self-initiated nose poke and presentation of the sound onset requires that rats pay attention to the stimulus, as the time for reward availability becomes contingent on the presentation of the stimulus and not on the nose-poke. If the rat exited the hold port during the random delay this was referred to as a "too early" trial and resulted in a time-out. The reward window was defined as the time window in which the rat needed to release the nose poke hold in order to receive reward. In order to obtain the reward, the animal had a reward window in which to respond. The reward window began 2.25 s after the start of the cue and lasted 1 s after the end of cue. Upon nose poke release in the reward window a reward pellet could be triggered by the first nose poke into the reward port and resulted in a correct trial. Nose poke releases that occurred after stimulus onset but before the reward window resulted in an incorrect trial indicated to the rat by a time-out period. Nose poke releases that occurred beyond the reward window were unpunished and unrewarded and were registered as "too late" trials. The time it took for the rat to move from the hold port to the reward port was defined as the reward latency. The animals had a duration of 1.5 s to collect their reward following release from the hold port. After reward collection, a new trial could be initiated after an ITI of 6 s. The ITI is used to indicate a pause between reward and next trial availability. Rats could make nose pokes during the ITI as the nosepokes were not conditioned during that period. Nosepokes registered in the reward port during the ITI were used as

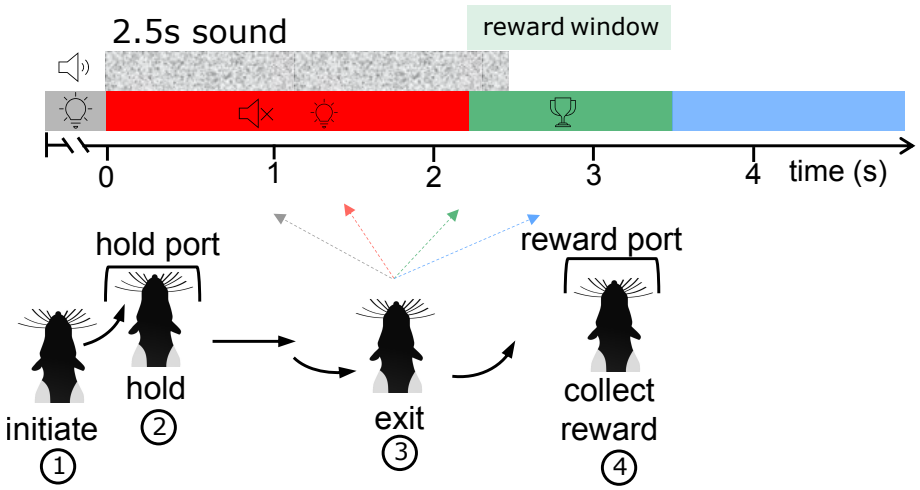

Figure 3.6: **Trial sequence in single-interval timing task with predictable time cue.** The timeline gives the sequence of possible stimulus events in the operant chamber and the numbers indicate the action sequence of the rat. A rat initiates a trial by poking into the hold port (1), triggering, after a random delay, an auditory stimulus of 2.5 s during which the rat has to fixate its nose into the hold port (2). The trial outcome depends on when the rat exits the hold port with respect to the reward window (light green). The grey arrow indicates a trial in which the rat exited too early, the red bar and arrow indicate an incorrect trial in which the sound is turned off and stimulus lights are on, green bar and arrow indicate a correct trial in which a reward can be triggered in the reward port, blue bar and arrow indicate a trial in which the rat did not exit from the hold port in the reward window and is referred to as too late trials.

a proxy for **reward-seeking** behaviour since the reward conditioned sound during this period is absent and nose poking is presumably habit driven (Duuren et al., 2009). Nosepokes registered in the hold port during the ITI were used as a proxy for anticipatory responding (Wood et al., 2006).

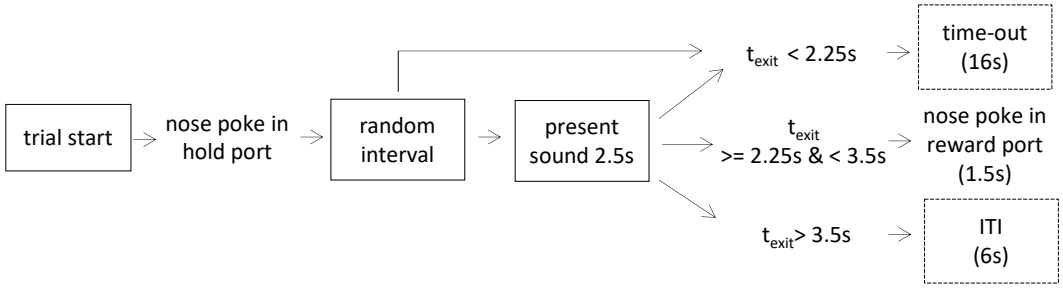

Figure 3.7: **Trial structure of interval timing stage with predictable time cue.** Boxes represent states during a trial, unboxed text indicates action required from the rat, arrows indicate transitions between states. Dashed boxes indicate states that goes back to the start to initiate a new trial and nose poke in the reward port will also result in a new trial. Trials are self initiated by poking into the hold port which triggers the onset of a sound of 2.5 s. The trial outcome will now depend on the time that the rat exits from the hold port.

The rats could learn this single interval timing behaviour with predictable time cue

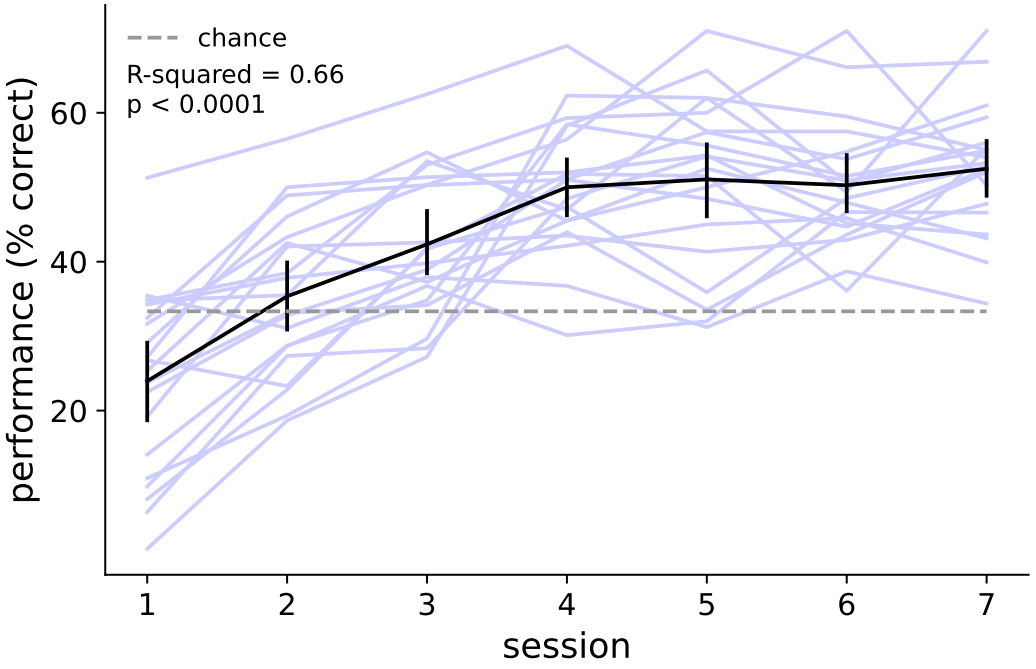

Figure 3.8: **Learning of interval timing stage with predictable time cue.** Learning across 1h training sessions for the first 7 days. Performance is quantified as the number of correct trials over the total number of trials during a session. Black line indicates mean ± SD; light lines indicate individual animals; error bars represent SD; dotted gray line indicates the chance level performance (33% correct).

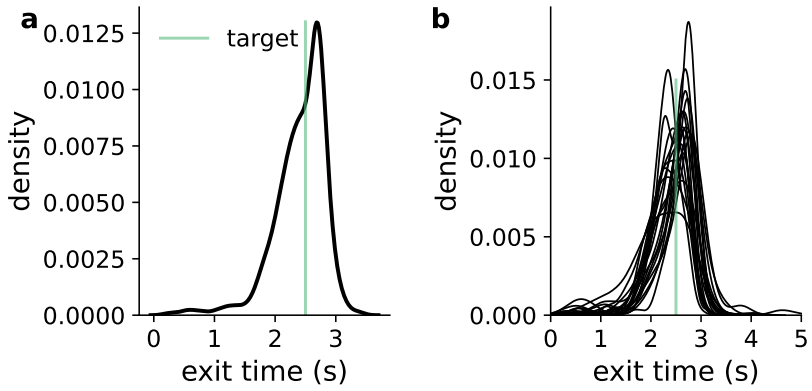

Figure 3.9: **Response distributions during interval timing stage with predictable time cue.**(a) Response distributions across all animals. (b) Individual response distributions. Data represented excluded too early trials.

after about 7 days of training (Fig. 3.8). A GLM was fitted, with percentage trials correct as the dependent variable and session number as the independent variables and rat as the random variable, indicating a significant effect of session number on learning ($R^2 = 0.66$ and p-value < 0.0001). After learning, rats produced the required time interval as average and individual probability density functions of exit times peak after the target duration (Fig. 3.9a, b). A training session was terminated

after 60 min in which rats could perform as many trials as possible. Experimental testing was performed once the rats have reached the criteria listed in Table 3.1.

3.2.4.1.7 Single-interval timing task with unpredictable time cue

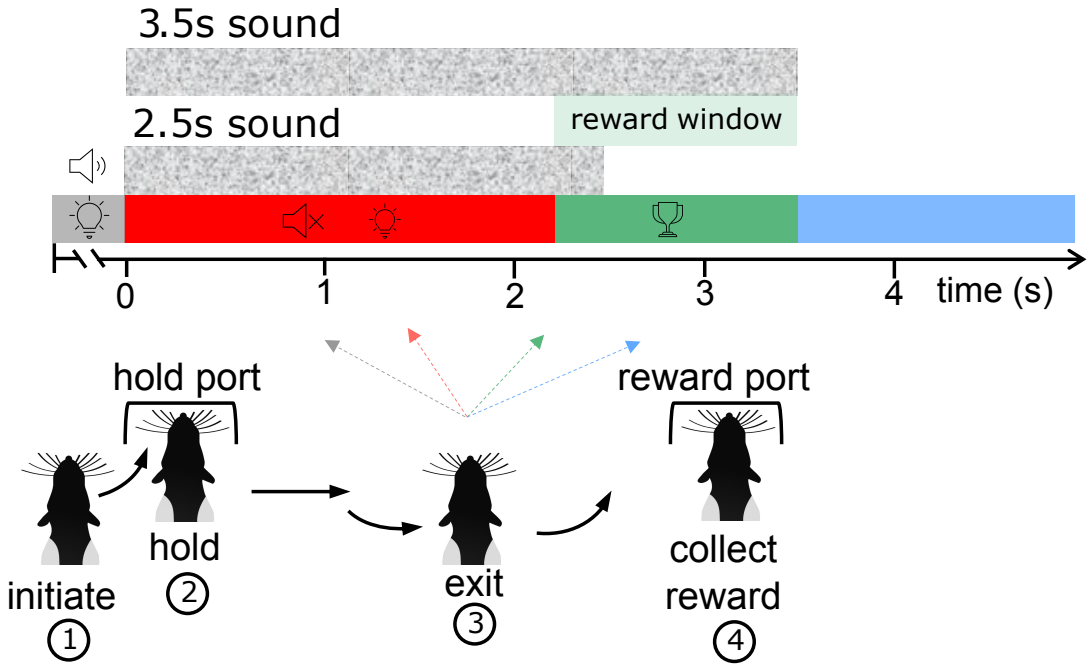

Figure 3.10: **Trial sequence in single-interval timing task with unpredictable time cue.** A rat initiates a trial by poking into the hold port (1), triggering, after a random delay, an auditory stimulus during which the rat has to fixate its nose into the hold port (2). In 50% of the trials the duration is 2.5 s and in randomized other 50% of the trials the sound has a duration of 3.5 s. The rest of the trial structure is the same as in Fig. 3.6.

After rats were trained and tested on the single interval timing task with predictable time cue, they moved on to the next stage of the task where trials with predictable time cue occurred randomly in 50% of the trials (Fig. 3.10 and Fig. 3.11). In the other 50% of trials, the same sound was played but for a longer duration (3.5 s). These trials are referred to as uncued trials, because exit from the hold port is not be cued by offset of the sound (Fig. 3.10). This stage tested the rats' ability to estimate a time interval rather than respond to or anticipate a sensory cue. Overall this stage used the same task parameters, i.e. random delay, reward window, ITI and time-out as in section 3.2.4.1.6. The trials in which the duration of the sound was the instructed target duration are referred to as cued trials. A training session was terminated after 60 min, in which rats could perform as many trials as they could. Experimental testing was performed once the rats have reached the criteria listed in Table 3.1. When reaching the criterion, rats produced the required time interval as average and individual probability density functions of exit times for both the cued and uncued trials peak around the target duration (Fig. 3.12a, b and c).

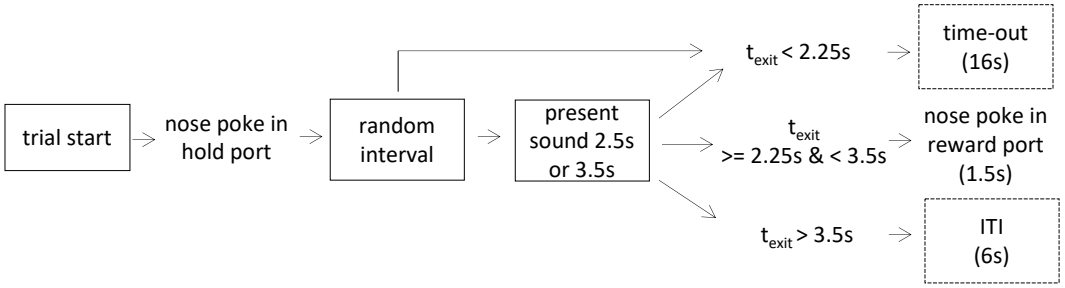

Figure 3.11: **Trial structure of interval timing stage with unpredictable time cue.** Boxes represent states during a trial, unboxed text indicate action required from the rat, arrows indicate transitions between states. Dashed boxes indicate states that go back into trial start and nose poke in the reward port will also result in a new trial. Trial structure is the same as in section 3.2.4.1.6, but now in 50% of the trials the duration is not indicated by a tone offset.

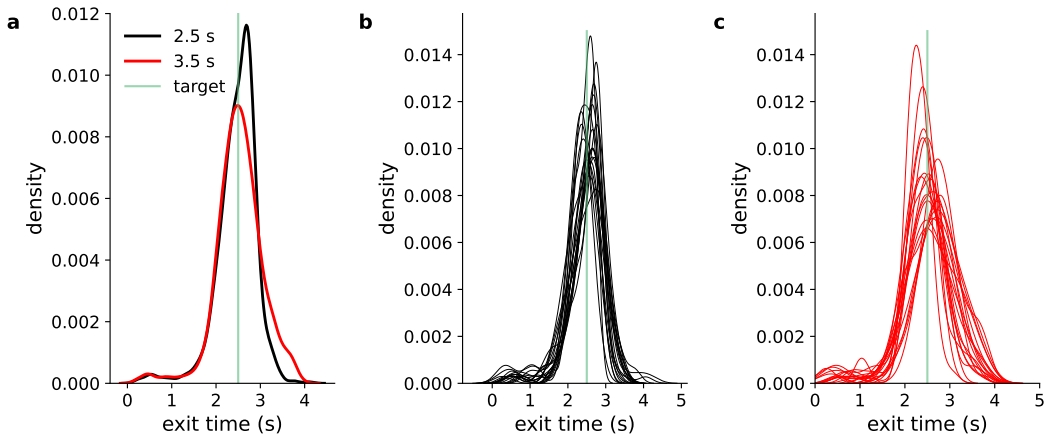

Figure 3.12: **Response distributions during interval timing stage with unpredictable time cue.**(a) Response distributions across all animals. (b, c) Individual response distributions across cued trials (black) and uncued trials (red). Data represented excluded too early trials.

3.2.4.2 Open field

Open field behavioural testing (n=12, batch 2) was performed to determine if chemogenetic inhibition of cerebellar output had any general effect on motor performance. Open field performance was assessed 30 minutes following CNO injection. Days of open field testing was separate from behavioural testing on the interval timing task. Rats were placed in the centre of a cylindrical arena (90 cm diameter, 51 cm height) which was placed on a black matte plastic base on the floor. Rats were allowed to freely explore the arena for 10 minutes. The behavioural testing occurred in white light (± 140 lux). Behaviour was monitored by an overhead webcam at 30 frames per second (fps). The arena was cleaned with 70% ethanol between each animal. A second open field behavioural test (n=12) was performed approximately 3 months after the first in the same animals. To minimize change in ambulation due to repeated open field exposure, the open field setup was placed in a different experimental room. For the second open field one animal from the control group

was excluded from the analysis due to faulty video recording.

3.2.5 Video recordings

During behavioural training and experimental testing animal behaviour was monitored via a camera (Microsoft LifeCam HD-3000) which was attached to the ceiling of the operant chamber above the hold port. Behaviour during experimental sessions in which a manipulation was applied were recorded at 30 frames per second (fps).

3.2.6 Behavioural measures

3.2.6.1 Open field

After data acquisition, rats were tracked using DeepLabCut software (Mathis et al., 2018) with the position of the implanted cannula used to extract the distance travelled as well as the average velocity using custom written scripts in Matlab.

3.2.6.2 Single-interval timing task

In order to test if chemogenetic manipulation of cerebellar circuits affected general motor performance in the operant box while performing single interval timing a number of parameters were measured. This included (i) the total number of trials performed; (ii) a measure of **reward-seeking** behaviour extracted by summing the number of nosepokes in the hold port during the ITI; and (iii) a measure of anticipatory behaviour extracted by summing the number of nosepokes in the reward port during the ITI. Then, to test if chemogenetic manipulation of cerebellar circuits affected the rats' ability to perform the single interval timing task, three metrics were calculated: (i) overall task performance (eq. 3.1), is the percentage of correct trials, calculated as the number of trials in which the cue was presented and the rat exited the hold port in the reward window, over the total number of trials that the rat initiated, calculated as

$$\text{Performance } (\%) = \frac{N_{2.25<t_{exit}<3.5}}{N_{total}} \times 100 \tag{3.1}$$

(ii) exit time for each trial (eq. 3.2), which is time of hold port release released subtracted by sound onset, both measures with respect to trial start, calculated as

$$t_{exit}(\text{s}) = t_{release} - t_{onset} \tag{3.2}$$

with t(0)=trial start, and (iii) reward latency for each correct trial (eq. 3.3), measured as the time between exit from the hold port and nose poke in the reward port on correct trials, calculated as

$$t_{reward}(\text{s}) = t_{reward} - t_{release} \tag{3.3}$$

with t(0)=trial start All the behavioural measures were extracted from the raw output of each session via custom written scripts in MATLAB, 2010.

3.2.7 Drug administration

Drug administration during behavioural testing was performed first on the single-interval timing task with predictable time cue and then on the single-interval timing task with unpredictable time cue. Rats achieved steady state performance on either stage in order to undergo behavioural testing (see Table 3.1). Rats performing the single-interval timing task (n=20) were administered with either vehicle or CNO. Typically, drug or vehicle was administered on two days (Tuesday and Thursday) interleaved with 3 baseline sessions (Monday, Wednesday and Friday). During a baseline session the animals did not receive a drug. At each stage rats first completed behavioural testing with intraperitoneal injections and then with intracranial infusions.

3.2.7.1 Intraperitoneal injections

All animals were injected intraperitoneally (IP) using a single handed modified restrained method to minimize stress and improve welfare (Stuart et al., 2015). Animals were habituated to the modified restrained method for approximately one week. On the day of injection either ClozepineN-Oxide (CNO; Tocris, UK), dissolved in 5% DMSO and diluted with 0.9% NaCl to a final concentration of 2.5 $\frac{ml}{kg}$, or an equivalent vehicle was, 1 $\frac{ml}{kg}$, 0.9%saline with 5% DMSO. Behavioural testing began 30 minutes following the injection.

3.2.7.2 Infusions

Rats were habituated to the infusion procedure during one session where animals were lightly restrained and the stylet removed and then replaced. During infusions, rats were gently restrained while the dust cap and guide cannula were removed and a bilateral 33-gauge internal cannula extending 1 mm beyond the length of the guide cannula was inserted. The internal cannula were attached to PVC tubing (0.5 x 0.5mm, Appleton woods Ltd., UK) containing drug or vehicle solution backfilled with oil. Infusions of 500 nl per hemisphere were delivered over 1 minute, and the cannula was left in place for a further 3 minutes before the dummy cannula was replaced. Behavioural testing began 15 minutes after the start of the infusion. CNO was prepared 3 μM (with final concentration of DSMO 0.005%) and vehicle was 0.9% saline with 0.005% DMSO.

3.2.8 Randomisation and blinding

Unless stated otherwise, this study used a 2-x-2 experimental design where the experimenter was blinded to the combinations of experimental and control viruses with treatment administration of either CNO or vehicle delivery. Randomisation was performed by a researcher detached from the experimental study. First, animals within a batch were randomly assigned to one of the experimental groups: control group (n=10) or the treatment group termed 'DREADD' (n=10). During surgery (see section 3.2.3), the experimenter was blinded to the identity of the virus that was used for transfection. During behavioural testing on interval timing task (see section 3.2.4.1) randomisation to treatment administration (see section 3.2.7), vehicle or CNO, was performed in a similar way unless stated otherwise. For the open field (see section 3.2.4.2) there was no vehicle comparison.

3.2.9 Histology

Upon completion of the experiments, all animals were anaesthetised with a lethal dose of Euthatal (200 $\frac{mg}{kg}$, Merial Animal Health Ltd, Harlow, UK) and transcardically perfused with 0.9% saline followed by 4% paraformaldehyde. Each brain was dissected and postfixed in paraformaldehyde. After several days, it was transferred to 30% sucrose in phosphate buffer (PB) and stored until sectioning. Prior to being cut, each brain was embedded in gelatin. Blocks containing either the cerebellum or the thalamus were mounted separately on a microtome (SM2000R, Leica) using Cryomatrix embedding medium (Thermo Scientific) and frozen for sectioning. All sections were cut at 40 µm, for the cerebellum sections were cut sagitally and for the thalamus coronally. Sections were collected in 0.01% PB and prepared for immunohistochemistry to visualize viral expression of the control or DREADD receptor. In brief, sections were washed 3 times in 0.01% PBS and placed in 50% ethanol for 30 minutes. After a further 3 washes, sections were placed overnight in a primary antibody (chicken anti-eGFP (Abcam) or rabbit anti-mCherry (Biovision), 1:2000, 5% normal horse serum). On day 2, after 3 washes, sections were incubated for 2h in a secondary antibody (goat anti-chicken (Alexa 488) or donkey anti-rabbit (Alexa 594), 1:1000, in PBS-T; Jackson). Finally, sections were mounted using 1% gelatin and 0.1% chromium potassium sulphate solution. Fluoromount with DAPI, a stain for all cell nuclei, was applied to the slides before they were cover slipped to prepare for imaging.

3.2.10 Microscopy

To assess transfection of the virus and placement of the cannula (Figure 3.8), sections were visualised using a fluorescent Axioskop 2 Plus microscope (Zeiss) fitted with a CoolLED pE-100 excitation system and images acquired using AxioVision software. Locations of the final injector tip positions in the thalamus were mapped onto standardized coronal sections of a rat brain stereotaxic atlas (add ref Paxinos and Watson, 1998). Transfection of the virus in the deep cerebellar nuclei

was assessed as follows: cerebellar sections were mapped onto standardized sagittal sections of a rat brain using a stereotaxic atlas (George et al., 2007). Sections at key anatomical points 0.18 mm, 0.9 mm, 1.4 mm, 1.9mm, 2.4mm, 2.9mm, 3.4mm, 3.9mm, 4.2mm and 4.6mm from midline were identified and used for manual scoring of fluorescence intensity. Fluorescence intensity was scaled from 0-5, with 0 no fluorescence and 5 maximal fluorescence across sections. In each animal, sections with maximum and minimum fluorescence were determined by comparing the sections to each other while keeping illumination settings constant. The section with maximum fluorescence was determined as the section with the largest fluorescent halo around the injection site. Then each section was divided in three regions: cortex, nuclei and fibers. A fluorescence score was determined per region by comparing within and across sections. The scores were registered in .xlsx files. As a first approximation in determining spread of fluorescence, the fluorescence scores of the nuclei were used to visualize the spread of the injection (see figure 3.13).

3.2.11 Data Processing

All analyses were done using custom-written scripts in Matlab (version 2021a), Python (version 3.9) and RStudio (version 4.0.3). The output from the K-limbic operant control system software was saved as a table structured format. Custom code was developed in Matlab to read through the output forms, map the data into a common table format and pre-process the data. Both Matlab and Python scripts were used for extracting parameters of the preprocessed data and plotting. Statistical analysis was completed in R or Python.

3.2.12 Statistical analysis

Independent-samples t-test was used to compare the scores of each behavioural metric in the open field test separately. The comparison was made to test if there was a statistically significant difference on each score between the control and DREADD virus group when given systemic injection of CNO. General linear models, a generalization of linear models, were used to represent the independent variables, which were the behavioural metrics of the interval timing experiment, as a linear combination of the dependent variables given by experimental design and a random term (equation 3.4). These statistical techniques take into consideration multiple levels of correlation in the dataset and were therefore preferred over classic statistical tests in neuroscience, such as t-test and ANOVA. Animals were split via two experimental factors, with compound administration as the within-subject factor, with levels vehicle and CNO, and virus group as the between-subject factor with levels control and DREADD group. The compound administration route is either a systemic injection or intracranial infusion depending on the experiment. Thus, for each behavioural metric the GLM was formulated as:

$$Y \approx administration \times group$$

Assuming the behavioural measure of interest follows a gaussian distribution, the hypothesis can be formalized as shown below:

$$Y_{group,administration} = \beta_0 + Group\beta_{group} + administration\beta_{administration} + \epsilon \quad (3.4)$$

More specifically, the effects, denoted by β, of compound administration, group and interaction between compound administration and group are estimated using statistical optimization methods (maximum likelihood; Farrell et al., 2018) with a random term ϵ. Where appropriate an extension to the GLM was used, called the generalized linear mixed model (GLMM) that allows the effects of compound administration and group via maximum likelihood, but also estimates correlated variability in the behavioural measures that are assumed to come from repeated measures. These arise from collecting multiple trials as each animal underwent saline and CNO administration over two different sessions. Where appropriate we considered rat ID, session date and trial number as repeated measures.

3.3 Results: systemic modulation of cerebellar output pathway during interval timing

3.3.1 Cerebellar manipulation using chemogenetics

In order to gain a better understanding of the role of the dentate cerebellar nuclei in interval timing an inhibitory DREADD virus was used to chronically manipulate cerebellar output during the single-interval timing task. Either a control or DREADD virus was stereotaxically infused bilaterally into the cerebellum, centred on the dentate nucleus on both sides (for further details see Methods section 3.2.3, Fig. 3.13a). Following successful transfection of cerebellar neurons, intraperitoneal injection of clozapine N-oxide (CNO), should lead to a systemic activation of the inhibitory DREADD receptor (hM4D(Gi)) but not the control protein (EGFP) (Fig. 3.13b). Histological processing and microscopic verification showed that both

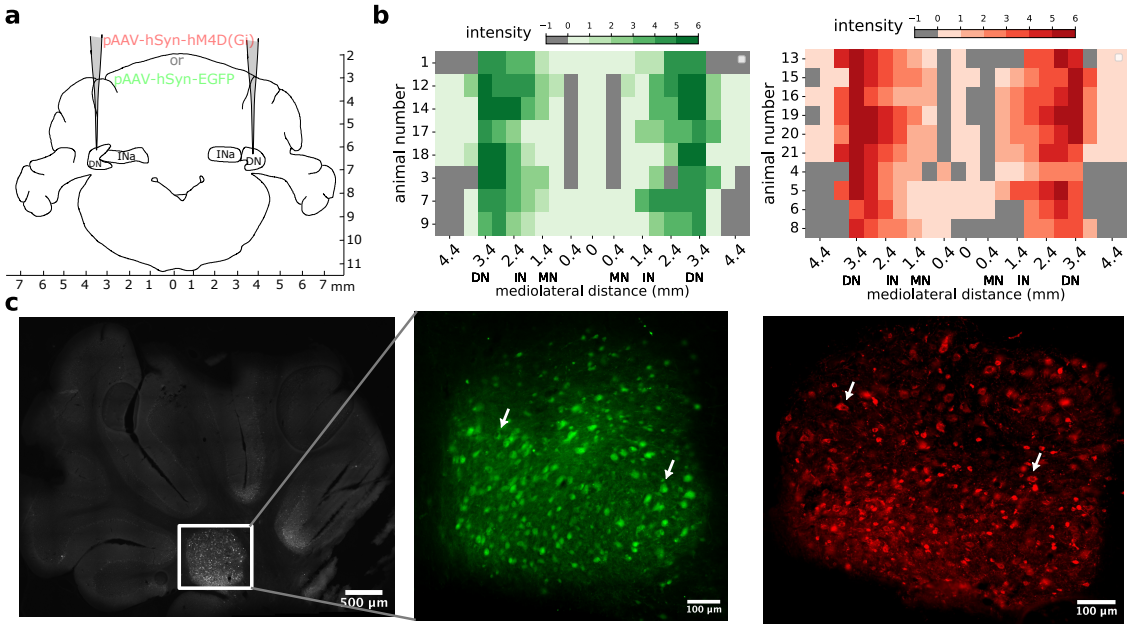

Figure 3.13: **Cerebellar manipulation using chemogenetics.** (**a**) Schematic of viral-mediated delivery of control or DREADD receptor. Bilateral injections targeted the dentate nucleus (DN; INa=anterior interpositus) of the cerebellum. (**b**) Heatmaps showing the extent of EGFP and hM4D(Gi) mCherry expression across the mediolateral axis of the cerebellar nuclei respectively (DN=dentate nucleus, IN=interpositus nucleus, MN=medial nucleus). Colours of heatmap indicate level of expression with no expression at 0 and maximal expression at 5, grey indicates sections in which expression could not be quantified. (**c**) A sagittal section of the dentate nucleus on the left, white frame indicating the cerebellar dentate nucleus. Representative example of viral vector expression at the dentate showing EGFP expression (white arrows) in DTITET 12 of the control group (middle) and hM4D(Gi) mCherry expression (white arrows) in DTITET 21 of the DREADD group (right).

the control and DREADD virus were reliably expressed in the dentate nucleus

(Fig. 3.13c). Semi quantitative mapping of the expression across the cerebellar nuclei (Fig. 3.13b and see section 3.2.10 for details) showed that expression was generally centred on, but not restricted to, the dentate nucleus. Therefore, the subsequent results are presented as a result of manipulation of cerebellar output.

3.3.2 Effect of cerebellar manipulation on open field exploration

As a first step it was important to assess whether chemogenetic inhibition of cerebellar output had any general effect on motor performance. The effect of systemic CNO administration on open field exploration in the DREADD group ($n = 6$) was compared to the control group ($n = 6$) (Fig. 3.14a, b). During an initial exposure (Fig. 3.14a-d, first exposure) to the open field arena the DREADD group, compared to control, showed a statistically significant reduction in open field exploration, expressed as total distance travelled (Fig. 3.14c, DREADD (n=6): tot. dist. (m) = 29.45 ∓ 19.5; control (n=5): tot.dist (m) = 61.37 ∓ 11.71, p-value < 0.01); as well as a lower average velocity (Fig. 3.14d, DREADD (n=6): av. vel. $(cm/s) = 5.63 \mp 3.75$; control (n=5): av. vel. $(cm/s) = 12.78 \mp 2.0$, p-value < 0.01). These results provide a positive control that CNO activation of DREADD transfected cells in the cerebellar nuclei was effective but that general motor effects may be a confound in the interval timing task. Moreover, open field exploration in the DREADD group was more variable than the control group (Fig. 3.14c, d) presumably because of differences in expression levels between animals.

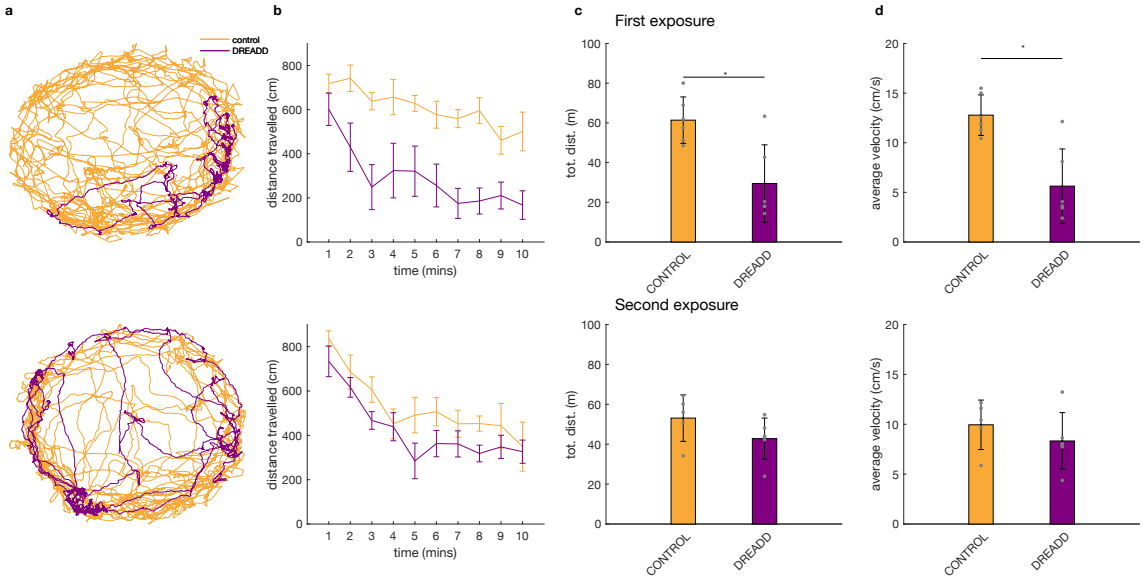

Figure 3.14: **Non-stationary effect of cerebellar manipulation on open field exploration.** (**a**) Example trajectories of exploration in two animals for control and DREADD during first (top) and second (bottom) exposure (**b**) Average distance travelled for control (orange) and DREADD (purple) groups across the 10 minute session during first and second exposure. (**c**) Average total distance travelled for control (orange) and DREADD (purple) groups across the 10 minute session during first and second exposure. (**d**) Same as c but average velocity.

An additional consideration is the possibility that the effectiveness of the DREADD and CNO interaction changed over time (Claes et al., 2022). Indeed, home-cage monitoring performed by the experimenter indicated a transient effect of repeated systemic CNO injection on home cage exploration. In order to evaluate this change, the open field test was repeated approximately 90 days after the first exposure to the arena. To minimize any changes in motor activity due to repeated open field exposure (Russell et al., 1973; Donald et al., 2011), the second open field exploration (Fig. 3.14a-d, second exposure) was performed in a novel experimental room. During this second exposure, exploration was reduced in DREADD versus the control group (Fig. 3.14a bottom), however this was less pronounced than during the first exposure (Fig. 3.14b bottom). Similarly, there was a reduction in average total distance travelled and average velocity but this was not statistically different (DREADD (n=6): tot. dist. (m)= 42.81 $\mp$ 10.32, av. vel. (cm/s) = 8.33 $\mp$ 2.84; control (n=5) tot. dist. (m) = 53.1 $\mp$ 11.67, av. vel. (cm/s) = 9.95 $\mp$ 2.48, p-value > 0.05). These results indicate that repeated CNO administration on hM4D(Gi) function would appear to diminish over time, that is the effect on general motor activity is non-stationary.

3.3.3 General motor performance during cerebellar manipulation in single-interval timing task

To further assess whether chemogenetic inhibition of cerebellar output via systemic CNO injection had a general effect on motor performance, behavioural activity in the operant box was analyzed while rats performed the single-interval timing task with predictable time cue. The behavioural sessions were divided into 4 groups: (i) control virus with vehicle, (ii) DREADD virus with vehicle, (iii) control virus with CNO and (iv) DREADD virus with CNO . In terms of experimental classification for analysis 'Vehicle' involved groups (i) and (ii) while 'Manipulation' involved groups (iii) and (iv). Since the dataset contains repeated measures and multiple groups, general linear mixed-effects models (GLMM) were used to interrogate the results. The GLMMs included data from two batches of animals (n=20 rats in total). The first batch of animals involved groups (iii) (n=4) and (iv) (n=4) , that is manipulation only sessions (n=8 rats in total). The second batch included all 4 groups, that is vehicle and manipulation sessions (n=12 rats).

First, the total number of trials executed in the operant box was analysed using a GLM with number of trials per session as the dependent variable and group and manipulation as the independent variables. Results of the model indicated that there was no statistically significant difference in the total number of trials performed ($p > 0.05$)(Fig. 3.15a). To quantify reward-seeking behaviour the number of nose pokes in the reward port during the inter-trial interval (ITI, see Methods Section 3.2.4.1.5) was also assessed (Fig. 3.15b). Nose pokes during this time period occur in the absence of a conditioned stimulus and are presumably therefore thought to be mainly the result of reward-seeking behaviour (Duuren et al., 2009). A GLM, with a negative binomial distribution, was fitted with the number of nosepokes in the reward port as the dependent variable and manipulation and group as the independent variables and session date as the random variable. There was a significant

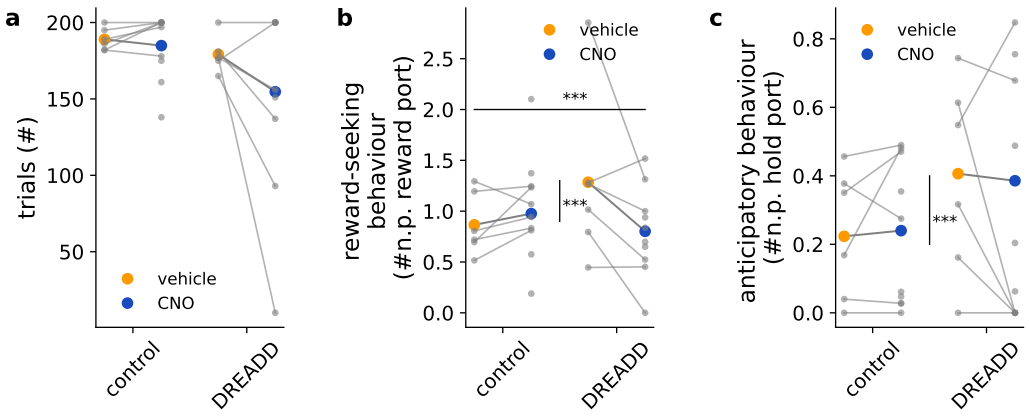

Figure 3.15: **General motor performance during cerebellar manipulation in single-interval timing task with predictable time cue.** (**a**) Interaction plot of total number of trials during a behavioural session given by the population means for CNO (blue, n=10) and vehicle (orange, n=10) in each group respectively. Individual means of each group are given by the grey circles and trend lines. (**b**) Interaction plot of average reward-seeking behaviour during a behavioural session, plotted in the same way as in **a**. (**c**) Interaction plot of average anticipatory behaviour during a behavioural session. *:$p < 0.01$, **: $p < 0.001$ ***: $p < 0.0001$.

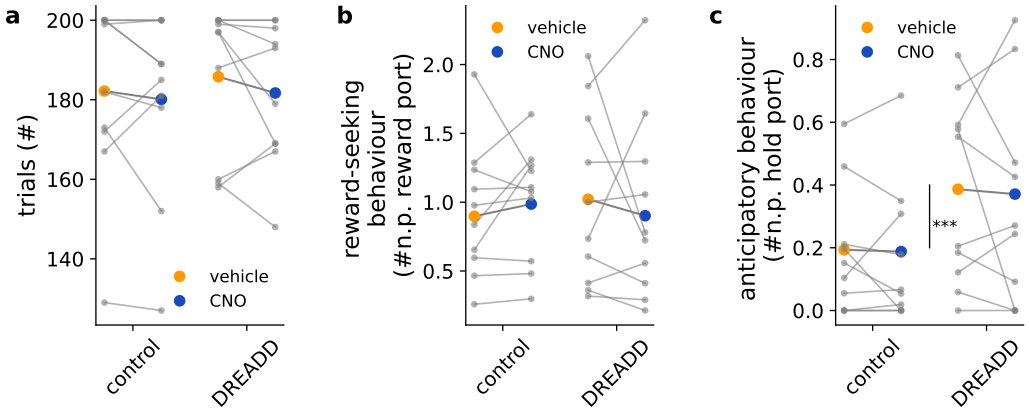

Figure 3.16: **General motor performance during cerebellar manipulation in single-interval timing task with unpredictable time cue.** (**a**) Interaction plot of total number of trials during a behavioural session given by the population means for CNO (blue, n=10) and vehicle (orange, n=10) in each group respectively. Individual means of each group are given by the grey circles and trend lines. (**b**) Interaction plot of average reward-seeking behaviour during a behavioural session, plotted in the same way as in **a**. (**c**) Interaction plot of average anticipatory behaviour during a behavioural session. *:$p < 0.01$, **: $p < 0.001$ ***: $p < 0.0001$.

effect of the interaction between group and manipulation (p-value < 0.0001), indicating reward-seeking behaviour was 0.553 times lower in the DREADD group when injected with CNO (95% CI=[0.445, 0.687]). While there was no significant effect of manipulation alone, there was a significant effect of group independent of manipulation on reward-seeking behaviour, indicating that the DREADD group exhibited increased reward-seeking behaviour by a factor of 1.49 (95% CI=[1.254,

1.758], p-value < 0.0001). Similarly, to evaluate anticipatory behaviour the number of nose pokes in the hold port during the ITI (Fig. 3.15c) was quantified in the same way. While there was no significant effect of the interaction between group and manipulation nor manipulation alone, there was a significant effect of group independent of manipulation, indicating that the DREADD group exhibited 1.82 times (95% CI=[1.413, 2.347], p-value < 0.0001) more anticipatory behaviour than the control group.

General motor performance was also assessed in the same group of animals (n=20) performing the single-interval timing task with unpredictable time cue. Now, the GLMs included data from all 4 groups, i.e vehicle and manipulation sessions. The GLMs were defined in the same way as in the previous training stage. Overall, the trend was similar to the previous training stage. A similar number of trials was executed by both the control and DREADD group during vehicle and CNO manipulation, as during the earlier training stage (3.16a). There was no significant effect of the interaction between group and manipulation on reward-seeking behaviour (3.16b). Similarly, to evaluate anticipatory behaviour the number of nose pokes in the hold port during the ITI (Fig. 3.16c) was quantified. There was a significant effect of group, indicating that the DREADD group exhibited a 2.0 fold increase (95% CI=[1.649, 2.424], p-value < 0.0001) in anticipatory behaviour.

Taken together these results indicate that, although chemogenetic manipulation of cerebellar output (especially when the animals received their first systemic CNO injection) leads, on average, to reduced open field exploration, there is a less profound effect on general motor activity in the operant box. Although cerebellar manipulation, as a result of the interaction between group and manipulation, leads to reduced reward-seeking behaviour, there is no detectable effect on anticipatory behaviour. However there is an effect of group on both reward-seeking and anticipatory behaviour, indicating DREADD expression might have an effect on general motor performance independent of CNO. On the contrary, there is no detectable effect of manipulation that might be indicative of any off target effects of CNO.

3.3.4 Cerebellar manipulation during single-interval timing task with predictable time cue

As a first step to assess if chemogenetic manipulation of cerebellar output affects a rat's ability to perform interval timing, rats were trained to predict the duration of a sound (see section 3.2.4.1.6 for details). In brief, a white noise with a duration of 2.5 s was presented on every trial. Food reward was delivered if the rat nose poked in the reward port after exiting the hold port in a time window of 2.25 s to 3.5 s. When rats achieved stable performance (see Table 3.1) on this single-interval timing task with predictable time cue, CNO or vehicle was injected intraperitoneally in two separate behavioural sessions. Three measures were taken per session: (i) overall task performance, measured as percentage of correct trials, (ii) exit time for each trial (the time from sound offset for the rat to remove its nose from the hold port), and (iii) reward latency for each correct trial (the time between exit from the hold port and nose poke in the reward port on correct trials). The data presented originated

from the same animals and sessions as when the general motor performance was quantified. As such the behavioural sessions were divided in the same way. In brief, the GLMs included data from two batches of animals (n=20 rats in total). The first batch of animals involved groups (iii) (n=4) and (iv) (n=4) , that is manipulation only sessions (n=8 rats in total). The second batch included all 4 groups, that is vehicle and manipulation sessions (n=12 rats).

First, to assess if cerebellar manipulation affects performance a GLM was fitted to the data, where reward was the dependent variable and manipulation and group were the independent variables (Fig. 3.17a). While there was a significant effect of manipulation alone, indicating an increase of 4.1% (95% CI [0.438, 7.824], p-value < 0.01) in performance when given CNO, there was no significant effect of group nor interaction between group and manipulation. This indicates that although the mean performance after administering CNO is somewhat higher than after administering vehicle, regardless of group, there is no effect of cerebellar manipulation as a consequence of the interaction of group and manipulation.

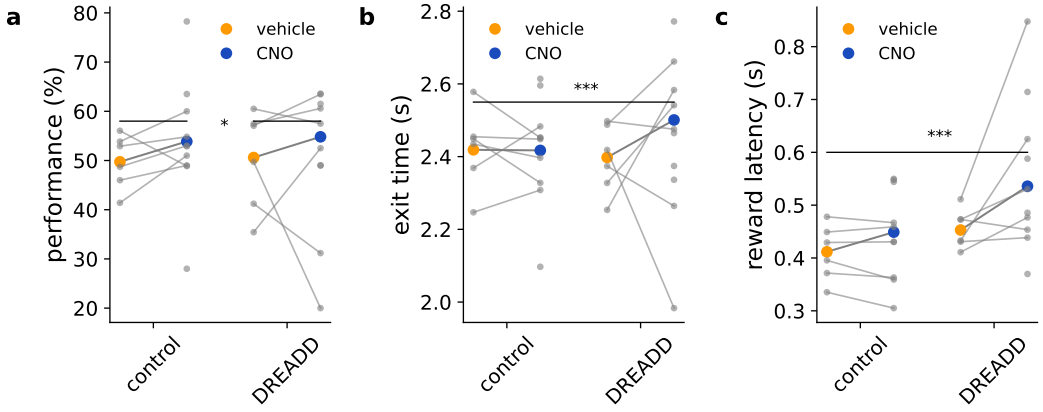

Figure 3.17: **Effect of cerebellar manipulation during single-interval timing task with predictable time cue.** (**a**) Interaction plot of overall performance during a behavioural session given by the population means for CNO (blue, n=10) and vehicle (orange, n=6) in each group respectively. Individual means of each group are given by the grey circles and trend lines. (**b**) Interaction plot of average exit time during a behavioural session, plotted in the same way as in **a**. (**c**) Interaction plot for reward latency. *:$p < 0.01$, **: $p < 0.001$ ***: $p < 0.0001$.

Next, to assess if cerebellar manipulation affects the time it takes for the rat to exit from the hold port a GLMM model was fitted to the data, setting exit time as the dependent variable, manipulation and group as the independent variables and animal ID, trials and session date as the random term (Fig. 3.17b). There was a significant effect of the interaction between group and manipulation, indicating an increase of 0.16 seconds (95% CI [0.079-0.237], p-value < 0.0001) in exit time for the DREADD group with CNO. Similarly, there was a significant effect of the interaction between injection and group on reward latency (Fig. 3.17c), indicating an increase of 0.08 seconds (95% CI [0.06 0.09], p-value < 0.0001) for the DREADD group upon CNO injection. This suggests that cerebellar manipulation affects exit time and reward latency such that rats from the DREADD group, when given CNO, maintain their position in the hold port for longer while being slower when moving to the reward

port. Overall, these results suggest that although cerebellar manipulation has no detectable effect on overall performance, it induces slowing of movement, resulting in delayed exit time and increased reward latency.

To further evaluate the effect of vehicle versus manipulation on task performance in the single interval timing task with predictable time cue, cumulative plots of exit time per session were constructed. Examples from 3 animals representative of the material as a whole are shown in (Fig. 3.18). By comparison to vehicle the pattern of response after systemic CNO injection in DREADD animals could be divided into three types: animals in which there was an increase in exit time (Fig. 3.18a); animals in which there was a decrease in exit time (Fig. 3.18b), and animals in which there was no change (Fig. 3.18c). The results for all animals in each group are summarised in the bar charts in (Fig. 3.18d), indicating that the proportion of DREADD and control animals grouped according to three categories indicated there is a larger proportion of DREADD animals with delayed exit time in the CNO session compared to vehicle.

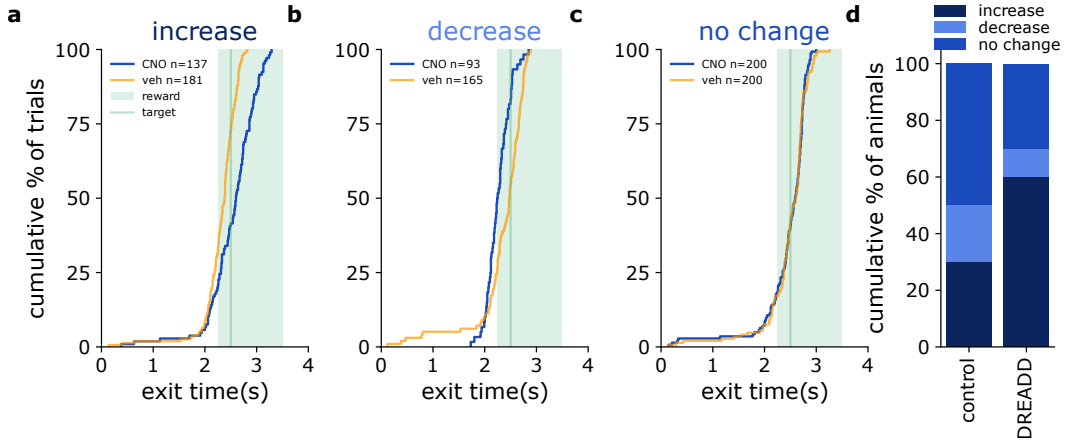

Figure 3.18: **Cumulative plots of exit time during single-interval timing task with predictable time cue** (**a**) Example animal showing a rightward shift of the cumulative plot of exit times, indicating a delay in exit from the hold port. The number of trials per CNO and vehicle session is given. (**b**) Example animal showing an leftward shift of the cumulative plot of exit times, indicating earlier exits from the hold port. The number of trials per CNO and vehicle session is given. (**c**) Example animal showing no change in exit times. The number of trials per CNO and vehicle session is given. (**d**) Bar plot showing the cumulative percentage of animals clustered according to the three observed responses for the control and DREADD virus group.

These results suggest that, on average, cerebellar manipulation during a single-interval timing task with predictable time cue results in delayed temporal judgements, manifested by maintaining nose poke in the hold port for longer and delayed exit times.

3.3.5 Cerebellar manipulation during the single-interval timing task with unpredictable time cue

In the single-interval timing task with predictable time cue the sound offset signals the time at which the animals can terminate nose poke in the hold port (cued trials). This means that the task is predictable because animals can learn to use stimulus offset to exit the hold port to obtain their food reward. In order to dissociate stimulus offset from reward, an element of unpredictability was therefore introduced into sessions in which the duration of the sound was randomly varied between a duration of 2.5 s (cued trials for reinforcement) and 3.5 s (uncued trials), with the reward time window in both cases occurring around 2.5 s (as in the single-interval timing task with predictable time cue, section 3.3.4). Over each session the number of cued and uncued trials was balanced and randomized. In these sessions, uncued trials therefore tested if rats can reliably estimate the time interval from the sound onset to exit the hold port to receive the reward.

As above GLMs were used to estimate the effect of cerebellar manipulation on single-interval timing task with unpredictable time cue. All GLMs included data from the same two batches of animals, each batch included all 4 groups, that is vehicle and manipulation sessions (n=20 rats).

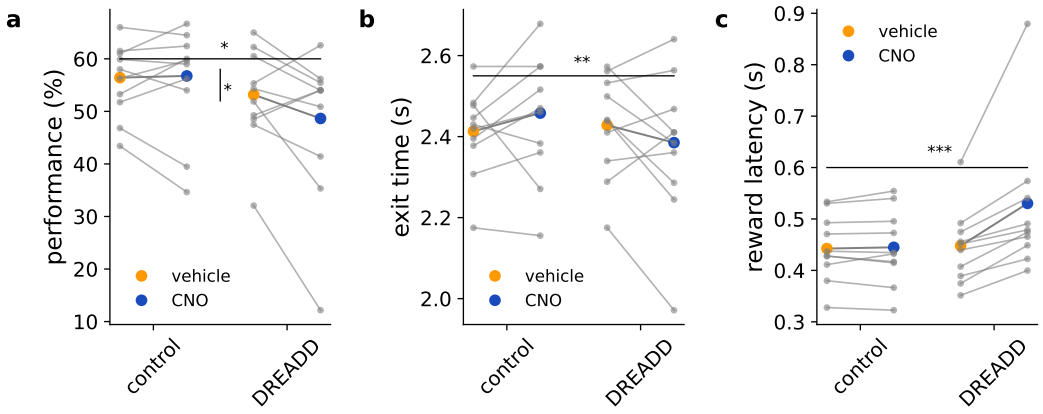

Figure 3.19: **Effect of cerebellar manipulation during single-interval timing task with unpredictable time cue.** (**a**) Interaction plot of overall performance during a behavioural session given by the population means for CNO (blue, n=10) and vehicle (orange, n=6) in each group respectively. Individual means of each group are given by the grey circles and trend lines. (**b**) Interaction plot of average exit time during a behavioural session, plotted in the same way as in **a**. (**c**) Interaction plot for reward latency. *:$p < 0.05$, **: $p < 0.001$ ***: $p < 0.0001$.

First to assess if cerebellar manipulation affects performance a GLM was fitted to the data, setting reward as the dependent variable and manipulation and group as independent variables (Fig. 3.19a). There was a significant effect of the interaction between group and manipulation, indicating that the DREADD group performed on average 4.82% (95% CI [0, 9.442], p-value < 0.05) worse when given CNO (Fig. 3.19a. While there was no effect of manipulation alone, there was a significant effect of group, indicating that the DREADD group performed on average 3.25% (95% CI

[0, 6.515], p-value < 0.01) worse. This indicates that although the mean performance for the DREADD group is lower overall, cerebellar manipulation, a consequence of CNO and DREADD interaction, reduces interval timing performance.

To assess if cerebellar manipulation affects the time it takes for the rat to exit from the hold port a LMM was fitted to the data, setting exit time as the dependent variable and manipulation and group as the independent variables, with rat ID, trial number and session date as the random term (Fig. 3.19b). There was a significant effect of the interaction between group and manipulation, indicating a decrease of 0.09 seconds (95% CI [0.045, 0.141], p-value < 0.001) in exit time for the DREADD group with CNO. There was no effect of manipulation or group alone on exit time. There was also a significant effect of the interaction between manipulation and group on reward latency, indicating an increase of 0.06 seconds (95% CI [0.056 0.08], p-value < 0.0001) for the DREADD group upon CNO injection. Similarly, there was no effect of manipulation or group alone on exit time. This suggests that cerebellar manipulation, affects exit time and reward latency differently, such that rats from the DREADD group, when given CNO, exited from the hold port earlier but are slower when moving to the reward port. Overall, these results suggest that cerebellar manipulation reduces performance in a single interval timing task with unpredictable time cue. Cerebellar manipulation causes rats to prematurely exit the hold port, but then move more slowly to the reward port.

In order to understand if animals were using a timing behaviour and not the tone offset as a cue to predict when they should move, separate analysis for cued and uncued trials was considered. First, to assess if cerebellar manipulation affects the time it takes for the rat to exit from the hold port a LMM was fitted to the data only including cued trials, setting exit time as the dependent variable and manipulation and group as the independent variables, with rat ID, trial number and session date as the random term. The results indicated that there was no significant effect of the interaction between manipulation and group nor an effect of manipulation or group alone. However, when including only the uncued trials there was a significant effect of the interaction between group and manipulation, indicating a decrease of 0.12 seconds (95% CI [0.005, 0.20], p-value < 0.0001) in exit time for the DREADD group with CNO. There was no effect of manipulation or group alone on exit time. These results indicate that the animals are using timing behaviour.

To further evaluate the effect of vehicle versus manipulation on task performance in the single interval timing task with unpredictable time cue, cumulative plots of exit time per session were constructed. Examples from 3 animals representative of the material as a whole are shown in Fig. 3.20. Similar to the interval timing task with predictable time cue (Fig. 3.18) the pattern of response after systemic CNO injection in DREADD animals by comparison to the vehicle could be divided into three types: animals in which there was an increase in exit time (Fig. 3.20a); animals in which there was a decrease in exit time (Fig. 3.20b), and animals in which there was no change (Fig. 3.20c). However, the relative proportion of these types were different (Fig. 3.20d). In particular, there was now a larger proportion of DREADD animals with earlier exit time in the CNO session compared to vehicle.

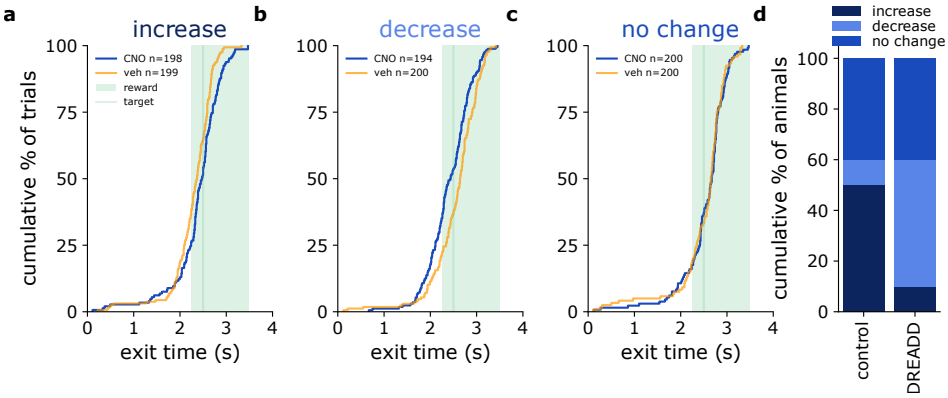

Figure 3.20: **Cumulative plots of exit time during single-interval timing task with unpredictable time cue** (**a**) Example of animal showing a rightward shift of the cumulative plot of exit time, indicating a delay in exit from the hold port. The number of trials per CNO and vehicle session is given. (**b**) Example of animal showing an leftward shift of the cumulative plot of exit time, indicating earlier exits from the hold port. The number of trials per CNO and vehicle session is given. (**c**) Example of animal showing no change in exit time. The number of trials per CNO and vehicle session is given. (**d**) Bar plot showing the cumulative percentage of animals clustered according to the three observed responses for the control and DREADD virus group.

3.4 Modulation of cerebello-thalamic pathway during interval timing

3.4.1 Modulation of cerebello-thalamic pathway

In order to study the role of the cerebello-thalamic pathway in interval timing, CNO was infused intracranially into the ventro-lateral (VL) thalamus. Therefore, the same group of animals (control n=10 and DREADD n=8) were stereotaxically implanted with bilateral cannula (for further details see section 3.2.3, 3.21a, b). Following successful transfection of cerebello-thalamic terminals, intracranial infusion of CNO, should lead to chronic modulation of neurotransmission of the inhibitory DREADD receptor (hM4Di) but not the control protein (EGFP). Histological processing and microscopic verification showed that cerebello-thalamic terminals were consistently labelled following bilateral injection in the dentate nuclei across animals in control and DREADD group (Fig. 3.21c).

3.4.2 General motor performance during cerebello-thalamic modulation in single-interval timing task

The total number of trials executed in the operant box was analyzed using a GLM with the total number of trials per session as the dependent variable and group and manipulation as the independent variables. There was no statistically significant dif-

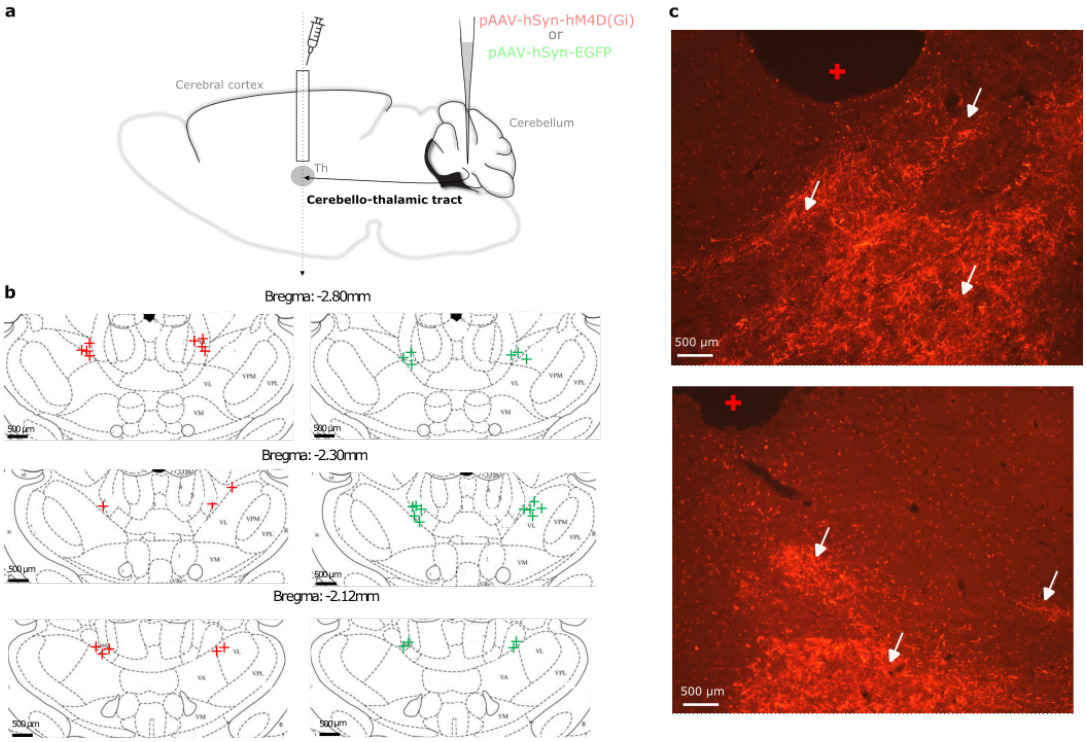

Figure 3.21: **Modulation of cerebello-thalamic pathway using chemogenetics.** (**a**) Schematic overview of intracranial infusion targeting terminals from cerebellar nuclei in the thalamus. (**b**) Summary of infusion sites for the control group (n=10, green crosses) and DREADD group (n=8, red crosses). Crosses indicate the location of cannula tips (i.e. infusion sites) in bilateral thalamus from around 2.12mm-2.80mm posterior to the bregma. VL = ventrolateral; VM = ventromedial; VPM = ventral posteromedial, VPL = ventral posterolateral (**c**) A section showing bilateral cannula placement targeting the VL thalamus for an example of the DREADD group, crosses refer to the location of the cannula tip (see **b**) and arrows indicate groups of labelled terminals.

ference in the total number of trials (3.22a). Next, reward-seeking and anticipatory behaviour were quantified similarly as before and analyzed using GLMMs, with a negative binomial distribution, with the number of nosepokes in the reward port or hold port, respectively, as the dependent variables and manipulation and group as the independent variables and session date as the random term. For both predictable and unpredictable time cue sessions there was no effect of the interaction between group and manipulation, both for reward-seeking and anticipatory behaviour (3.22b, c and 3.23b, c respectively). There was no significant effect for group or manipulation alone on reward-seeking behaviour. However, there was a significant effect of group on anticipatory behaviour, indicating that the DREADD group exhibited increased anticipatory behaviour with a factor of 3.254 (95% CI=[2.452; 4.352], p-value < 0.0001) during sessions with predictable time cue (Fig. 3.22) and 2.26 (95% CI=[1.85, 2.78], p-value < 0.0001) during session with unpredictable time cue (Fig. 3.23). Taken together these results therefore indicate that rats belonging to the DREADD group exhibit more reward-seeking behaviour but that there is no significant effect of the interaction between group and manipulation on all behavioural measures. Thus, chemogenetic modulation of cerebello-thalamic pathway does not

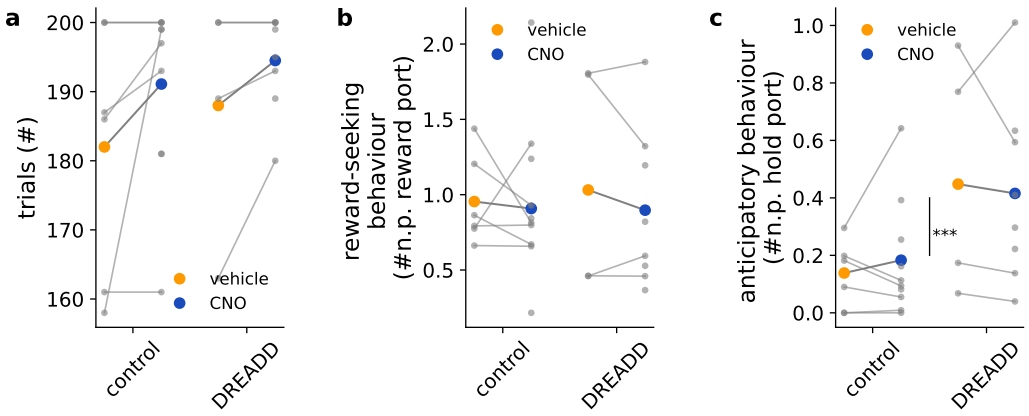

Figure 3.22: **General motor performance during cerebello-thalamic modulation in single-interval timing task with predictable time cue.** (**a**) Interaction plot of total number of trials during a behavioural session given by the population means for CNO (blue, n=10) and vehicle (orange, n=10) in each group respectively. Individual means of each group are given by the grey circles and trend lines. (**b**) Interaction plot of average reward-seeking behaviour during a behavioural session, plotted in the same way as in **a**. (**c**) Interaction plot of average anticipatory behaviour during a behavioural session. *: $p < 0.01$, **: $p < 0.001$ ***: $p < 0.0001$.

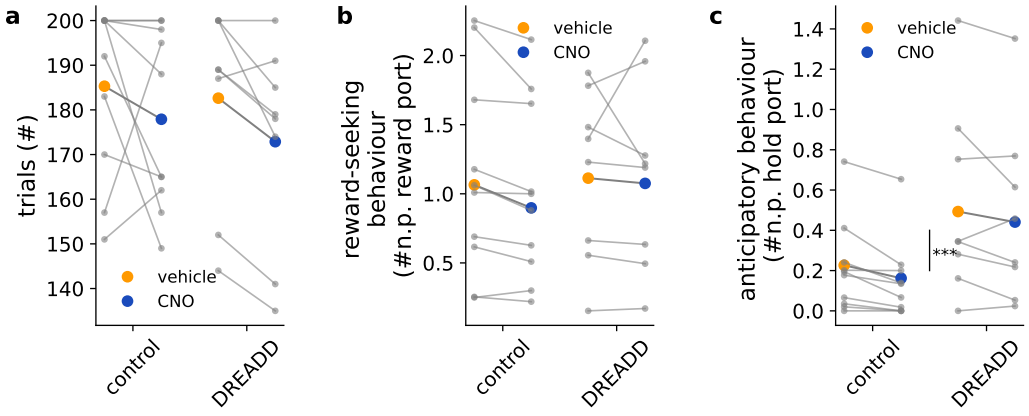

Figure 3.23: **General motor performance during cerebello-thalamic modulation in single-interval timing task with unpredictable time cue.** (**a**) Interaction plot of total number of trials during a behavioural session given by the population means for CNO (blue, n=10) and vehicle (orange, n=10) in each group respectively. Individual means of each group are given by the grey circles and trend lines. (**b**) Interaction plot of average reward-seeking behaviour during a behavioural session, plotted in the same way as in **a**. (**c**) Interaction plot of average anticipatory behaviour during a behavioural session. *: $p < 0.01$, **: $p < 0.001$ ***: $p < 0.0001$.

affect motor behaviour in the operant box.

3.4.3 Modulation of cerebello-thalamic pathway during single-interval timing task with predictable time cue

First, to assess if modulation of the cerebello-thalamic pathway on a rat's ability to perform interval timing to a predictable time cue GLMs were used to interrogate the results. The GLMs included data from two batches of animals (18 rats in total), two animals from the DREADD group were excluded from the dataset as canula tip locations were off target (see 3.21 for distribution of on target locations). The first batch of animals (n=7) involved groups (iii) (n=4) and (iv) (n=3) , i.e. manipulation only sessions. The second batch (n=12) included all 4 groups with group (i) & (iii) (n=6) and (ii) & (iv) (n=5).

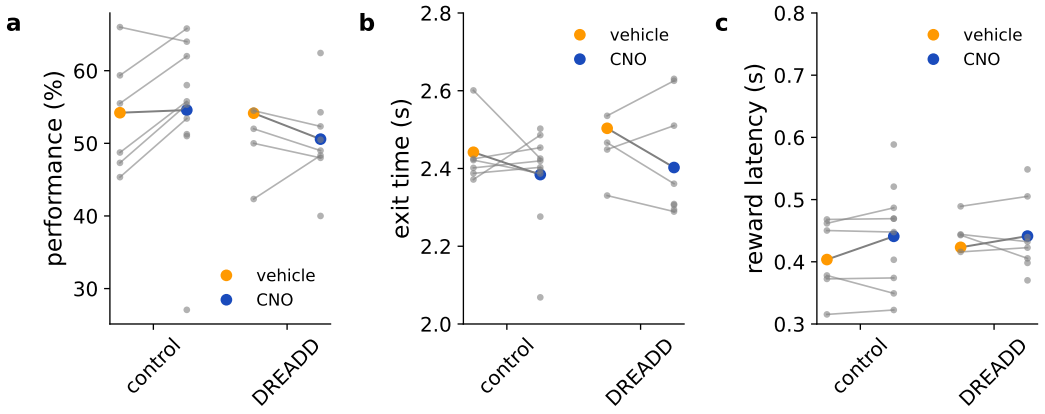

Figure 3.24: **Effect of cerebello-thalamic manipulation during single-interval timing task with predictable time cue.** (**a**) Interaction plot of overall performance during a behavioural session given by the population means for CNO (blue, n=10) and vehicle (orange, n=10) in each group respectively. Individual means of each group are given by the grey circles and trend lines. (**b**) Interaction plot of average exit time during a behavioural session, plotted in the same way as in (a). (**c**) Interaction plot for reward latency. *: $p < 0.01$, **: $p < 0.001$ ***: $p < 0.0001$.

First this study assessed if cerebellar manipulation affects performance by fitting a GLM where reward was the dependent variable and manipulation and group the independent variables (Fig. 3.24a). There was no effect of cerebellar manipulation on performance. Next it was assessed if cerebellar manipulation affects the time it takes for the rat to exit from the hold port. This was assessed using a LMM with exit time as the dependent variable and manipulation and group as the independent variables and rat, session date and trial number as the random term (Fig. 3.24b). There was no effect of the interaction of manipulation and group, nor was there a significant effect of manipulation or group alone. Similarly, there was no effect of either, group, manipulation or the interaction between group and manipulation on reward latency (Fig. 3.24c). Overall, these results suggest that, on average, modulation of the cerebello-thalamic pathway does not affect the rat's ability to perform a single-interval timing task with predictable time cue.

3.4.4 Modulation of cerebello-thalamic pathway during single-interval timing task with unpredictable time cue

As above GLMs were used to estimate the effect of cerebellar manipulation on single-interval timing task with unpredictable time cue. All GLMs included data from two batches of animals, each batch included all 4 groups, i.e. vehicle and manipulation sessions (n=18 rats).

First this study assessed if cerebello-thalamic manipulation affects performance by fitting a GLM with reward as the dependent variable and group and manipulation as the independent variables (Fig. 3.25a). The results indicated that there was no significant effect of the interaction between manipulation and group. However, there was a significant effect of group, indicating that the DREADD group performed on average 6.246% (95% CI [2.829, 9.677], p-value < 0.0001) worse independent of manipulation. There was also a significant effect of the manipulation, indicating that the performance decreased upon CNO administration 4.48% (95% CI [1.239, 7.757], p-value < 0.01; Fig. 3.25a). This indicates that although there is no effect of the interaction between group and manipulation, the mean performance for the DREADD group is overall lower and the average performance decreases with CNO.

Next it was assessed if cerebellar manipulation affects the time it takes for the rat to exit from the hold port by fitting a LMM where exit time was the dependent variable and group and manipulation were the independent variables (Fig. 3.25b). Although there was no significant effect of the interaction between manipulation and group, there was a significant effect of manipulation alone, indicating that exit time decreases, with 0.054 seconds (95% CI [0.02, 0.09], p-value < 0.01), after CNO infusion. There was no effect of modulation of cerebello-thalamic pathway on reward latency (Fig. 3.25c). Overall these results suggest that modulation of the cerebello-thalamic pathway does not affect the rat's ability to perform a single-interval timing task with unpredictable time cue.

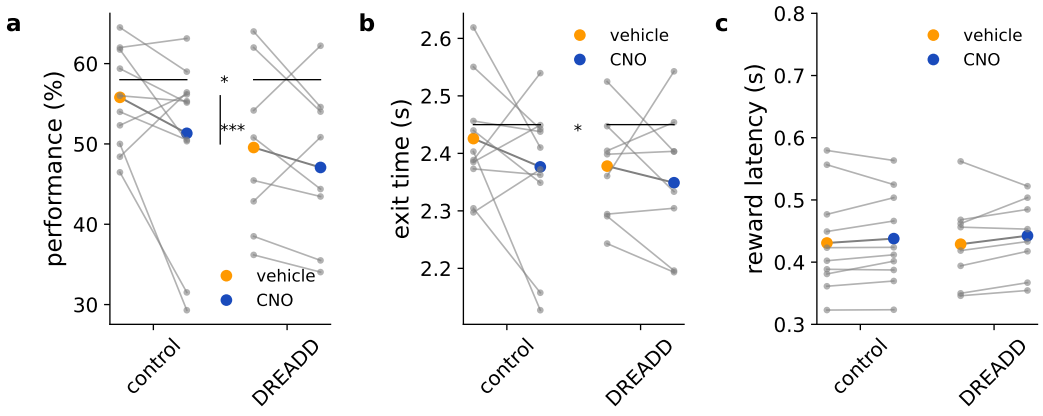

Figure 3.25: **Effect of cerebello-thalamic manipulation during single-interval timing task with unpredictable cue.** (**a**) Interaction plot of overall performance during a behavioural session given by the population means for CNO (blue, n=10) and vehicle (orange, n=10) in each group respectively. Individual means of each group are given by the grey circles and trend lines. (**b**) Interaction plot of average exit time during a behavioural session, plotted in the same way as in **a**. (**c**) Interaction plot for reward latency. *: $p < 0.01$, **: $p < 0.001$ ***: $p < 0.0001$.

3.5 Discussion

The data presented in this chapter, demonstrate that systemic manipulation of the cerebellar output pathway affects interval timing behaviour while targeted manipulation of the cerebello-thalamic pathway does not.

When cerebellar output was manipulated during the single-interval timing task with a predictable and unpredictable time cue, the present study observed two opposite effects of cerebellar manipulation on interval timing. When the time cue is predictable, cerebellar manipulation causes a delayed exit from the waiting port, whereas when the time cue is unpredictable, rats exhibited premature exits.

This conclusions made in this study were based on studying the average behaviour across rats using both a between-subject and within subject control. Examples of individual responses were studied using cumulative response distributions, indicating that there was individual variability underlying this average response. How this perceived stochasticity arises in the nervous system remains an important question in neuroscience (Brembs, 2023). In order to capture within subject variability repeated measures from the same individual are often required (Asahina et al., 2022), which has not been considered in this study. Future analysis of the dataset presented here could consider including anatomical maps of viral expression patterns in order to account for differences that could arise presumably because of differences in viral expression levels between animals.

The response distributions across animals in the single interval timing task indicate a biphasic response. This could indicate that there were two different populations of

rats, with one population showing predictive behaviour and others showing reactive behaviour to the cue. Another possibility is that the same rat switches strategies and the individual response distributions are the result of two distributions, one following the predictive strategy and one following the reactive strategy. The possibility that response distributions between or within animals arise from different underlying distributions is important to consider. The analysis in this study did not directly consider this type of variability, instead GLMs were used to analyse data. Such models are a practical choice for data in which such different sources of variability can be considered but are not of direct interest (Yu et al., 2021) Another point to consider when looking at the different strategies rats develop during the task is the learning of the task. During learning of the target interval of 2.5 s the average performance of rat's plateaus around 55%, above chance level and that training significantly increases performance. For future studies it would be interesting to consider if slight changes to the experimental set up could increase this performance plateau. For example, the nose poke sensitivity and reliability can indicate how sensitive the nose poke hold is to small movements, as it is very hard for rats to remain completely still for a long duration. In this study the IR beam aperture and the width of the nose poke port will have an influence on how sensitive the IR beam is to spontaneous snout movements. It would be interesting to consider if smaller widths of the nose poke port increase the nose poke reliability and sensitivity. A setup with a smaller width of nose poke port relative to this study was considered in Xu et al., 2014 however this paper does not provide detailed measures on the actual performance of the rats in this task. For future studies it might be interesting to consider designated measures for nose poke reliability as this is likely to influence learning and plateau performance. Such measures could be extracted from detailed high-speed behavioural videos.

The analysis performed in this study indicated that the observed effects of cerebellar manipulation on interval timing were not due to off-targets effects of CNO on behaviour (MacLaren et al., 2016; Mahler et al., 2018; Gomez et al., 2017; Manvich et al., 2018), as there was no effect of CNO in control rats on exit time. However, the present study did observe differences in open field exploration, which are indicative of general motor deficits, and should be considered as a potential confound in this experiment. On the contrary, effects on general motor behaviour in the conditioning box were more subtle and seemed to be confined to reward-seeking behaviour. An additional confounding factor is that the observed cerebellar deficits on general motor behaviour were non-stationary. Previous studies suggest that repeated administration of CNO can lead to decreased efficacy of the DREADD (Rogers et al., 2021; Nawreen et al., 2020). However, in the present study additional task-related motor activity was observed and expressed as the reward latency. These results indicated that reward latency was similarly impaired in both the interval timing task with predictable and unpredictable time cue, which suggests that CNO is still effective. Although reduced CNO efficacy cannot be excluded, it might be that different underlying factors cause the non-stationary general motor deficits. First of all it should be noted that motor deficits were not observed in all rats expressing the DREADD virus. One possibility is thus that subtle differences in the underlying expression patterns of the DREADD virus might correlate with the observed motor deficits. Indeed, it is known that different parts of the cerebellar circuit contribute

to motor deficits differently (Amrani et al., 1996). Therefore this needs to be considered in future studies that want to understand role of cerebellum in behaviours using chemogenetic approaches. Even though the reasons for the non-stationary effect of cerebellar output manipulation on motor behaviour remain unclear, the observed effect on exit time in the interval timing task cannot be fully explained by motor deficits as the effect of cerebellar manipulation on more fine motor behaviour, such as the reward latency remained constant across the experiments.

Throughout this chapter it was assumed that the effect of interaction between group and manipulation is fixed and thus does not vary per rat. This assumption was made given that currently the effect of cerebellar manipulation on interval timing behaviour at supra-second timescales is unknown and was followed when performing the LMM analysis. However, as discussed above, the results from the open field and histology suggest that there is some variability in effect of chemogenetic cerebellar manipulation on open field exploration as well as some variability in control and DREADD receptor expression. There exist LMM methods to include such varying effects, these are referred to as random effects (Yu et al., 2021). However, the effect of including random effects in the statistical approach used has not been tested in this study. While GLMs and LMMs provide a useful statistical approach to be adopted in Neuroscience, the flexibility that comes with this approach in combination with an apparent increase in the number of experimenter-based decisions can prevent their appropriate and consistent use (Yu et al., 2021).

Given that the observed effects of cerebellar manipulation on exit time were specific to DREADD-expressing rats, the present study observed that manipulation of cerebellar output affects interval timing behaviour differently depending on the predictability of the time cue. Interestingly, while slowed movements are a representative cardinal symptom of cerebellar disease (Holmes, 1939; Hallett et al., 1991; Mark et al., 1993), impaired time estimation at the supra-second time scale is more commonly observed in schizophrenia, a complex disorder that is thought to mainly involve the cerebral cortex (Lewis et al., 2008). One the one hand, dysmetria is a lack of muscle coordination and control. People with dysmetria have trouble with movement, fine motor tasks and maintaining balance. Dysmetria leads to a delay in movement initiation which can underlie delayed time estimation (Mark et al., 1993). On the other hand, schizophrenic patients show increased anticipatory responses and an increasing number of studies have suggested the cerebellum is also involved in this psychological disorder (Andreasen et al., 2008). This is thought to be because of an acceleration of the internal clock, caused by dopaminergic dysregulation, which leads to a decreased performance in time estimation. Previous studies indicate that the degree of anticipatory responses in schizophrenic patients is linked to task demands (Peterburs et al., 2013). Similarly Gooch et al., 2010 have described different effects of time measurements in cerebellar patients in time production versus time estimation tasks. More specifically, the authors reported that cerebellar patients had increased time measurements in time production tasks but decreased time measurements in time estimation tasks. Although it is unclear how these tasks in humans directly relate to behavioural paradigms in rodents, the effect seems analogous to the differential effect on exit time observed in this study. One possibility is that in the single-interval timing task with predictable time cue there is no requirement of the animal to keep track of time, but the rats can perform the task using another

predictive strategy for reward collection that might not be directly related to time. Whereas in the interval timing task with unpredictable time cue, rats are required to pay attention to the passage of the stimulus as sound offset does not indicate reward anymore (Freestone et al., 2010; Freestone et al., 2013). Another possibility is that, given the non-stationary effect of cerebellar manipulation on motor deficits, in the single-interval timing task with predictable time cue, the effects of cerebellar manipulation on time estimation were masked by the motor deficits which resulted in a delayed exit time. Whereas in the single-interval timing task with unpredictable time cue the effects of cerebellar manipulation on time estimation became evident. Interestingly, when the time cue was unpredictable, rats still displayed a delayed reward latency. However in the interval timing task with unpredictable time cue, rats are required to pay attention to the passage of the stimulus as sound offset does not indicate reward anymore. After the rat has estimated the timing of reward, there is no more requirement of keeping track of the stimulus and the rat now can move to get the reward. Thus the difference in exit time can be because there are clear differences between the goals of each response: reward prediction response versus reward collection.

During the single-interval timing task with unpredictable time cue the analysis separated the cued and uncued trials to verify that animals were using timing behaviour. In theory, rats can only distinguish between cued and uncued trials by accumulating evidence across the trial. For future analysis one could consider the differences between cued and uncued trials by separating the time component from the cue component. In the cued trials, if the manipulation affects the timing then the part of the time component where the cue is on should be affected but the time component where the cue is off should not be affected, as in the latter the rats will have external evidence that the time has passed. In the uncued trials, the time component before and after the target time should be affected. This implies that a mere separation between the cued and uncued trials would not be sufficient, rather the interpretation of the data could be improved by modelling the data with two state transition vectors: a state transition vector related to the passing of time and a state transition indicating the state of the external world. Together, the interaction of these state transition vectors can pinpoint to differences in the relative distributions of exit time readout. Another way to consider behavioural differences in cued and uncued trials would be to work with a block experimental design in which the trial types are interleaved in blocks rather than randomly interleaved, as was done in this study.

Although the results of the current study are in agreement with findings from human literature, studies on the role of cerebellum in interval timing using rodents have been variable and inconclusive (Parker, 2016; Ohmae et al., 2017). A recent study by Heslin et al., 2022 did not find any effects of the role of the cerebellum in interval timing. An important difference with the present study is that Heslin et al., 2022 considered longer time windows, ranging from 4-12 seconds, than the present study. In addition, Heslin et al., 2022 used neuropharmacological approaches to study cerebellar impairment whereas the current study employed chemogenetics restricted to excitatory and inhibitory neurons (Kuhn et al., 2012). Another important difference between the two approaches is the type of movement that animals use to indicate how much time has elapsed. While in this study animals were required to perform

a discrete movement, Heslin et al., 2022 used repetitive movements. It might be that the cerebellar contributes to timing of discrete versus repetitive movement differently (Huys et al., 2008). Together, this suggests that experimental factors such as the time range, ranging from a couple of seconds to tens of seconds, type of intervention and the type of movement, being discrete or repetitive, that is used as a readout of timing are important factors that should be considered and reviewed in order to guide future studies.

Previous studies suggest that the ability to encode a precise temporal structure relies on a cerebellar-prefrontal loop via thalamus (Mathiak et al., 2004). In this study results suggested that cerebello-thalamic modulation does not influence interval timing behaviour. It is possible that the chemogenetic modulation of the cerebello-thalamic pathway was not sufficient to cause a change in pathway transmission. Other studies have described an effect on modulating the cerebellar-thalamocortical pathway on movement initiation (Dacre et al., 2021). However, in that study a more targeted viral approach using retrograde and anterograde labelling was employed, whereas in the current study the cerebello-thalamic modulation resulted in targeting anterograde labelled cerebellar terminals in thalamus. Future studies should thus consider a positive control for cerebello-thalamic modulation. In addition, it is known that the cerebellum exerts its effect on timing behaviour via ascending pathways targeting other different subcortical structures. One pathway via which the cerebellum can influence timing processes is via its monosynaptic projections to the ventral tegmental area (VTA, Carta et al., 2019), a dopaminergic brain region known to be involved in temporal control (Narayanan et al., 2012). In addition, it has been shown that DREADD manipulation of specific neural populations in the VTA can disrupt responses to reward-predictive cues by altering temporal processing (Shields et al., 2021). The direct cerebellum-VTA pathway thus forms a good candidate for future studies on the role of cerebellum in interval timing.

While this study did not observe an effect of cerebello-thalamic modulation on interval timing, off-target CNO effects were observed in the single-interval timing task with unpredictable cue. Such off-target effects of CNO on behaviour have been widely described and discussed in the neuroscientific community (Manvich et al., 2018; MacLaren et al., 2016; Campbell et al., 2018) and novel compounds with increased selectivity (Nagai et al., 2020) should be considered for future experiments. In addition, throughout this study a baseline change in the anticipatory behaviour arising from the DREADDs virus was observed. In contrary to the off-target CNO effects such DREADD receptor specific effects have been reported less in the literature. The baseline change observed in the DREADD group could be due to the different nature of the receptor expression. While the GFP receptor is a fluorescent molecule dissolved in the cytosol, the DREADD receptor is incorporated in the cell membrane. These exogenic membrane bound molecule could be inserted instead of naturally occurring, endogenic, membrane bound receptors and potentially disturbing the natural physiology of the cell by affecting its firing properties.

In this chapter the role of cerebellar output and cerebello-thalamic pathway during interval timing was studied using experienced subjects. However, the theoretical results presented in Chapter II suggest that the cerebellum might not only play a role in precisely executing acquired behaviour but contribute to the learning of the

behaviour as well. Therefore, the results presented in this study might have missed a critical time window during which the cerebellum might be involved (Heslin et al., 2022).

Chapter 4

Concluding statement

The findings reported in this thesis suggest a novel role for how cerebellar output modulates cerebral learning and that the cerebellum is behaviourally relevant for supra-second processing, which has typically been attributed to cortico-striatal circuits.

Evidence from simulating cerebro-cerebellar circuitry using deep learning models, as presented in Chapter II, suggests that the main function of the cerebellar circuit during learning is to provide a feedback signal that enables efficient temporal credit assignment in the cerebral cortex (Richards et al., 2019a). By implementing biologically realistic assumptions and simulating neuroscience-inspired tasks with limited degrees of backpropagation gradient descent to generate feedback signals (Lillicrap et al., 2019) the model makes a range of predictions that suggest specific experimental hypotheses regarding the role of the cerebellum in temporal credit assignment during learning (see Section 2.5.0.7). Specifically, the cerebellar feedback signal increases the amount of temporal information available to the cerebral network during learning and as such facilitates the acquisition of efficient task-relevant representations. The cerebellar feedback signals facilitate learning especially when there is a limited amount of feedback information coming from the environment or internal body state. This is highly relevant for reward-based learning.

The body of modelling work presented in Chapter II suggests that the cerebellum is critical for temporal tasks. The experimental evidence presented in Chapter III indicates that the cerebellum influences performance in a supra-second time estimation task. Moreover, this study was able to differentiate between effects of cerebellar impairment on movement itself and its effects on time prediction. Future studies are required to understand the neural circuit mechanisms by which the cerebellum supports encoding of supra-second intervals. It is possible that, given its mainly feedforward structure, the cerebellum contributes to supra-second time by continuously processing different types of information over a millisecond timescale. Indeed, given the cerebellum's feedforward structure and intricate connectivity with the rest of the brain it is likely that it makes predictions, and provides feedback, over multiple time horizons: from milliseconds (motor control) to seconds or more (decision-making). While its ability to support millisecond timescales might be intrinsic to cerebellar

circuitry, the ability to support supra-second timescales might result from cerebellar interactions with other brain regions, such as the prefrontal cortex (PFC).

While in Chapter III cerebellar contributions to interval timing were studied in a previously learnt skilled behaviour that is thought to be dependent on the PFC (Xu et al., 2014), the findings in Chapter II proposed a framework for studying cerebro-cerebellar interactions during learning that can be extended to higher-order behaviours (Tsay et al., 2022; Sadeghihassanabadi et al., 2022). The overarching dual role of the cerebellum in learning and execution of behaviour can be related to two distinct projection pathways to the cerebral cortex via the thalamus. The cerebellar nuclei have projection pathways via thalamic core cells onto basal dendrites of cortical pyramidal cells (dense) and via thalamic matrix cells onto apical dendrites of cortical pyramidal cells (Anastasiades et al., 2021). While the input onto the basal dendrites are thought to carry bottom-up signals that drive feedforward processing, input into the apical dendrites is thought to carry top-down signaling (Müller et al., 2020). Input onto apical dendrites are thought to drive plasticity underlying learning (Payeur et al., 2021; Greedy et al., 2022). Together, evidence coming from these studies investigating the cellular mechanism of learning in the brain and top-down studies such as presented in this thesis will form the basis of more targeted experiments.

Moreover, as a step towards a mechanistic understanding of cerebellar contributions to interval timing, it is useful to consider a computational model of cerebro-cerebellar circuits like the one presented in the first results chapter or variants thereof (Tanaka et al., 2020; Sussillo et al., 2009; Pemberton et al., 2021). The overarching idea being that the cerebral RNN is connected to a cerebellar network which receives a copy of the RNN activity and returns a prediction of the desired task outcome or feedback signals necessary for learning. Thus, future experimental studies could consider such a network architecture while implementing timing tasks such as the one presented in Chapter III. For example, such networks can be used to train on a single-interval timing task which required producing a timed output. Subsequent analysis of the RNN dynamics during this task with, for example, principal component analysis (PCA), could then elucidate how the population dynamics change with the length of the encoded duration. For example, it is known that both frontal cerebral areas as well as RNNs display ramping dynamics, which are commonly thought to underlie temporal control during adaptive behaviour in the cerebral cortex (Xu et al., 2014; Zhou et al., 2022). Additionally, precise circuit interrogation with focal lesions of the cerebellum combined with activity recordings in the cerebral cortex could then be used to test any predictions resulting from this modelling work. While the present research has focused solely on neural networks trained using supervised learning, another framework that is of particular interest to study brain circuits underlying goal-directed behaviour is reinforcement learning (RL) (Botvinick et al., 2020). Indeed, the ccRNN model is of particular relevance to RL given the prevalence of the sparse feedback and the converging ideas on bootstrapping for efficient learning (Sutton, 1984). Moreover, the study of the neural circuits of interval timing have been previously shown to have integrated views with RL models (Petter et al., 2018). For future studies it would thus be interesting to consider RL implementations that are analogous to the ccRNN presented in this thesis (Garibbo et al., 2022). Using this combination of behavioural experiments testing cerebellar

involvement in combination with models that can be used to probe the dynamical system of neural circuits underlying behaviour might provide a common language to talk about behaviour and neural activity (Savage, 2019).

Overall, in this thesis I hope to have provided unifying perspectives for our understanding of the contribution of cerebral-cerebellar networks for time-based behaviours in the brain.

References

Abbott, Larry and Karel Svoboda (2020). "Brain-wide interactions between neural circuits". In: *Current Opinion in Neurobiology* 65.C.

Adams, Jack A (1968). "Response feedback and learning." In: *Psychological Bulletin* 70.6p1, p. 486.

Ahmad, Nasir, Marcel A J van Gerven, and Luca Ambrogioni (2020). "GAIT-prop: A biologically plausible learning rule derived from backpropagation of error". In: *arXiv preprint arXiv:2006.06438*.

Albus, JS (1973). "The control of a manipulator by a computer model of the cerebellum." In: *National Conference on Remotely manned systems: Exploration and operation in space*.

Amrani, Khalil, Robert W Dykes, and Yves Lamarre (1996). "Bilateral contributions to motor recovery in the monkey following lesions of the deep cerebellar nuclei". In: *Brain research* 740.1-2, pp. 275–284.

Anastasiades, Paul G, David P Collins, and Adam G Carter (2021). "Mediodorsal and ventromedial thalamus engage distinct L1 circuits in the prefrontal cortex". In: *Neuron* 109.2, pp. 314–330.

Andreasen, Nancy C and Ronald Pierson (2008). "The role of the cerebellum in schizophrenia". In: *Biological psychiatry* 64.2, pp. 81–88.

Apps, Richard and Martin Garwicz (2005). "Anatomical and physiological foundations of cerebellar information processing". In: *Nature Reviews Neuroscience* 6.4, pp. 297–311.

Apps, Richard and Thomas C Watson (2013). "Cerebro-cerebellar connections". In: *Handbook of the Cerebellum and Cerebellar Disorders* 1, pp. 1131–53.

Apps, Richard et al. (2018). "Cerebellar Modules and Their Role as Operational Cerebellar Processing Units: A Consensus paper". In: *The Cerebellum* 17.5, pp. 683–684. ISSN: 1473-4222. DOI: 10.1007/s12311-018-0959-9.

Armstrong, RA (2022). "Basic Structure of the Brain and Neurology". In: *Handbook of Substance Misuse and Addictions: From Biology to Public Health*. Springer, pp. 1–21.

Aronov, Dmitriy and Michale S Fee (2011). "Analyzing the dynamics of brain circuits with temperature: design and implementation of a miniature thermoelectric device". In: *Journal of neuroscience methods* 197.1, pp. 32–47.

Asahina, Kenta et al. (2022). "Revisiting Behavioral Variability: What It Reveals About Neural Circuit Structure and Function". In: *Frontiers in Behavioral Neuroscience* 16.

Ashida, Reiko et al. (July 2019). "Sensorimotor, language, and working memory representation within the human cerebellum". In: *Human Brain Mapping* 40.16, pp. 4732–4747.

Attinger, Alexander, Bo Wang, and Georg B Keller (2017). "Visuomotor coupling shapes the functional development of mouse visual cortex". In: *Cell* 169.7, pp. 1291–1302.

Baker, S C et al. (1996). "Neural systems engaged by planning: a PET study of the Tower of London task". In: *Neuropsychologia* 34.6, pp. 515–526.

Bellec, Guillaume et al. (2019). "Biologically inspired alternatives to backpropagation through time for learning in recurrent neural nets". In: *arXiv preprint arXiv:1901.09049*.

Ben-Shushan, Nadav and Misha Tsodyks (2017). "Stabilizing patterns in time: Neural network approach". In: *PLoS computational biology* 13.12, e1005861.

Beppu, Hirokuni, Minami Suda, and Reisaku Tanaka (1984). "Analysis of cerebellar motor disorders by visually guided elbow tracking movement". In: *Brain* 107.3, pp. 787–809.

Berezovskii, Vladimir K, Jonathan J Nassi, and Richard T Born (2011). "Segregation of feedforward and feedback projections in mouse visual cortex". In: *Journal of Comparative Neurology* 519.18, pp. 3672–3683.

Botvinick, Matthew et al. (2020). "Deep reinforcement learning and its neuroscientific implications". In: *Neuron* 107.4, pp. 603–616.

Boven, Ellen et al. (2022). "Cerebro-cerebellar networks facilitate learning through feedback decoupling". In: *bioRxiv*.

Brembs, Björn (2023). "Watching a paradigm shift in neuroscience". In: *Authorea Preprints*.

Buckner, Randy L (Oct. 2013). "The Cerebellum and Cognitive Function: 25 Years of Insight from Anatomy and Neuroimaging". In: *Neuron* 80.3, pp. 807–815.

Buetfering, Christina et al. (2022). "Behaviorally relevant decision coding in primary somatosensory cortex neurons". In: *Nature neuroscience* 25.9, pp. 1225–1236.

Buhusi, Catalin V and Warren H Meck (2005). "What makes us tick? Functional and neural mechanisms of interval timing". In: *Nature reviews neuroscience* 6.10, pp. 755–765.

Butcher, Peter A. et al. (2017). "The cerebellum does more than sensory prediction error-based learning in sensorimotor adaptation tasks". In: *Journal of Neurophysiology* 118.3, pp. 1622–1636. ISSN: 15221598. DOI: 10.1152/jn.00451.2017.

Campbell, Erin J and Nathan J Marchant (2018). "The use of chemogenetics in behavioural neuroscience: receptor variants, targeting approaches and caveats". In: *British journal of pharmacology* 175.7, pp. 994–1003.

Carr, Catherine E et al. (1993). "Processing of temporal information in the brain". In: *Annual review of neuroscience* 16.1, pp. 223–243.

Carta, Ilaria et al. (2019). "Cerebellar modulation of the reward circuitry and social behavior". In: *Science* 363.6424, eaav0581.

Cavanagh, Sean E, Laurence T Hunt, and Steven W Kennerley (2020). "A diversity of intrinsic timescales underlie neural computations". In: *Frontiers in Neural Circuits* 14, p. 615626.

Cayco-Gajic, N Alex and R Angus Silver (2019). "Re-evaluating circuit mechanisms underlying pattern separation". In: *Neuron* 101.4, pp. 584–602.

Cerminara, Nadia L. and Richard Apps (2011). "Behavioural significance of cerebellar modules". In: *Cerebellum* 10.3, pp. 484–494. ISSN: 14734222. DOI: 10.1007/s12311-010-0209-2.

Cerminara, Nadia L, Richard Apps, and Dilwyn E Marple-Horvat (2009). "An internal model of a moving visual target in the lateral cerebellum". In: *The Journal of physiology* 587.2, pp. 429–442.

Cerminara, Nadia L et al. (2015). "Redefining the cerebellar cortex as an assembly of non-uniform Purkinje cell microcircuits". In: *Nature Reviews Neuroscience* 16.2, pp. 79–93.

Chabrol, Francois P, Antonin Blot, and Thomas D Mrsic-Flogel (2019). "Cerebellar contribution to preparatory activity in motor neocortex". In: *Neuron* 103.3, pp. 506–519.

Chen, Janice, Uri Hasson, and Christopher J Honey (2015). "Processing timescales as an organizing principle for primate cortex". In: *Neuron* 88.2, pp. 244–246.

Chen, Jerry L et al. (2013). "Behaviour-dependent recruitment of long-range projection neurons in somatosensory cortex". In: *Nature* 499.7458, pp. 336–340.

Claes, Marie, Lies De Groef, and Lieve Moons (2022). "The DREADDful Hurdles and Opportunities of the Chronic Chemogenetic Toolbox". In: *Cells* 11.7, p. 1110.

Costa, Rui Ponte et al. (2017). "Cortical microcircuits as gated-recurrent neural networks". In: *Advances in neural information processing systems*, pp. 272–283.

Criscimagna-Hemminger, Sarah E, Amy J Bastian, and Reza Shadmehr (2010). "Size of error affects cerebellar contributions to motor learning". In: *Journal of neurophysiology* 103.4, pp. 2275–2284.

Cruz, K Guadalupe et al. (2022). "Cortical-subcortical interactions in goal-directed behavior". In: *Physiological reviews* 103.1, pp. 347–389.

Czarnecki, Wojciech Marian et al. (2017). "Understanding synthetic gradients and decoupled neural interfaces". In: *Proceedings of the 34th International Conference on Machine Learning-Volume 70*. JMLR. org, pp. 904–912.

Dacre, Joshua et al. (2021). "A cerebellar-thalamocortical pathway drives behavioral context-dependent movement initiation". In: *Neuron* 109.14, pp. 2326–2338.

Dash, Suryadeep and Peter Thier (2014). "Cerebellum-dependent motor learning: lessons from adaptation of eye movements in primates". In: *Progress in Brain Research* 210, pp. 121–155.

De Schutter, Erik and Reinoud Maex (1996). "The cerebellum: cortical processing and theory". In: *Current opinion in neurobiology* 6.6, pp. 759–764.

De Zeeuw, Chris I, Stephen G Lisberger, and Jennifer L Raymond (2021). "Diversity and dynamism in the cerebellum". In: *Nature neuroscience* 24.2, pp. 160–167.

Dean, Paul and John Porrill (2008). "Adaptive-filter models of the cerebellum: computational analysis". In: *The Cerebellum* 7.4, pp. 567–571.

Deuschl, G et al. (1996). "Adaptation motor learning of arm movements in patients with cerebellar disease." In: *Journal of Neurology, Neurosurgery & Psychiatry* 60.5, pp. 515–519.

Deverett, Ben et al. (2019). "Cerebellar disruption impairs working memory during evidence accumulation". In: *bioRxiv*, p. 521849.

Diedrichsen, Jörn, Sarah E Criscimagna-Hemminger, and Reza Shadmehr (2007). "Dissociating timing and coordination as functions of the cerebellum". In: *Journal of Neuroscience* 27.23, pp. 6291–6301.

Diedrichsen, Jörn et al. (2019). "Universal transform or multiple functionality? understanding the contribution of the human cerebellum across task domains". In: *Neuron* 102.5, pp. 918–928.

Donald, Ramona D et al. (2011). "Emotionality in growing pigs: is the open field a valid test?" In: *Physiology & behavior* 104.5, pp. 906–913.

Douglas, Rodney and Kevan Martin (1998). "Neocortex." In.

Douglas, Rodney J et al. (1995). "Recurrent excitation in neocortical circuits". In: *Science* 269.5226, pp. 981–985.

Doyon, Julien, Virginia Penhune, and Leslie G Ungerleider (2003). "Distinct contribution of the cortico-striatal and cortico-cerebellar systems to motor skill learning". In: *Neuropsychologia* 41.3, pp. 252–262.

Dum, Richard P and Peter L Strick (2003). "An unfolded map of the cerebellar dentate nucleus and its projections to the cerebral cortex". In: *Journal of neurophysiology* 89.1, pp. 634–639.

Dussutour, Audrey (2021). "Learning in single cell organisms". In: *Biochemical and Biophysical Research Communications* 564, pp. 92–102.

Duuren, Esther van et al. (2009). "Single-cell and population coding of expected reward probability in the orbitofrontal cortex of the rat". In: *Journal of Neuroscience* 29.28, pp. 8965–8976.

Ebbesen, Christian Laut and Michael Brecht (2017). "Motor cortex—to act or not to act?" In: *Nature Reviews Neuroscience* 18.11, pp. 694–705.

Eyono, Roy Henha et al. (2022). "Current State and Future Directions for Learning in Biological Recurrent Neural Networks: A Perspective Piece". In: *Neurons, Behavior, Data analysis, and Theory*, p. 35302.

Farrell, Simon and Stephan Lewandowsky (2018). *Computational Modeling of Cognition and Behavior*. Cambridge University Press. DOI: 10.1017/CBO9781316272503.

Fiez, Julie A et al. (1992). "Impaired non-motor learning and error detection associated with cerebellar damage: A single case study". In: *Brain* 115.1, pp. 155–178.

Foulkes, Alexander J McC and R Chris Miall (2000). "Adaptation to visual feedback delays in a human manual tracking task". In: *Experimental brain research* 131.1, pp. 101–110.

Freestone, David M and Russell M Church (2010). "The importance of the reinforcer as a time marker". In: *Behavioural processes* 84.1, pp. 500–505.

Freestone, David M, Mika LM MacInnis, and Russell M Church (2013). "Response rates are governed more by time cues than contingency". In: *Timing & Time Perception* 1.1, pp. 3–20.

Galea, Joseph M et al. (2011). "Dissociating the roles of the cerebellum and motor cortex during adaptive learning: the motor cortex retains what the cerebellum learns". In: *Cerebral cortex* 21.8, pp. 1761–1770.

Galliano, Elisa et al. (2013). "Silencing the majority of cerebellar granule cells uncovers their essential role in motor learning and consolidation". In: *Cell reports* 3.4, pp. 1239–1251.

Gallistel, Charles R (1990). *The organization of learning*. The MIT Press.

Gao, Zhenyu et al. (2018). "A cortico-cerebellar loop for motor planning". In: *Nature* 563.7729, pp. 113–116.

Garcia, Keith S and Michael D Mauk (1998). "Pharmacological analysis of cerebellar contributions to the timing and expression of conditioned eyelid responses". In: *Neuropharmacology* 37.4-5, pp. 471–480.

Garibbo, Michele et al. (2022). "What deep reinforcement learning tells us about human motor learning and vice-versa". In: *arXiv preprint arXiv:2208.10892*.

George, Paxinos and Charles Watson (2007). *The Rat Brain in Stereotaxic Coordinates (version 6th ed). 6th ed.* Elsevier.

Gerlai, Robert et al. (1996). "Impaired motor learning performance in cerebellar En-2 mutant mice." In: *Behavioral neuroscience* 110.1, p. 126.

Gill, Jason S and Roy V Sillitoe (2019). "Functional outcomes of cerebellar malformations". In: *Frontiers in Cellular Neuroscience* 13, p. 441.

Gomez, Juan L et al. (2017). "Chemogenetics revealed: DREADD occupancy and activation via converted clozapine". In: *Science* 357.6350, pp. 503–507.

Gooch, Cynthia M. et al. (2010). "Interval timing disruptions in subjects with cerebellar lesions". In: *Neuropsychologia* 48.4, pp. 1022–1031. ISSN: 00283932. DOI: 10.1016/j.neuropsychologia.2009.11.028.

Goudar, Vishwa and Dean V Buonomano (2018). "Encoding sensory and motor patterns as time-invariant trajectories in recurrent neural networks". In: *Elife* 7, e31134.

Gouvêa, Thiago S et al. (2014). "Ongoing behavior predicts perceptual report of interval duration". In: *Frontiers in neurorobotics* 8, p. 10.

Grasselli, Giorgio and Christian Hansel (2014). "Cerebellar long-term potentiation: cellular mechanisms and role in learning". In: *International review of neurobiology* 117, pp. 39–51.

Greedy, Will et al. (2022). "Single-phase deep learning in cortico-cortical networks". In: *arXiv preprint arXiv:2206.11769*.

Guell, Xavier, Franziska Hoche, and Jeremy D Schmahmann (2015). "Metalinguistic deficits in patients with cerebellar dysfunction: empirical support for the dysmetria of thought theory". In: *The Cerebellum* 14.1, pp. 50–58.

Guerguiev, Jordan, Timothy P Lillicrap, and Blake A Richards (2017). "Towards deep learning with segregated dendrites". In: *ELife* 6, e22901.

Hallett, M et al. (1991). "Physiological analysis of simple rapid movements in patients with cerebellar deficits." In: *Journal of Neurology, Neurosurgery & Psychiatry* 54.2, pp. 124–133.

Hardy, NICHOLAS F and Dean V Buonomano (2018). "Encoding time in feedforward trajectories of a recurrent neural network model". In: *Neural computation* 30.2, pp. 378–396.

Harris, Kenneth D and Gordon MG Shepherd (2015). "The neocortical circuit: themes and variations". In: *Nature neuroscience* 18.2, pp. 170–181.

Haruno, Masahiko, Daniel M Wolpert, and Mitsuo Kawato (2003). "Hierarchical MOSAIC for movement generation". In: *International congress series*. Vol. 1250. Elsevier, pp. 575–590.

Hasson, Uri et al. (2008). "A hierarchy of temporal receptive windows in human cortex". In: *Journal of Neuroscience* 28.10, pp. 2539–2550.

He, Kaiming et al. (2015). "Delving deep into rectifiers: Surpassing human-level performance on imagenet classification". In: *Proceedings of the IEEE international conference on computer vision*, pp. 1026–1034.

Heffley, William et al. (2018). "Coordinated cerebellar climbing fiber activity signals learned sensorimotor predictions". In: *Nature neuroscience* 21.10, pp. 1431–1441.
Herculano-Houzel, Suzana (2009). "The human brain in numbers: a linearly scaled-up primate brain". In: *Frontiers in Human Neuroscience* 3, p. 31. ISSN: 1662-5161. DOI: 10.3389/neuro.09.031.2009. URL: https://www.frontiersin.org/article/10.3389/neuro.09.031.2009.
Herzog, Michael H and Manfred Fahle (1997). "The role of feedback in learning a vernier discrimination task". In: *Vision research* 37.15, pp. 2133–2141.
Heslin, Kelsey A et al. (2022). "A limited cerebellar contribution to suprasecond timing across differing task demands." In: *Behavioral Neuroscience* 136.5, p. 479.
Hochreiter, Sepp and Jürgen Schmidhuber (1997). "Long short-term memory". In: *Neural computation* 9.8, pp. 1735–1780.
Holmes, Gordon (1917). "The symptoms of acute cerebellar injuries due to gunshot injuries". In: *Brain* 40.4, pp. 461–535.
– (1939). "The cerebellum of man". In: *Brain* 62.1, pp. 1–30.
Honda, Takuya, Masaya Hirashima, and Daichi Nozaki (2012). "Adaptation to visual feedback delay influences visuomotor learning". In: *PLoS one* 7.5, e37900.
Hore, J, B Wild, and HC Diener (1991). "Cerebellar dysmetria at the elbow, wrist, and fingers". In: *Journal of neurophysiology* 65.3, pp. 563–571.
Hua, Sherwin E and James C Houk (1997). "Cerebellar guidance of premotor network development and sensorimotor learning." In: *Learning & Memory* 4.1, pp. 63–76.
Huys, Raoul et al. (2008). "Distinct timing mechanisms produce discrete and continuous movements". In: *PLoS computational biology* 4.4, e1000061.
Ikegami, Tsuyoshi et al. (2012). "Intermittent visual feedback can boost motor learning of rhythmic movements: evidence for error feedback beyond cycles". In: *Journal of Neuroscience* 32.2, pp. 653–657.
Iosif, Cristiana I et al. (2022). "Cerebellar Prediction and Feeding Behaviour". In: *The Cerebellum*, pp. 1–18.
Ito, Masao (1970). "Neurophysiological aspects of the cerebellar motor control system". In: *Int. J. Neurol.* 7, pp. 126–179.
– (2008). "Control of mental activities by internal models in the cerebellum". In: *Nature Reviews Neuroscience* 9.4, pp. 304–313. ISSN: 1471-003X. DOI: 10.1038/nrn2332. URL: www.nature.com/reviews/neurohttp://www.nature.com/articles/nrn2332.
Ivry, Richard B et al. (2002). "The cerebellum and event timing". In: *Annals of the new York Academy of Sciences* 978.1, pp. 302–317.
Jaderberg, Max et al. (2017). "Decoupled neural interfaces using synthetic gradients". In: *Proceedings of the 34th International Conference on Machine Learning-Volume 70*. JMLR. org, pp. 1627–1635.
Jaeger, Dieter (2003). "No parallel fiber volleys in the cerebellar cortex: evidence from cross-correlation analysis between Purkinje cells in a computer model and in recordings from anesthetized rats". In: *Journal of computational neuroscience* 14.3, pp. 311–327.
Jordan, Rebecca and Georg B Keller (2020). "Opposing influence of top-down and bottom-up input on excitatory layer 2/3 neurons in mouse primary visual cortex". In: *Neuron* 108.6, pp. 1194–1206.

Jordan, Rebecca and Georg B Keller (2022). "The locus coeruleus broadcasts prediction errors across the cortex to promote sensorimotor plasticity". In: *bioRxiv*.

Kaiser, Jacques, Hesham Mostafa, and Emre Neftci (2018). "Synaptic plasticity dynamics for deep continuous local learning". In: *arXiv preprint arXiv:1811.10766*.

Kaushik, Akanksha, Jyotsna Singh, and Shilpa Mahajan (2023). "Recurrent Neural Network: A Flexible Tool of Computational Neuroscience Research". In: *Proceedings of the Third International Conference on Information Management and Machine Intelligence*. Springer, pp. 377–384.

Kawai, Risa et al. (2015). "Motor cortex is required for learning but not for executing a motor skill". In: *Neuron* 86.3, pp. 800–812.

Kawato, Mitsuo and Daniel Wolpert (2007). "Internal models for motor control". In: *Novartis Foundation Symposium 218-Sensory Guidance of Movement: Sensory Guidance of Movement: Novartis Foundation Symposium 218*. Wiley Online Library, pp. 291–307.

Keiflin, Ronald and Patricia H Janak (2015). "Dopamine prediction errors in reward learning and addiction: from theory to neural circuitry". In: *Neuron* 88.2, pp. 247–263.

Kiebel, Stefan J, Jean Daunizeau, and Karl J Friston (2008). "A hierarchy of timescales and the brain". In: *PLoS computational biology* 4.11, e1000209.

King, Maedbh et al. (Aug. 2019). "Functional boundaries in the human cerebellum revealed by a multi-domain task battery". In: *Nature Neuroscience* 22.8, pp. 1371–1378.

Kingma, Diederik P and Jimmy Ba (2014). "Adam: A method for stochastic optimization". In: *arXiv preprint arXiv:1412.6980*.

Kishore, Asha, Sabine Meunier, and Traian Popa (2014). "Cerebellar influence on motor cortex plasticity: behavioral implications for Parkinson's disease". In: *Frontiers in neurology* 5, p. 68.

Kitazawa, Shigeru, Takashi Kohno, and Takanori Uka (1995). "Effects of delayed visual information on the rate and amount of prism adaptation in the human". In: *Journal of Neuroscience* 15.11, pp. 7644–7652.

Kobak, Dmitry et al. (2016). "Demixed principal component analysis of neural population data". In: *Elife* 5, e10989.

Kostadinov, Dimitar and Michael Häusser (2022). "Reward signals in the cerebellum: origins, targets, and functional implications". In: *Neuron*.

Kostadinov, Dimitar et al. (2019). "Predictive and reactive reward signals conveyed by climbing fiber inputs to cerebellar Purkinje cells". In: *Nature neuroscience* 22.6, pp. 950–962.

Krupa, David J and Richard F Thompson (1997). "Reversible inactivation of the cerebellar interpositus nucleus completely prevents acquisition of the classically conditioned eye-blink response." In: *Learning & Memory* 3.6, pp. 545–556.

Kuhn, Bernd et al. (2012). "An amplified promoter system for targeted expression of calcium indicator proteins in the cerebellar cortex". In: *Frontiers in neural circuits* 6, p. 49.

Laje, Rodrigo and Dean V Buonomano (2013). "Robust timing and motor patterns by taming chaos in recurrent neural networks". In: *Nature neuroscience* 16.7, pp. 925–933.

Lee, Daeyeol (2020). *Birth of intelligence: from RNA to artificial intelligence*. Oxford University Press.

Legg, CR, B Mercier, and M Glickstein (1989). "Corticopontine projection in the rat: the distribution of labelled cortical cells after large injections of horseradish peroxidase in the pontine nuclei". In: *Journal of Comparative Neurology* 286.4, pp. 427–441.

Leiner, Henrietta C, Alan L Leiner, and Robert S Dow (1993). "Cognitive and language functions of the human cerebellum". In: *Trends in neurosciences* 16.11, pp. 444–447.

Levy, Noa et al. (2010). "Adaptation to delayed force perturbations in reaching movements". In: *PLoS one* 5.8, e12128.

Lewis, David A and Guillermo González-Burgos (2008). "Neuroplasticity of neocortical circuits in schizophrenia". In: *Neuropsychopharmacology* 33.1, pp. 141–165.

Lewis, David I (2019). "Animal experimentation: implementation and application of the 3Rs". In: *Emerging Topics in Life Sciences* 3.6, pp. 675–679.

Li, Nuo and Thomas D Mrsic-Flogel (2020). "Cortico-cerebellar interactions during goal-directed behavior". In: *Current opinion in neurobiology* 65, pp. 27–37.

Lillicrap, Timothy P and Adam Santoro (2019). "Backpropagation through time and the brain". In: *Current opinion in neurobiology* 55, pp. 82–89.

Lillicrap, Timothy P et al. (2020). "Backpropagation and the brain". In: *Nature Reviews Neuroscience* 21.6, pp. 335–346.

Lim, Dong-Hyun et al. (2020). "Active maintenance of eligibility trace in rodent prefrontal cortex". In: *Scientific reports* 10.1, pp. 1–11.

Llinás, Rodolfo et al. (1975). "Inferior olive: its role in motor learning". In: *Science* 190.4220, pp. 1230–1231.

Locke, Timothy M et al. (2018). "Dopamine D1 receptor–positive neurons in the lateral nucleus of the cerebellum contribute to cognitive behavior". In: *Biological psychiatry* 84.6, pp. 401–412.

Maass, Wolfgang, Thomas Natschläger, and Henry Markram (2002). "Real-time computing without stable states: A new framework for neural computation based on perturbations". In: *Neural computation* 14.11, pp. 2531–2560.

MacLaren, Duncan AA et al. (2016). "Clozapine N-oxide administration produces behavioral effects in Long–Evans rats: implications for designing DREADD experiments". In: *eneuro* 3.5.

Mahler, Stephen V and Gary Aston-Jones (2018). "CNO evil? Considerations for the use of DREADDs in behavioral neuroscience". In: *Neuropsychopharmacology* 43.5, pp. 934–936.

Mangels, Jennifer A, Richard B Ivry, and Naomi Shimizu (1998). "Dissociable contributions of the prefrontal and neocerebellar cortex to time perception". In: *Cognitive Brain Research* 7.1, pp. 15–39.

Mante, Valerio et al. (2013). "Context-dependent computation by recurrent dynamics in prefrontal cortex". In: *nature* 503.7474, pp. 78–84.

Manto, Mario (2009). "Mechanisms of human cerebellar dysmetria: experimental evidence and current conceptual bases". In: *Journal of neuroengineering and rehabilitation* 6.1, pp. 1–18.

Manvich, Daniel F et al. (2018). "The DREADD agonist clozapine N-oxide (CNO) is reverse-metabolized to clozapine and produces clozapine-like interoceptive stimulus effects in rats and mice". In: *Scientific reports* 8.1, pp. 1–10.

Mark, Hallet and G Massaquoi Steve (1993). "Physiologic studies of dysmetria in patients with cerebellar deficits". In: *Canadian journal of neurological sciences* 20.S3, S83–S92.

Marr, David (1969). "A theory of cerebellar cortex". In: *The Journal of Physiology* 202.2, pp. 437–470. ISSN: 00223751. DOI: 10.1113/jphysiol.1969.sp008820. URL: http://doi.wiley.com/10.1113/jphysiol.1969.sp008820.

Mathiak, Klaus et al. (2004). "Discrimination of temporal information at the cerebellum: functional magnetic resonance imaging of nonverbal auditory memory". In: *Neuroimage* 21.1, pp. 154–162.

Mathis, Alexander et al. (2018). "DeepLabCut: markerless pose estimation of user-defined body parts with deep learning". In: *Nature neuroscience* 21.9, pp. 1281–1289.

MATLAB (2010). *version 7.10.0 (R2010a)*. Natick, Massachusetts: The MathWorks Inc.

Medina, Javier F and Michael D Mauk (2000). "Computer simulation of cerebellar information processing". In: *nature neuroscience* 3.11, pp. 1205–1211.

Miall, R. C. et al. (1993). "Is the cerebellum a smith predictor?" In: *Journal of Motor Behavior* 25.3, pp. 203–216. ISSN: 19401027. DOI: 10.1080/00222895.1993.9942050.

Mnih, Volodymyr et al. (2015). "Human-level control through deep reinforcement learning". In: *nature* 518.7540, pp. 529–533.

Mojtahedian, S et al. (2007). "Dissociaton of conditioned eye and limb responses in the cerebellar interpositus". In: *Physiology & behavior* 91.1, pp. 9–14.

Molinari, M, V Filippini, and MG Leggio (2002). "Neuronal plasticity of interrelated cerebellar and cortical networks". In: *Neuroscience* 111.4, pp. 863–870.

Monteiro, Tiago et al. (2020). "Manipulation of striatal population dynamics using temperature warps judgment of time". In: *bioRxiv*.

Müller, Eli J et al. (2020). "Core and matrix thalamic sub-populations relate to spatio-temporal cortical connectivity gradients". In: *NeuroImage* 222, p. 117224.

Murray, John D et al. (2014). "A hierarchy of intrinsic timescales across primate cortex". In: *Nature neuroscience* 17.12, pp. 1661–1663.

Murugan, Pushparaja (2018). "Learning the sequential temporal information with recurrent neural networks". In: *arXiv preprint arXiv:1807.02857*.

Muscinelli, Samuel, Mark Wagner, and Ashok Litwin-Kumar (2022). "Optimal routing to cerebellum-like structures". In: *bioRxiv*.

Nagai, Yuji et al. (2020). "Deschloroclozapine, a potent and selective chemogenetic actuator enables rapid neuronal and behavioral modulations in mice and monkeys". In: *Nature neuroscience* 23.9, pp. 1157–1167.

Narayanan, Nandakumar S et al. (2012). "Prefrontal D1 dopamine signaling is required for temporal control". In: *Proceedings of the National Academy of Sciences* 109.50, pp. 20726–20731.

Narayanan, Sriram, Aalok Varma, and Vatsala Thirumalai (2021). "Adaptable internal representations drive cerebellum-mediated predictive control of an innate behavior". In: *bioRxiv*.

Nashef, Abdulraheem et al. (2019). "Reversible Block of Cerebellar Outflow Reveals Cortical Circuitry for Motor Coordination". In: *Cell Reports* 27.9, 2608–2619.e4. ISSN: 22111247. DOI: 10.1016/j.celrep.2019.04.100. URL: https://doi.org/10.1016/j.celrep.2019.04.100.

Nawreen, Nawshaba et al. (2020). "Chemogenetic inhibition of infralimbic prefrontal cortex GABAergic parvalbumin interneurons attenuates the impact of chronic stress in male mice". In: *Eneuro* 7.5.

Nectow, Alexander R and Eric J Nestler (2020). "Viral tools for neuroscience". In: *Nature Reviews Neuroscience* 21.12, pp. 669–681.

Nguyen, Tri M et al. (2022). "Structured cerebellar connectivity supports resilient pattern separation". In: *Nature*, pp. 1–7.

Nichelli, Paolo, David Alway, and Jordan Grafman (1996). "Perceptual timing in cerebellar degeneration". In: *Neuropsychologia* 34.9, pp. 863–871.

Odeh, Francis et al. (2005). "Pontine maps linking somatosensory and cerebellar cortices are in register with climbing fiber somatotopy". In: *Journal of Neuroscience* 25.24, pp. 5680–5690.

Ohmae, Shogo (2022). "The temporal-difference error signals of the climbing fibers and their originas during cerebellar learning in mice". John Hopkins Cerebellum seminar. URL: `urllinktotalkabstractifany`.

Ohmae, Shogo, Jun Kunimatsu, and Masaki Tanaka (2017). "Cerebellar roles in self-timing for sub-and supra-second intervals". In: *Journal of Neuroscience* 37.13, pp. 3511–3522.

Ohmae, Shogo and Javier F Medina (2015). "Climbing fibers encode a temporal-difference prediction error during cerebellar learning in mice". In: *Nature neuroscience* 18.12, pp. 1798–1803.

Oprisan, Sorinel A and Catalin V Buhusi (2014). "What is all the noise about in interval timing?" In: *Philosophical Transactions of the Royal Society B: Biological Sciences* 369.1637, p. 20120459.

O'Reilly, Jill X, M Marsel Mesulam, and Anna Christina Nobre (2008). "The cerebellum predicts the timing of perceptual events". In: *Journal of Neuroscience* 28.9, pp. 2252–2260.

Parker, Krystal L (2016). "Timing tasks synchronize cerebellar and frontal ramping activity and theta oscillations: implications for cerebellar stimulation in diseases of impaired cognition". In: *Frontiers in psychiatry* 6, p. 190.

Paulin, Michael (1989). "A Kalman filter theory of the cerebellum". In: *Dynamic interactions in neural networks: Models and data*. Springer, pp. 239–259.

Payeur, Alexandre et al. (2021). "Burst-dependent synaptic plasticity can coordinate learning in hierarchical circuits". In: *Nature neuroscience*, pp. 1–10.

Pemberton, Joseph, Paul Chadderton, and Rui Ponte Costa (2022). "Cerebellar-driven cortical dynamics enable task acquisition, switching and consolidation". In: *bioRxiv*. DOI: `10.1101/2022.11.14.516257`. eprint: `https://www.biorxiv.org/content/early/2022/11/21/2022.11.14.516257.full.pdf`. URL: `https://www.biorxiv.org/content/early/2022/11/21/2022.11.14.516257`.

Pemberton, Joseph et al. (2021). "Cortico-cerebellar networks as decoupling neural interfaces". In: *Advances in Neural Information Processing Systems* 34, pp. 7745–7759.

Penhune, Virginia B and Julien Doyon (2005). "Cerebellum and M1 interaction during early learning of timed motor sequences". In: *Neuroimage* 26.3, pp. 801–812.

Peterburs, Jutta et al. (2013). "Impaired representation of time in schizophrenia is linked to positive symptoms and cognitive demand". In: *PloS one* 8.6, e67615.

Petter, Elijah A, Samuel J Gershman, and Warren H Meck (2018). "Integrating models of interval timing and reinforcement learning". In: *Trends in Cognitive Sciences* 22.10, pp. 911–922.

Pisano, Thomas J et al. (2021). "Homologous organization of cerebellar pathways to sensory, motor, and associative forebrain". In: *Cell reports* 36.12, p. 109721.

Ponzi, Adam and Jeff Wickens (2022). "Ramping activity in the striatum". In: *Frontiers in Computational Neuroscience* 16.

Popa, Laurentiu S and Timothy J Ebner (2019). "Cerebellum, predictions and errors". In: *Frontiers in cellular neuroscience* 12, p. 524.

Popa, T et al. (2013). "Cerebellar processing of sensory inputs primes motor cortex plasticity". In: *Cerebral cortex* 23.2, pp. 305–314.

Prestori, Francesca et al. (2020). "The optogenetic revolution in cerebellar investigations". In: *International Journal of Molecular Sciences* 21.7, p. 2494.

Raby, Caroline R et al. (2007). "Planning for the future by western scrub-jays". In: *Nature* 445.7130, pp. 919–921.

Rahmati, Negah et al. (2014). "Cerebellar potentiation and learning a whisker-based object localization task with a time response window". In: *Journal of Neuroscience* 34.5, pp. 1949–1962.

Rajan, Kanaka, Christopher D Harvey, and David W Tank (2016). "Recurrent network models of sequence generation and memory". In: *Neuron* 90.1, pp. 128–142.

Raut, Ryan V, Abraham Z Snyder, and Marcus E Raichle (2020). "Hierarchical dynamics as a macroscopic organizing principle of the human brain". In: *Proceedings of the National Academy of Sciences* 117.34, pp. 20890–20897.

Raymond, Jennifer L and Javier F Medina (2018). "Computational principles of supervised learning in the cerebellum". In: *Annual review of neuroscience* 41, pp. 233–253.

Richards, Blake A and Timothy P Lillicrap (2019a). "Dendritic solutions to the credit assignment problem". In: *Current opinion in neurobiology* 54, pp. 28–36.

Richards, Blake A et al. (2019b). "A deep learning framework for neuroscience". In: *Nature neuroscience* 22.11, pp. 1761–1770.

Rilling, James K and Thomas R Insel (1998). "Evolution of the cerebellum in primates: differences in relative volume among monkeys, apes and humans". In: *Brain, Behavior and Evolution* 52.6, pp. 308–314.

Rogers, Stephanie et al. (2021). "Mechanisms and plasticity of chemogenically induced interneuronal suppression of principal cells". In: *Proceedings of the National Academy of Sciences* 118.2, e2014157118.

Rosenblatt, Frank (1958). "The perceptron: a probabilistic model for information storage and organization in the brain." In: *Psychological review* 65.6, p. 386.

Roth, Bryan L (2016). "DREADDs for neuroscientists". In: *Neuron* 89.4, pp. 683–694.

Ruigrok, Tom JH (2011a). "Ins and outs of cerebellar modules". In: *The cerebellum* 10.3, pp. 464–474.

Ruigrok, Tom J.H. (2011b). "Ins and outs of cerebellar modules". In: *Cerebellum* 10.3, pp. 464–474. ISSN: 14734222. DOI: 10.1007/s12311-010-0164-y.

Russell, PA and DI Williams (1973). "Effects of repeated testing on rats' locomotor activity in the open-field". In: *Animal behaviour* 21.1, pp. 109–111.

Sacramento, João et al. (2018). "Dendritic cortical microcircuits approximate the backpropagation algorithm". In: *Advances in Neural Information Processing Systems*, pp. 8721–8732.

Sadeghihassanabadi, Fatemeh et al. (2022). "Structural cerebellar reserve positively influences outcome after severe stroke". In: *Brain Communications* 4.6, fcac203.

Sanes, Jerome N, Bozhidar Dimitrov, and Mark Hallett (1990). "Motor learning in patients with cerebellar dysfunction". In: *Brain* 113.1, pp. 103–120.

Savage, Neil (2019). "How AI and neuroscience drive each other forwards". In: *Nature* 571.7766, S15–S15.

Schöll, Eckehard et al. (2009). "Time-delayed feedback in neurosystems". In: *Philosophical Transactions of the Royal Society A: Mathematical, Physical and Engineering Sciences* 367.1891, pp. 1079–1096.

Schultz, Wolfram, Peter Dayan, and P Read Montague (1997). "A neural substrate of prediction and reward". In: *Science* 275.5306, pp. 1593–1599.

Sejnowski, Terrence J, Christof Koch, and Patricia S Churchland (1988). "Computational neuroscience". In: *Science* 241.4871, pp. 1299–1306.

Sendhilnathan, Naveen, Anna E Ipata, and Michael E Goldberg (2020). "Neural correlates of reinforcement learning in mid-lateral cerebellum". In: *Neuron*.

Shadmehr, Reza, Maurice A Smith, and John W Krakauer (2010). "Error correction, sensory prediction, and adaptation in motor control". In: *Annual review of neuroscience*.

Shields, Andrea K et al. (2021). "Activation of VTA GABA neurons disrupts reward seeking by altering temporal processing". In: *Behavioural brain research* 410, p. 113292.

Shipman, Megan L and John T Green (2020). "Cerebellum and cognition: does the rodent cerebellum participate in cognitive functions?" In: *Neurobiology of learning and memory* 170, p. 106996.

Silva, N Tatiana et al. (2022). "Neural instructive signals for associative cerebellar learning". In: *bioRxiv*.

Skinner, Burrhus F (1971). "Operant conditioning". In: *The encyclopedia of education* 7, pp. 29–33.

Sohn, Hansem et al. (2021). "A network perspective on sensorimotor learning". In: *Trends in Neurosciences* 44.3, pp. 170–181.

Sompolinsky, Haim, Andrea Crisanti, and Hans-Jurgen Sommers (1988). "Chaos in random neural networks". In: *Physical review letters* 61.3, p. 259.

Song, H Francis, Guangyu R Yang, and Xiao-Jing Wang (2016). "Training excitatory-inhibitory recurrent neural networks for cognitive tasks: a simple and flexible framework". In: *PLoS computational biology* 12.2, e1004792.

– (2017). "Reward-based training of recurrent neural networks for cognitive and value-based tasks". In: *Elife* 6, e21492.

Spitmaan, Mehran et al. (2020). "Multiple timescales of neural dynamics and integration of task-relevant signals across cortex". In: *Proceedings of the National Academy of Sciences* 117.36, pp. 22522–22531.

Sternson, Scott M and Bryan L Roth (2014). "Chemogenetic tools to interrogate brain functions". In: *Annual review of neuroscience* 37, pp. 387–407.

Stevens, Eli, Luca Antiga, and Thomas Viehmann (2020). *Deep learning with PyTorch*. Manning Publications.

Streng, Martha L, Laurentiu S Popa, and Timothy J Ebner (2018). "Modulation of sensory prediction error in Purkinje cells during visual feedback manipulations". In: *Nature communications* 9.1, pp. 1–12.

Stuart, Sarah A and Emma SJ Robinson (2015). "Reducing the stress of drug administration: implications for the 3Rs". In: *Scientific reports* 5.1, pp. 1–8.

Sultan, Fahad (2002). "Analysis of mammalian brain architecture". In: *Nature* 415.6868, pp. 133–134.

Sussillo, David and Larry F Abbott (2009). "Generating coherent patterns of activity from chaotic neural networks". In: *Neuron* 63.4, pp. 544–557.

Sutton, Richard S and Andrew G Barto (2018). *Reinforcement learning: An introduction*. MIT press.

Sutton, Richard Stuart (1984). *Temporal credit assignment in reinforcement learning*. University of Massachusetts Amherst.

Synofzik, Matthis, Axel Lindner, and Peter Thier (2008). "The Cerebellum Updates Predictions about the Visual Consequences of One's Behavior". In: *Current Biology* 18.11, pp. 814–818. ISSN: 09609822. DOI: 10.1016/j.cub.2008.04.071.

Tanaka, Gouhei et al. (2019). "Recent advances in physical reservoir computing: A review". In: *Neural Networks* 115, pp. 100–123.

Tanaka, Hirokazu et al. (2020). "The cerebro-cerebellum as a locus of forward model: a review". In: *Frontiers in systems neuroscience* 14, p. 19.

Tanaka, Yasuyo H et al. (2018). "Thalamocortical axonal activity in motor cortex exhibits layer-specific dynamics during motor learning". In: *Neuron* 100.1, pp. 244–258.

Tanji, Jun and Eiji Hoshi (2008). "Role of the lateral prefrontal cortex in executive behavioral control". In: *Physiological reviews* 88.1, pp. 37–57.

Tracy, Joseph I et al. (2000). "Functional localization of a "Time Keeper" function separate from attentional resources and task strategy". In: *Neuroimage* 11.3, pp. 228–242.

Tsay, Jonathan S, Lauren Schuck, and Richard B Ivry (2022). "Cerebellar degeneration impairs strategy discovery but not strategy recall". In: *The Cerebellum*, pp. 1–11.

Tseng, Ya-weng et al. (2007). "Sensory prediction errors drive cerebellum-dependent adaptation of reaching". In: *Journal of neurophysiology* 98.1, pp. 54–62.

Uusisaari, Marylka and Erik De Schutter (2011). "The mysterious microcircuitry of the cerebellar nuclei". In: *The Journal of physiology* 589.14, pp. 3441–3457.

Voogd, Jan and Mitchell Glickstein (1998). "The anatomy of the cerebellum". In: *Trends in cognitive sciences* 2.9, pp. 307–313.

Wagner, Mark J. et al. (2019). "Shared Cortex-Cerebellum Dynamics in the Execution and Learning of a Motor Task". In: *Cell* 177.3, 669–682.e24. ISSN: 10974172. DOI: 10.1016/j.cell.2019.02.019. URL: https://doi.org/10.1016/j.cell.2019.02.019.

Wang, Xiaolu et al. (2020). "A FN-MdV pathway and its role in cerebellar multimodular control of sensorimotor behavior". In: *Nature communications* 11.1, pp. 1–20.

Wang, Xiaolu et al. (2022). "Input and output organization of the mesodiencephalic junction for cerebro-cerebellar communication". In: *Journal of Neuroscience Research* 100.2, pp. 620–637.

Watson, Thomas C, Matthew W Jones, and Richard Apps (2009). "Electrophysiological mapping of novel prefrontal-cerebellar pathways". In: *Frontiers in integrative neuroscience*, p. 18.

Watson, Thomas C. et al. (2014). "Back to front: Cerebellar connections and interactions with the prefrontal cortex". In: *Frontiers in Systems Neuroscience* 8.FEB, pp. 1–11. ISSN: 16625137. DOI: 10.3389/fnsys.2014.00004.

Werbos, Paul J (1990). "Backpropagation through time: what it does and how to do it". In: *Proceedings of the IEEE* 78.10, pp. 1550–1560.

Werfel, Justin, Xiaohui Xie, and H Seung (2003). "Learning curves for stochastic gradient descent in linear feedforward networks". In: *Advances in neural information processing systems* 16.

Whittington, James CR and Rafal Bogacz (2019). "Theories of error back-propagation in the brain". In: *Trends in cognitive sciences* 23.3, pp. 235–250.

Wolff, Annemarie et al. (2022). "Intrinsic neural timescales: temporal integration and segregation". In: *Trends in cognitive sciences*.

Wolpert, Daniel M and Zoubin Ghahramani (2000). "Computational principles of movement neuroscience". In: *Nature neuroscience* 3.11, pp. 1212–1217.

Wolpert, Daniel M, R Chris Miall, and Mitsuo Kawato (1998). "Internal models in the cerebellum". In: *Trends in cognitive sciences* 2.9, pp. 338–347.

Wood, David A, Amy K Siegel, and George V Rebec (2006). "Environmental enrichment reduces impulsivity during appetitive conditioning". In: *Physiology & behavior* 88.1-2, pp. 132–137.

Xu, Min et al. (2014). "Representation of interval timing by temporally scalable firing patterns in rat prefrontal cortex". In: *Proceedings of the National Academy of Sciences of the United States of America* 111.1, pp. 480–485. ISSN: 00278424. DOI: 10.1073/pnas.1321314111.

Yamazaki, Tadashi (2021). "Evolution of the Marr-Albus-Ito Model". In: *Cerebellum as a CNS Hub*. Springer, pp. 239–255.

Yang, Guangyu Robert et al. (2019). "Task representations in neural networks trained to perform many cognitive tasks". In: *Nature neuroscience* 22.2, pp. 297–306.

Yu, Zhaoxia et al. (2021). "Beyond t test and ANOVA: applications of mixed-effects models for more rigorous statistical analysis in neuroscience research". In: *Neuron*.

Zhou, Shanglin and Dean V Buonomano (2022). "Neural population clocks: Encoding time in dynamic patterns of neural activity." In: *Behavioral Neuroscience*.

Zhu, Hu and Bryan L Roth (2014). "Silencing synapses with DREADDs". In: *Neuron* 82.4, pp. 723–725.